

ARDHI UNIVERSITY



**ASSESSMENT OF GLOBAL ATMOSPHERIC REANALYSIS PRODUCTS
USING LOCAL ATMOSPHERIC WATER VAPOUR RETRIEVED FROM
GNSS SIGNALS IN TANZANIA**

KILUSWA JOHNSON Y

BSc Geomatics

Dissertation

Ardhi University, Dar es Salaam

July, 2023

ASSESSMENT OF GLOBAL ATMOSPHERIC REANALYSIS PRODUCTS
USING LOCAL ATMOSPHERIC WATER VAPOUR RETRIEVED FROM
GNSS SIGNALS IN TANZANIA

KILUSWA JOHNSON Y

A Dissertation Submitted to the department of geospatial sciences and Technology in Partially
Fulfilment of the Requirements for the Degree of Bachelor of Science in Geomatics (BSc.in
Geomatics) of Ardhi University on June, 2023.

Certification

The undersigned certify that they have proof read and hereby recommend for acceptance by Ardhi University, a dissertation entitled, “**Assessment of Global Atmospheric Reanalysis Products Using Local Atmospheric Water Vapour Retrieved from GNSS Signals in Tanzania**” in partial fulfillment of the requirements for the award of degree of Bachelor of Science in Geomatics, Ardhi University, Dar es salaam.

.....

Name; Dr. Elifura Saria

(Main Supervisor)

Date

.....

Name; Ms. Valerie Ayubu

(Second Supervisor)

Date

Declaration and Copyright

I, **Kiluswa, Johnson Y**, declare that this dissertation titled, ‘Assessment of Global Atmospheric Reanalysis Products Using Local Atmospheric Water Vapour Retrieved from GNSS Signals in Tanzania’ and the work presented in it are my own. I confirm that:

- This work was done wholly while in candidature for a research degree at this University and no part of this thesis has previously been published or submitted for a degree or any other qualification anywhere else
- Any reference to work done by any other person or institution or any material obtained from other sources have been duly cited and referenced.

.....

Kiluswa, Johnson Y

22792/T.2019

(Candidate)

Copyright © 1999 This dissertation is copyright material protected under the Berne Convention, the Copyright Act of 1999 and other international and national enactments, in that behalf, on intellectual property. It may not be reproduced by any means, in full or in part, except for short extracts in fair dealing; for research or for private study, critical scholarly review or discourse with an acknowledgement, without the written permission of the Directorate of Undergraduate studies, on behalf of both the author and Ardhi University

Acknowledgement

First of all, I would humbly like to thank Lord, the Almighty for taking me this far and for sure; he didn't bring me this far to abandon me.

I would to express my appreciation toward Dr. Elifuraha Saria and Ms. Valerie Ayubu whose greatly inspired me towards this study and for their memorable and valuable supervision towards accomplishment of this Dissertation. I would also like to thank Mr. Timothy Joseph and Mr. Daudi Ntambila for their fully cooperation towards this research. I would like to thank all academic staff of Department of Geospatial Sciences and Technology (DGST) for their guidance in four years at Ardhi University.

I would also like to express my gratitude and appreciation towards my fellow colleagues Daniel Sylvanus, Anna Emmanuel, Hussein Mgalawe, Jairos Ulema, Salma Kodi, Masatu John, Machemba Abdallah, Stella Msuya, Rugabilana Ahmed, together with all Geomatics classmate for their help and gratefully memories we had in four years.

Last but not least, I would like to happily thank my lovely family members: my dear late father, Eng. Yonas Kiluswa, my dear mother, Mrs. Mary Kiluswa, my dear brother, Yedaya , and my dear sister, Diana. It is with immense joy that I express my appreciation for your unwavering love and support. May God always watch over and protect each one of you.

Dedication

I dedicate to my beloved mother, Mrs. Mary Kiluswa, and in loving memory of my departed father, Eng. Yonas Kiluswa, alongside the entire Kiluswa family, this dissertation stands as a symbol of the immense love, strength, and guidance that I have received from each one of you throughout my academic journey. With profound gratitude and admiration, I dedicate this work to honor the unwavering support and inspiration that you have bestowed upon me.

To my late father, Eng. Yonas Kiluswa, this research report is a tribute to your enduring legacy. Your unyielding passion for knowledge, your insatiable curiosity, and your unwavering pursuit of excellence have left an indelible mark on my journey. Though you are no longer physically with us, your presence resonates within my every achievement, urging me to surpass my limits and make you proud.

To the Kiluswa family, I dedicate this report with deep gratitude. Your unwavering support, encouragement, and collective wisdom have been pillars of strength throughout my academic pursuit. From the cherished moments spent discussing ideas with my aunts and uncles, to the shared laughter and heartfelt conversations with my cousins, each interaction has contributed to my growth and understanding. It is through the collective strength of our family that I draw inspiration and purpose. May it stand as a testament to the resilience, determination, and intellectual curiosity that define our shared heritage.

With deep affection and appreciation, May the blessings of God be bestowed upon each and every one of you, and may you be blessed with a long and prosperous life.

Abstract

Atmospheric water vapor is an environmentally significant component of the atmosphere, playing a crucial role in the Earth's natural greenhouse effect and influencing weather patterns. Understanding and monitoring the quantity and distribution of atmospheric water vapor are vital for analyzing and forecasting short and long-term changes in climate. This dissertation focuses on the assessment of global atmospheric reanalysis datasets for representing atmospheric water vapor in Tanzania using ground-based GPS receivers. These reanalysis datasets are widely used for weather forecasting, climate research, and environmental monitoring purposes. The study used atmospheric water vapour measurement obtained from GNSS signals of three GPS stations to evaluate the performance and accuracy of ERA5, ERA-Interim, JRA55, NASA's MERRA2, NCEP1, NCEP2 reanalysis products. The GPS used were ARSH, DODM, and MTVE which are found in Tanzania main land. The GPS processing software GAMIT/GLOBK was employed to determine the GPS-precipitable water (GPS-pw), which serves as a reference for evaluating the reanalysis datasets. Performance metrics such as weighted mean bias, weighted root mean squared deviation, and weighted coefficient correlation were computed to assess the agreement between the reanalysis datasets and GPS-pw. The overall results indicate a good agreement between the global reanalysis datasets and GPS-pw. The weighted mean bias, weighted root mean squared deviation, and weighted coefficient correlation averaged across all datasets were -1.980mm, 5.067mm, and 0.817, respectively. Among o the reanalysis products, the results based on Pearson correlation coefficient were ERA-5 from ECMWF and NASA's MERRA 2 demonstrate the best performance (0.934 and 0.902) respectively, ERA-interim and JRA55 also exhibits favorable results of (0.897 and 0.860) respectively, while NCEP1 and NCEP2 show poorer performance of (0.638 and 0.674) respectively. Based on the findings, it can be concluded that global reanalysis datasets, particularly ERA-5, can be utilized in Tanzania for weather prediction and climate monitoring purposes. These reanalysis products successfully reproduce the spatiotemporal variability of precipitable water vapor over Tanzania, as assessed against the GPS-pw dataset.

Key words: GNSS, GPS, GAMIT/GLOBK, Reanalysis products, Precipitate water vapour, Correlation

Table of Contents

Certification.....	i
Declaration and Copyright	ii
Acknowledgement.....	iii
Dedication	iv
Abstract	v
Table of Contents	vi
List of Tables.....	ix
List of Figures	x
Acronym and abbreviations	xi
CHAPTER ONE	1
INTRODUCTION.....	1
1.1 Background of study	1
1.1.1 Station used in this study.....	5
1.2 Statement of the research problem	6
1.3 Research Objectives	6
1.3.1 Main Objective.....	6
1.3.2 Specific Objectives.....	6
1.4 Significant of the research.....	6
1.5 Beneficiaries of Research.....	6
1.6 Limitations of research.....	7
1.7 Structure of the dissertation.....	7
CHAPTER TWO.....	8
LITERATURE REVIEW.....	8
2.1 Meteorology.	8
2.1.1 Atmosphere and its layers.	8
2.1.2 Meteorological observation techniques.....	9
2.1.3 Weather forecasting.....	9
2.1.4 Reanalysis data.....	11
2.2 Atmospheric water vapour.	16
2.2.1 water vapour measurement techniques.	16
2.2.2 Relationship between water vapour and humidity	18
2.3 GNSS Meteorology	20
2.4 Tropospheric delay.....	20
2.4.1 Mapping function.	23

2.4.2 ZWD from total zenith delay.	24
2.4.3 PW/IWV from ZWD.....	25
2.5 Time series analysis.	25
2.6 Correlation analysis.....	26
2.7 Related studies.....	27
2.7.1 On this research.....	28
CHAPTER THREE.....	29
METHODOLOGY.....	29
3.1 Data identification.....	29
3.1.1 Reanalysis datasets.....	29
3.1.2 GNSS datasets.....	29
3.2 Data sources and acquisition.	30
3.2.1 Reanalysis datasets acquisition.	30
3.2.2 RINEX observation files, Metrological, Navigation files from GPS stations.	31
3.2.3 Precise ephemeris and precise clock files.	32
3.3 Data preparation & Quality check.....	32
3.3.1 RINEX observation files.....	32
3.3.2 RINEX meteorological file.....	33
3.3.3 Preparation of atmospheric reanalysis datasets.....	33
3.4 Data processing.....	33
3.4.1 Extraction PW/IWV from Reanalysis datasets.....	33
3.4.1 Determining PW/IWV from GAMIT/GLOBK.....	34
CHAPTER FOUR.....	38
RESULTS, ANALYSIS AND DISCUSSION.....	38
4.1 Time series analysis of GPS-pw.....	38
4.2 Time series analysis of RA-pw.....	39
4.3 Mean Bias, Root mean square (RMSD) and Correlation (r) Statistics analysis.	40
4.3.1 Arusha Statistics analysis.....	40
4.3.2 Dodoma Statistics analysis.....	45
4.3.3 Mtwara Statistics analysis.....	50
4.4 Summary discussion of the results.....	54
CHAPTER FIVE.....	56
CONCLUSION AND RECOMMENDATION.....	56
5.1 Conclusion.....	56
5.2 Recommendations.....	56

REFERENCE 57

APPENDICES..... 59

 Appendix 1: Sample of processed data and results from ARSH station 59

 Appendix 2: Sample of processed data and results from DODM station 62

 Appendix 3: Sample of processed data and results from MTVE station 65

 Appendix 4: Python script employed to merge daily reanalysis datasets 68

List of Tables

Table 1.1 Reanalysis datasets (UCAR, 2023)	2
Table 3.1 Reanalysis datasets identified	29
Table 3.2 GPS data identification	30
Table 3.3 Reanalysis data access.....	30
Table 3.4 Geographical position of GPS stations	34
Table 4.1 Descriptives statistics based on ARSH station.....	40
Table 4.2 Difference in descriptive statistics between GPS-pw and RA-pw	40
Table 4.3 Mean bias and Root mean squared deviation for ARSH station.....	41
Table 4.4 Pearson correlation coefficient in all datasets of ARSH station	43
Table 4.5 Descriptives statistics based of DODM station.....	45
Table 4.6 Difference in descriptive statistics between GPS-pw and RA-pw of DODM station.....	46
Table 4.7 Mean bias and Root mean squared deviation of DODM station	46
Table 4.8 Pearson correlation coefficient in all datasets of DODM station.....	47
Table 4.9 Descriptives statistics based of MTVE station.....	50
Table 4.10 Difference in descriptive statistics between GPS-pw and RA-pw of MTVE station	50
Table 4.11 Mean bias and Root mean squared deviation of MTVE station	50
Table 4.12 Pearson correlation coefficient in all datasets of DODM station.....	52
Table 4.13 weighted average of mean bias, RSMD, and correlation from all GPS stations	55

List of Figures

Figure 1.1 A Map Showing permanent GPS stations in Tanzania.....	5
Figure 2.1 atmosphere and its layers (physicalGeography.net, 2013)	8
Figure 3.1 UNAVCO Data Download center	31
Figure 3.2 Extraction of Observation files from Crinex to Rinex.....	32
Figure 3.3 Time series of ARSH-pw from reanalysis	34
Figure 3.4 Workflow for processing GNSS Data by using GAMIT/GLOBK Software	35
Figure 4.1 Time series plots of GPS-pw for ARSH, DODM, and MTVE stations.	38
Figure 4.2 The time series of RA-pw from all GPS stations.....	39
Figure 4.3 the graph shows the difference between GPS-pw and RA-pw in mean bias and RMSD of ARSH stations.....	42
Figure 4.4 the difference between GPS-pw and RA-pw against time of ARSH station.....	42
Figure 4.5 the graph shows a variation of Pearson correlation coefficient on all RA-pw against GPS-pw of ARSH station	43
Figure 4.6 the time series plots of GPS-pw with error bars and RA-pw of ARSH station.....	44
Figure 4.7 scatter plots of all RA-pw against GPS-pw of ARSH station.....	45
Figure 4.8 The graph shows the difference between GPS-pw and RA-pw in mean bias and RMSD of DODM stations.	47
Figure 4.9 The graph shows a variation of pearson correlation coefficient on all RA-pw against GPS-pw of DODM station.....	48
Figure 4.10 The time series plots of GPS-pw with error bars and RA-pw of DODM station	48
Figure 4.11 scatter plots of all RA-pw against GPS-pw of DODM station	49
Figure 4.12 The graph shows the difference between GPS-pw and RA-pw in mean bias and RMSD of MTVE stations	51
Figure 4.13 The graph shows a variation of pearson correlation coefficient on all RA-pw against GPS-pw of MTVE station	52
Figure 4.14 The time series plots of GPS-pw with error bars and RA-pw of MTVE station.....	53
Figure 4.15 scatter plots of all RA-pw against GPS-pw of DODM station	53
Figure 4.16 The pie chart shows the distribution of contribution of GPS station in data analysis and comparison.	54

Acronym and abbreviations

CFSR	Climate Forecast System Reanalysis
ECMWF	European Centre for Medium-Range Weather Forecasts
ERA	ECMWF Re-Analysis
GAMIT	Global Navigation Satellite Systems Analysis and Modeling Toolkit
GPS	Global Positioning System
GPS-pw	GPS integrated precipitate water
IGS	International GNSS Service
IPW	Integrated Precipitable Water
IWV	Integrated Water Vapor
JRA	Japan Meteorological Agency
MERRA	Modern-Era Retrospective analysis for Research and Applications
NASA	National Aeronautics and Space Administration
NCAR	National Center for Atmospheric Research
NCEP	National Centers for Environmental Prediction
NSF	National Science Foundation
PPP	Precise Point Positioning
PW	Precipitable Water
PWV	Precipitable Water Vapor
RA-pw	Reanalysis integrated precipitate water
RINEX	Receiver Independent Exchange Format
RMSD	Root Mean Square deviation
TMA	Tanzania Meteorological Agency
UCAR	University corporation for atmospheric research
ZTD	Zenith Total Delay

CHAPTER ONE

INTRODUCTION

1.1 Background of study

Atmospheric water vapours is an environmentally significant part of the atmosphere with about 99% of it being in the troposphere and 1% in the stratosphere. It is one of the fundamental greenhouse gasses which contributes to the Earth's natural greenhouse effect which keeps the surface of the Earth warmer and liveable (Wang *et al.*, 2016). The condensation of water vapour to liquid or ice phase is responsible for clouds, rain, snow, and other precipitation, all of which count among the most significant elements of weather (Moustafa, 1992). As water vapour moves in the atmosphere, it redistributes energy or latent heat of vaporization, which is released through condensation (Li *et al.*, 2014). This is one of the most important conditions in the atmospheric energy budget on both local and global scales and is an important climate variable in most major weather events such as tropical cyclones and severe thunderstorms (Sharifi *et al.*, 2015; Zhang *et al.*, 2018). Therefore, understanding and monitoring the quantity and distribution of atmospheric water vapour, and the effects on atmospheric radiation and circulation, is vital in the analysis and forecast of short and long-term changes in climate.

Global atmospheric reanalysis is a numerical weather prediction model that uses a combination of observations from weather stations, ships, balloons, satellites, and other sources to produce a complete representation of the state of the atmosphere. (Kalnay *et al.*, 1996). This record is created by using a combination of observations from weather stations, ships, aircraft, satellites, and other sources, as well as computer models that simulate the Earth's atmospheric processes. The goal of global atmospheric reanalysis is to provide a consistent and accurate representation of the Earth's atmospheric conditions over time, which can be used for a variety of purposes, including weather forecasting, climate research, and environmental monitoring. (Kalnay, *et al.*, 1996). Reanalysis datasets are widely used by scientists and researchers to study long-term climate trends, understand the processes that drive atmospheric circulation, and improve weather forecasting models. The following are different global atmospheric reanalysis datasets that are available, each of which is produced by a different organization or research group using slightly different methods and data sources.

Table 1.1 Reanalysis datasets (UCAR, 2023)

Atmospheric reanalysis products						
Name	Source	Years of record	Time Step	Spatial resolution	Formats	Scheme
ERA5-Atmospheric analysis	ECMWF	12-1979 up to 11-2021	Sub-Daily Daily Monthly	31km,137 levels to 1pa	netCDF, GRIB	4DVAR, 2016;IFS
ERA-Interim	ECMWF	1979-01 to 2019- 09	Sub-daily, Daily, Monthly	0.75°x0.75°x60 lev 0.1 hPA top	GRIB, netCDF	4DVAR 2006
NASA's MERRA 2 Reanalysis	NASA Global and assimilation office	1980-01 to 2017- 11	Sub-daily, Monthly	½° latitude by ⅝° longitude by 72 model levels (also interpolated to 42 pressure levels)	netCDF	3DVAR 2014
JRA-55	Japanese metrological Agency	12-1957 up to 02-2022	Sub-Daily Monthly	31km,137 levels to 1pa	GRIB	4DVAR 2009
NCEP Reanalysis (R2)	NCEP , DOE	1979-01 to 2022- 02	Sub-daily, Daily, Monthly	2.5°x2.5° 28 levels 3 hPA top	netCDF, GRIB	3DVAR 2001
NCEP-NCAR (R1)	NCEP , NCAR	1948-01 to 2022- 02	Sub-daily, Daily, Monthly	2.5°x2.5°; 3 hPA top	GRIB, netCDF	3DVAR 1995

Atmospheric reanalysis has been widely embraced as the primary data source for acquiring integrated water vapor (IWV) information over the past few decades. This preference is attributed to its advantages, including extensive regional/global coverage, consistent spatiotemporal resolution, and the availability of numerous other meteorological variables. However, it is important to note that reanalysis products may still exhibit considerable uncertainty. This uncertainty arises from various factors, such as inconsistencies in input data and assimilation schemes among different providers and versions. Additionally, disparities in the utilization of distinct physical schemes and representations contribute to the observed variations (Dee *et al.*, 2011).

The Global Navigation Satellite Systems (GNSS) has been exploited for water vapor retrieval by using its ground-based measurements since the 1990s (Bevis *et al.*, 1992). The concept is based on propagation delays due to a neutral atmosphere as the magnitude of signal delay was treated to be proportional to the amount of water vapor in the atmosphere (Bevis *et al.*, 1992). The delayed GPS signals by atmosphere and ionosphere are considered as errors and not needed in geodetic applications but interestingly they become useful atmospheric parameters when well modeled (Schüler, 2001). Sensing meteorological parameters using GNSS signals can be achieved using ground-based surface network of GNSS receivers or space-borne GNSS receivers on board a low Earth orbiting (LEO) satellite (De hand, 2008). From that possibility, we can observe integrated water vapour (IWV) from the atmosphere using GPS stations. So, as the measurements of water vapour may be expressed in terms of precipitable water vapour (PWV), which is the total

atmospheric water vapour contained in a vertical air column of unit area from the Earth's surface to the top of the atmosphere (Alshawaf *et al.*, 2017). Despite the introduction of radiosonde in the 1940 (Durre *et al.*, 2006), partly improved the availability of precipitable water vapour data, although at very low spatial and temporal resolutions. However, these techniques have limitations which have affected the accuracy of water vapour measurements and offer limited coverage. Ground-based GPS receivers are capable of providing IWV with a high temporal and spatial resolution (Yunk *et al.*, 2000). Compared to other techniques, they offer a number of advantages which include the capability to provide continuous data of good quality under all weather conditions and above all surfaces (Hangemann *et al.*, 2003). Since 1992, Global Positioning System (GPS) has been presented as an efficient meteorological tool (Bevis, *et al.*, 1992). and is being increasingly used for estimating atmospheric parameters such as precipitable water vapour (Alshawaf *et al.*, 2015).

Tanzania Meteorological Agency (TMA) is a Government Agency established by the Government Executive Agency Act no.30 of 1997 and it was then officially launched on 3rd December 1999. The Agency is responsible for the provision of Meteorological services; weather forecasts, climate services and warnings and advisories information for the country. Tanzania Meteorological Agency is currently operating under the Ministry of Works, Transport and Communications of the United Republic of Tanzania. Today observed meteorological parameters are Rainfall, Maximum, Minimum, Dry bulb, Dew Point, Wet bulb temperatures, Cistern Level Pressure, Relative Humidity, Vapor Pressure, Cloud Cover, Evaporation, Radiation, Sunshine hours, Wind run, Wind Speed, Wind Direction, Fog, Thunder, Hail, Mean Sea Level, Visibility and Evaporation. Among used method in TMA for weather forecasting and climatic monitoring include Global Weather Prediction Models in which are developed by the National Organization for the Atmosphere in America whereby the output is freely available and European Centre for Medium Range Weather Forecasts (ECMWF) that consists atmospheric reanalyzed datasets from ERA-5, ERA-interim.

TMA cooperates with ECMWF that provides global atmospheric reanalysis datasets ERA-5 and ERA interim for the numerical weather prediction and climatic monitoring. Although there are many other organizations that provide different atmospheric reanalysis datasets like Japanese Meteorological Agency (JRA-55), CFSR, NASA MERRA, NASA's MERRA 2, NCEP (R2) and NCEP, their products may still be subject to large uncertainty. On the one hand, this is due to the fact that the reanalysis from different providers and different versions are inconsistent in the input data, assimilation schemes, besides using different physical schemes and representations. Therefore, it's important to analyze their ability in representing atmospheric water vapour and

suggest a better global reanalysis product that may best fits local coverage in Tanzania for the reliable information for weather forecasting.

Different researches have been conducted to assess the accuracy of estimated integrated precipitate water vapour (IWV) from both GPS receiver and Global Atmospheric reanalysis datasets. For example, in 2020, research was conducted on Atmospheric water vapor determination using GNSS signals in Tanzania that was able obtain PW from GPS station by Precise Point Positioning (PPP) and those from Global reanalysis data, the result showed a positive correlation about with the lowest value of 0.9588. This is one of few researches on Atmospheric water vapor which was conducted in Tanzania based on DoDM GPS station. (Mlawwa, 2020).

Another research was aimed for assessing performance of ERA-5 in retrieving Precipitate water vapour over the East African Region. This research is interested in evaluate a challenge on estimating water vapour from Reanalysis datasets due to complexity of topographical nature in the East Africa region. Due to the essence of rift valley that creates mountainous features along the valley, because the differences in elevation generates variation of in situ data and predicted data. In the study for assessment obtained by comparing between the PWV determined from ERA-5 and GPS PWV from 13 GPS stations, the results shows that RMSE values at most the sites for the two datasets are in the range of 1.35mm-2.25mm with an average of RSME of 1.66mm (Ssenyunzi *et al.*, 2020).

Moreover, another research for Retrieving Precipitable Water Vapor Data Using GPS Zenith Delays and Global Reanalysis Data in China, in research they use The NCEP FNL dataset provided by the NCEP (National Centers for Environmental Prediction) and over 600 observed stations from different sources was selected to assess the quality of the results. A one-year experiment was performed in our study. The types of stations selected include meteorological sites, GPS stations, radio sounding stations, and a sun photometer station. At more than 96% of selected stations, PWV differences caused by the differences between the interpolation results and real measurements were less than 1.0 mm and study indicates that GPS PWV products that use interpolated surface meteorological elements were very close to those based on real meteorological observations, with differences within ± 0.4 mm and a RMSE mainly below 0.6 mm. (Jiang *et al.*, 2016).

This research assesses the performance of the global atmospheric reanalysis products will be using local atmospheric water vapor retrieved from ground GPS receivers as in situ measurement. Tanzania is a region of particular interest due to its complex topography and varied climate, which affects the distribution and variability of atmospheric water vapor.

1.1.1 Station used in this study

This study utilize data from African Array Meteorological sites located in Tanzania Mainland. Only three stations were used in this study (ARSH, DODM, and MTVE) which are located in Arusha, Dodoma, and Mtwara respectively, sites were selected because they had meteorological devices in which monitors temperature($^{\circ}\text{C}$) and pressure (hPa) which are essential elements for computation of IWV. The data coverage was over one-year (1st/January/2015-31st/December/2015), as well as global atmospheric reanalysis data. Figure 1.1 shows a permanent GPS station used in this study.



Figure 1.1 A Map Showing permanent GPS stations in Tanzania

1.2 Statement of the research problem

Despite extensive use of ERA-5, ERA-Interim, JRA-55, NASA's MERRA 2, NCEP (R2), NCEP1 reanalysis products by Tanzania Meteorological Agency (TMA), Meteorologists and scientific researchers. There is a lack of empirical evidence regarding their performance and accuracy. These reanalysis products may still be subject to significant uncertainty. This uncertainty arises from the fact that the reanalysis comes from different providers and different versions which are inconsistent in the input data, assimilation schemes. Furthermore, they employ different physical schemes and representations, resulting in different updates and advancements. Hence, it's important to evaluate their performance on representing atmospheric water vapour as measured by GNSS Signals that best fits local weather conditions in Tanzania.

1.3 Research Objectives

1.3.1 Main Objective

To evaluate the accuracy and performance of global atmospheric reanalysis products in representing local atmospheric water vapour conditions in Tanzania.

1.3.2 Specific Objectives

- i) To Determine Zenith Total Delays (ZTD) from GPS station.
- ii) To derive integrated precipitate water vapour (IWV) from Zenith Total Delays (ZTD).
- iii) To extract integrated precipitate water vapour (IWV) from Reanalysis products.
- iv) To comparing the global atmospheric reanalysis data with locally-derived GNSS data to assess the degree of agreement between the two datasets through Time series.

1.4 Significant of the research

- i) To provide evidence for best global atmospheric reanalysis that can be used by Tanzania Meteorological agency (TMA) for weather prediction in Tanzania
- ii) Increase range of applicability of Geomatics Course in Weather forecasting based on GNSS techniques.
- iii) It enables the identification of potential biases or errors in the global atmospheric reanalysis products, which can be used to improve the quality of the products.

1.5 Beneficiaries of Research

- i) Meteorologists and scientific researchers who use global atmospheric reanalysis products for their research that improves understanding of atmospheric water vapour and its variability as well as accuracy for forecasting.
- ii) Governments and policy makers who rely on accurate atmospheric data to make informed decisions related to climate change and weather-related policy.

- iii) The Tanzania Meteorological agency (TMA), who can benefit from improved weather forecasting and understanding of local atmospheric conditions.
- iv) The agricultural industry in Tanzania, which relies on accurate weather forecasting to optimize crop production and protect against adverse weather events.
- v) Environmental organizations and advocacy groups, who can use the research to better understand and address climate change and its impacts on local communities.

1.6 Limitations of research

- i) Limited geographical coverage, since the research will be based on three GPS stations which cover north, central and southern part of Tanzania due to limited GPS stations so it could not cover the whole country.
- ii) Limited data sources, the research will be based on atmospheric reanalysis based on water vapour and no other atmospheric parameters.

1.7 Structure of the dissertation

This dissertation consists of five chapters. Chapter one, had introduced main concepts regarding Reanalysis data sets with its significance. It gives a brief summary on similar researches regarding GNSS meteorology and stating the research problem together with the objectives of research. Chapter Two discusses some important concepts regarding meteorology, water vapour, GNSS, tropospheric delay and statistical analysis techniques from different literatures which are related to this research. Chapter Three gives a detailed methodology used to process the data in order to obtain the results from the research. Chapter Four, presents the results and discussion of obtained results and finally Chapter Five provides the conclusion and recommendations regarding to findings of this research.

CHAPTER TWO

LITERATURE REVIEW

This chapter will cover on essential components rationale to knowledge required for better understanding of the research topic based on variety topics which were discussed along the research topic

2.1 Meteorology.

Meteorology is part of atmospheric science which includes atmospheric physics and atmospheric chemistry with a major focus on weather forecasting (Weber, 2004). This study includes some concepts from such fields as explained in the following subsection.

2.1.1 Atmosphere and its layers.

Atmosphere is the layer of glasses that surrounds the earths and is held in place by gravity. It plays a critical role in regulating the planet's temperature, protecting it from harmful radiation and supporting life. The other gasses present in the atmosphere include helium, methane, ozone, neon, xenon and many other trace gasses (Balasubramanian, 2011). These gas constituents can be grouped into three main categories: dry air, water substance, and aerosols (Potter & Colman, 2003).

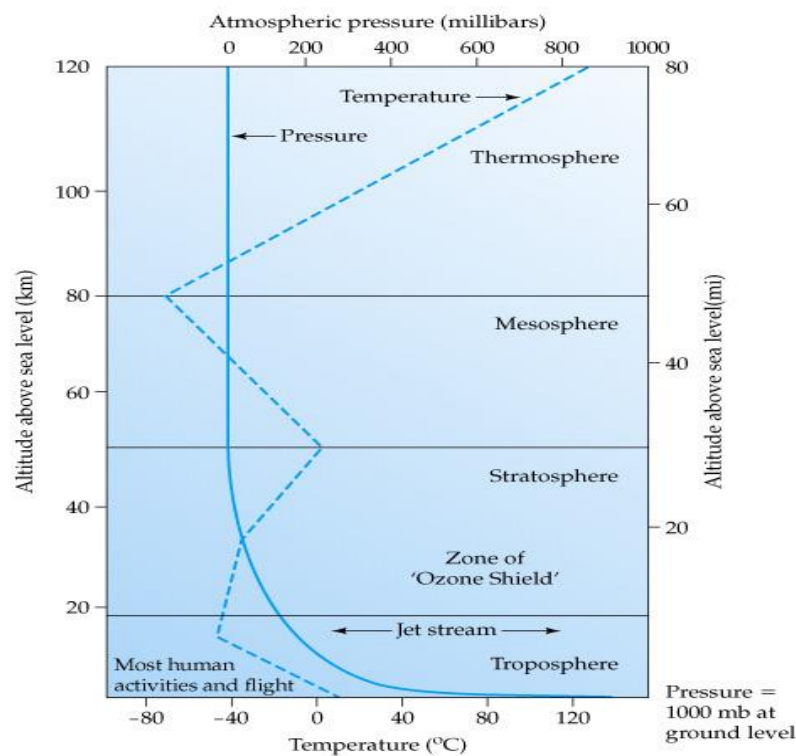


Figure 2.1 atmosphere and its layers (physicalGeography.net, 2013)

2.1.2 Meteorological observation techniques.

Meteorological observations are made for a variety of reasons. They are used for the real-time preparation of weather analyses, forecasts and severe weather warnings, for the study of climate, for local weather dependent operations (for example, local aerodrome flying operations, construction work on land and at sea), for hydrology and agricultural meteorology, and for research in meteorology and climatology (WMO, 2018). The requirements for observational data may be met using in situ measurements or remote-sensing (including space-borne) systems, according to the ability of the various sensing systems to measure the environmental elements needed.

The requirements in terms of global, regional and national scales and according to the application area. WMO Integrated Global Observing System (WIGOS), designed to meet these requirements, is composed of the surface-based subsystem and the space-based subsystem.

- i) The surface-based subsystem comprises a wide variety of types of stations according to the particular application (for example, surface synoptic station, upper-air station, climatological station, and so on).
- ii) The space-based subsystem comprises a number of spacecrafts with on-board sounding missions and the associated ground segment for command, control and data reception (WMO, 2018).

2.1.3 Weather forecasting.

One of the purposes for Meteorological observation is accurate weather forecasting which impacts a lot of human activities and survival. The impact of weather can be very dire if warnings are not given in time and the rate of change are not reported periodically. Almost all-weather phenomenon occurs in the tropospheric layer of the atmosphere. The atmosphere is a dynamic system with many degrees of freedom and predicting its state is very difficult and its state is described by tri-dimensional spatial distribution of weather variables (Taylor & Buizza, 2006). This shows that there is a need for good, well distributed and enough observations of such parameters so that atmospheric state can be modeled and be well predicted.

Weather forecasting means the prediction of the weather through the application of the principles of physics, supplemented by a variety of statistical and empirical techniques. In addition to predictions of atmospheric phenomena themselves, weather forecasting includes predictions of changes on the Earth's surface climate (Balasubramanian, 2016).

Weather forecasting irrespective of the technique used, involves three steps: observation and analysis, extrapolation to find the future state of the atmosphere, and prediction of particular variables (Huffman, 2020). Below are four approaches in weather forecasting

- i) **Analogue Technique:** - a compilation of previous weather events is used, with this a search is conducted into the analogous data to find weather phenomena similar to what is happening today. This method is a difficult method to use when predicting the weather because it requires finding a day in the past with weather similar to the current forecast, which is difficult to do. For example, suppose the current forecast indicates a warm day with a cold front imminent in the region of the forecast. The weather person might remember a similar day in the past month, a warm day with a cold front arriving, which led to the development of thunderstorms later in the day. The forecaster could predict the same type of weather based on the analog comparison, but even small differences between the past and the present can change the outcome, which is why the analog method may not be the right choice to compile a weather forecast (Brenner, 2020).
- ii) **Climatology Method:** -The climatology method offers a simple technique for generating a weather forecast. Meteorologists use this method after reviewing weather statistics gathered over multiple years and calculating the averages. They predict the weather for a specific day and location based on the weather conditions for that same day for several years in the past. The climatology method works when weather patterns remain in place, but in situations where outside factors change the weather frequently, as in climate changes due to global warming, the climatology method is not the best choice for predicting the weather, as it will more than likely not be accurate (Brenner, 2020).
- iii) **Persistence and Trends method:** -The persistence and trends method requires little to no skill to predict the weather because it relies on past trends. In an ideal world, the atmosphere changes slowly, which equates to a forecast tomorrow that stays the same as today, with a hat tip to the climate's norm for the specific time of year. This method requires only that you stay abreast of current temperatures and conditions and know the region's climate averages (Brenner, 2020).
- iv) **Numerical weather prediction:** -The complex physical process in the atmosphere is simulated using numerical models on highly powerful computers to predict how the atmosphere will evolve in time (Acheampong, 2015). The forecast is only as good as the algorithms used by the computer's software to predict the weather. If some of the equations lack precision, they lead to errors (Brenner, 2020). With Numerical Weather Prediction (NWP), predictions of the weather can be made for several days in advance

with high degrees of confidence as greater insights have been gained into the factors causing changes in the atmosphere, and their likely timing and severity and because of the chaotic nature and non-linearity of the atmospheric processes, time integrations of the NWP models are treated as an initial-value problem (Huffman, 2020).

2.1.4 Reanalysis data

Reanalysis is a scientific technique used to create comprehensive and physically consistent numerical descriptions of weather and climate trends over time. This involves combining observations and numerical models that simulate different aspects of the Earth system. Reanalysis data is generated by taking all available observations at constant time intervals over a period of time and using unchanging data assimilation schemes and models (Dee *et al.*, 2020). While there is a wealth of data from various sources, such as weather stations, radiosondes, airplanes, and satellites, the global coverage is incomplete and the quality of the data may vary (Gleisner & Thelji, 2016). To make the observations uniform, some form of data selection, interpolation, or processing is required, but purely mathematical interpolation is not physical and does not provide any additional information. In reanalysis, physical models are used to provide this additional information and produce a physically consistent description. This is why reanalysis data is preferred for research purposes when corresponding data from other sources is unavailable. Consider Figure 2.2 that shows global distribution of rain from NASA MERRA and ERA-Interim

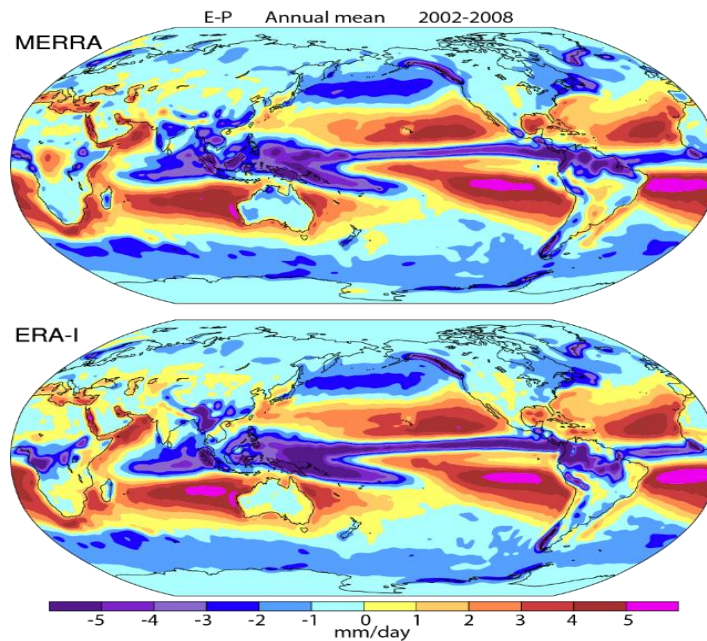


Figure 2.2: Global reanalysis (NCAR, 2023)

Reanalysis models are based on meteorological numerical weather prediction (NWP) models, which assimilate available observations and ensure that the numerical solution is as consistent as possible with the observations. The models start with a previous solution, calculate one time step forward, compare the solution to relevant observations, calculate the error, modify the starting conditions, and repeat the process until a consistent solution (reanalysis) is achieved. Reanalysis grew out of the NWP field, which uses physical models to forecast current observations, and it assimilates historical data going back more than a century. As more data becomes available through digitization and archival work, new reanalysis can be generated (Gleisner & Thelji, 2016). At the same time the descriptions of physical processes in the models are improved by researchers and new re-analyses of the updated body of data become available. (Gleisner & Thelji, 2016). Below are the Global reanalysis data sets from different organizations.

2.1.4.1 ERA 5

This stands for the fifth generation of the European Reanalysis, is a climate dataset produced by the European Centre for Medium-Range Weather Forecasts (ECMWF). It provides a comprehensive description of the Earth's climate system from 1979 to the present with a high spatial resolution of 0.25 degrees (around 31 km) and temporal resolution of one hour (Hersbach *et al.*, 2018). ERA 5 incorporates a wide range of observed data, including satellite, radar, and ground-based measurements, and assimilates them using a numerical weather prediction model, the ECMWF Integrated Forecasting System (IFS). The strengths of ERA 5 is its ability to represent different components of the climate system accurately. For example, it provides an accurate representation of the water cycle, including precipitation, evaporation, and soil moisture (Hersbach *et al.*, 2020). ERA 5 also includes several atmospheric variables, such as temperature, pressure, humidity, wind, and radiation fluxes, which are essential for studying the climate system and its interactions with the oceans, land, and ice (Dee *et al.*, 2011). In addition to the high resolution and comprehensive coverage, ERA 5 provides users with several features that enhance its usability. For instance, it provides seamless global coverage with no gaps, which makes it useful for applications such as weather forecasting, climate monitoring, and numerical modeling (Hersbach *et al.*, 2018). ERA 5 is also available through an open-access platform, which means that anyone can access and download the data free of charge (Hersbach *et al.*, 2020).

2.1.4.2 ERA-interim

This is a climate dataset produced by ECMWF that covers the period from 1979 to 2019. It is the predecessor of ERA 5 and was developed as an improvement over the first generation of the European Reanalysis (ERA-40) (Dee *et al.*, 2011). Like ERA 5, ERA-interim assimilates

observations from various sources, including satellites, aircraft, and surface stations, using the IFS model. However, it has a lower resolution of 0.75 degrees (around 79 km) and temporal resolution of three hours compared to ERA 5. Despite its lower resolution, ERA-interim has been widely used for a variety of applications, including weather forecasting, climate modeling, and atmospheric research. It provides a comprehensive set of atmospheric variables, such as temperature, pressure, humidity, and wind, which are useful for understanding the Earth's climate system (Dee *et al.*, 2011). ERA-interim also incorporates several features that make it useful for scientific research, including a continuous time series, a large spatial coverage, and a long-term record of atmospheric conditions. One of the limitations of ERA-interim is its lower resolution compared to ERA 5, which can affect its accuracy in representing small-scale features of the climate system. It also has limitations in representing some variables, such as soil moisture and snow cover, which are important for understanding the land-atmosphere interactions (Dee *et al.*, 2011). Despite these limitations, ERA-interim remains a valuable dataset for studying the Earth's climate system, especially for long-term climate analyses and for comparisons with other reanalysis datasets.

2.1.4.3 JRA-55

This is a widely used atmospheric reanalysis dataset that provides a comprehensive picture of the Earth's atmosphere from 1958 to the present day. It is created by the Japanese Meteorological Agency (JMA) in collaboration with various research institutions and organizations. The dataset is a result of combining observational data from various sources, including satellite measurements, with numerical models to create a continuous three-dimensional representation of the atmosphere. At the core of JRA-55 is the JMA global spectral model, which is run at a resolution of about 55 km horizontally and 60 vertical levels. This model assimilates observations from various sources, including surface stations, radiosondes, aircraft, and satellites, using the four-dimensional variational (4D-Var) data assimilation method (Chen *et al.*, 2015). The model also incorporates physical processes such as radiation, convection, and turbulence to create a comprehensive representation of the atmosphere. One of the main advantages of JRA-55 is its high spatial and temporal resolution. The dataset provides hourly estimates of various atmospheric variables, including temperature, pressure, wind, and humidity, at a resolution of 1.25 degrees horizontally and 60 vertical levels. This high-resolution data is useful for a wide range of applications, including weather forecasting, climate modeling, and air quality studies. JRA-55 has been extensively used in various studies related to climate and weather, such as the assessment of long-term climate variability, the investigation of atmospheric circulation patterns, and the prediction of extreme weather events. For instance, JRA-55 has been used to study the impact of Arctic Sea ice loss on

mid-latitude weather patterns (Inoue *et al.*, 2012) and to analyze the characteristics of the East Asian monsoon (Chen *et al.*, 2015). In addition to the standard JRA-55 dataset, several variations and extensions of the dataset have been developed to meet specific research needs. For instance, JRA-55C is a version of the dataset that includes corrections for systematic errors in the original dataset, while JRA-55AMIP is a version that is optimized for use in atmospheric model intercomparison projects.

2.1.4.4 NASA MERRA-2 (Modern-Era Retrospective Analysis for Research and Applications, Version 2)

This is a global reanalysis data product that provides long-term, high-resolution atmospheric data for scientific research and applications (Gelaro *et al.*, 2017). The data covers the time period from 1980 to present and has a horizontal resolution of 0.625 degrees (approximately 70 km) with 72 vertical levels. MERRA-2 is a continuation of the original MERRA dataset, which was first released in 2008 (Rienecker *et al.*, 2011). MERRA-2 has several improvements over its predecessor, including updates to the model physics, assimilation of new observations, and a higher resolution. MERRA-2 also includes a new aerosol reanalysis, which provides more accurate and comprehensive information on the distribution and evolution of aerosols in the atmosphere (Buchard *et al.*, 2017). The MERRA-2 dataset provides a wide range of atmospheric variables, including temperature, wind, precipitation, humidity, and aerosols. These variables can be used for a variety of applications, such as weather forecasting, climate studies, air quality monitoring, and renewable energy assessment. The data has been used in numerous studies, including investigations of Arctic Sea ice decline (Liu *et al.*, 2021), air pollution in Asia (Xu *et al.*, 2019), and drought monitoring in Africa (Hagos *et al.*, 2020). MERRA-2 is freely available to the public through the NASA Goddard Earth Sciences Data and Information Services Center (GES DISC).

2.1.4.5 The National Centers for Environmental Prediction (NCEP)

This is a division of the National Weather Service (NWS) responsible for providing environmental forecasting and analysis services to the United States government, the public, and other organizations around the world. The NCEP was established in 1954 with a focus on numerical weather prediction, and has since evolved into a comprehensive center for weather, ocean, and climate prediction (Saha *et al.*, 2015). One of the core services provided by NCEP is the Global Forecast System (GFS), which is a numerical weather prediction model used to produce weather forecasts for the entire globe. The GFS is run multiple times per day, and produces forecasts at various time horizons ranging from a few hours to several days in advance (Saha *et al.*, 2015). The GFS model is a complex system that uses a variety of data sources to produce its forecasts. One of the most important data sources is observational data, which is collected from a

wide variety of sources including ground-based weather stations, weather balloons, and satellites. This data is then ingested into the GFS model to produce a three-dimensional representation of the atmosphere, which is then used to generate forecasts of temperature, pressure, wind, and other meteorological variables. Another important component of the GFS model is the use of numerical methods to solve the equations governing atmospheric motion. These equations are solved using a combination of finite difference and spectral methods, and the resulting solutions are then used to predict the behavior of the atmosphere over time (NCEP, n.d.). The GFS model has undergone numerous upgrades and improvements over the years, and continues to be one of the most widely used numerical weather prediction models in the world. One of the most recent upgrades to the GFS model is the implementation of a new dynamical core known as the Finite-Volume on a Cubed-Sphere (FV3) dynamical core. This new core is designed to improve the accuracy and efficiency of the model by reducing numerical errors and increasing the resolution of the model (NCEP, n.d.). In addition to the GFS model, NCEP also operates a number of other forecasting models and data assimilation systems. These include the North American Mesoscale (NAM) model, the Rapid Refresh (RAP) model, and the Climate Forecast System (CFS) model. Each of these models is designed to address specific forecasting needs, such as short-term high-resolution forecasting or long-term climate prediction (NCEP, n.d.). Overall, NCEP plays a critical role in providing weather and climate prediction services to a wide variety of users around the world. Its forecasting models and data assimilation systems are essential tools for meteorologists, emergency managers, and many other professionals who rely on accurate weather forecasts to make critical decisions.

2.1.4.6 NCEP R2

This also known as the National Centers for Environmental Prediction Reanalysis 2, is a widely used atmospheric reanalysis dataset that provides a global, comprehensive and consistent record of atmospheric and land surface variables dating back to 1979 (Kalnay *et al.*, 1996; Kanamitsu *et al.*, 2002). Reanalysis datasets are generated by assimilating observations of various types and from various sources into numerical models of the atmosphere and the land surface. NCEP R2 is based on the NCEP Global Forecast System (GFS) model, which assimilates surface, upper-air, and satellite observations (Kanamitsu *et al.*, 2002). NCEP R2 is a valuable resource for a range of applications, including climate research, weather forecasting, and atmospheric science. It has been used extensively to study trends in temperature, precipitation, and other climate variables (Wang *et al.*, 2013; Zhang *et al.*, 2018). It has also been used to investigate the dynamics of atmospheric processes, such as the El Niño-Southern Oscillation (ENSO) and the Madden-Julian Oscillation (MJO) (e.g., Wang *et al.*, 2012; Kumar *et al.*, 2014). In addition, NCEP R2 has

been used as a source of boundary conditions for regional climate modeling studies (e.g., Racherla *et al.*, 2012; Jerez *et al.*, 2014). One of the strengths of NCEP R2 is its extensive spatial and temporal coverage. The dataset covers the entire globe, with a horizontal resolution of 2.5 degrees latitude by 2.5 degrees longitude, and is available at six-hourly intervals. The variables available in NCEP R2 include surface and upper-air meteorological variables (such as temperature, pressure, and wind), as well as land surface variables (such as soil moisture and snow cover). NCEP R2 has undergone several updates and improvements over the years. For example, in 2010, the dataset was extended back to 1948 (Kanamitsu *et al.*, 2010). In 2015, an update to the assimilation system improved the representation of atmospheric water vapor (Saha *et al.*, 2015). These updates have improved the quality and consistency of the NCEP R2 dataset, and have expanded its utility for a range of applications. In summary, NCEP R2 is a valuable resource for climate research, weather forecasting, and atmospheric science. It provides a global, comprehensive and consistent record of atmospheric and land surface variables dating back to 1979, with extensive spatial and temporal coverage. The dataset has undergone several updates and improvements over the years, which have expanded its utility for a range of applications.

2.2 Atmospheric water vapour.

Water is the only substance in the Earth's environment that exists naturally in significant quantities in all three states: solid (ice), liquid (water) and gas (water vapour) (Shakhashiri, 2010). Water vapour gets to the atmosphere through open-water evaporation (from the ocean, lakes and rivers), land surfaces, sublimation from ice and snow surfaces and evapo-transpiration from vegetation. As water vapour plays a vital role in maintaining earth's energy balance, the need to accurately and densely measure it is important and one of ways to meet this is through GNSS Meteorology. Water vapour density, water vapour mixing ratio, specific humidity and relative humidity are various definitions used to quantify the amount of water vapour in air (De haan, 2008). The total amount of water vapour in a vertical column which are widely used in meteorology are expressed using Total Precipitable Water (TPW) or Integrated Precipitable Water (IPW) or Integrated Water Vapour (IWV) (Acheampong, 2015).

2.2.1 water vapour measurement techniques.

water vapour has been obtained by use of different techniques in which its measurement still has been not enough as compared to its importance. Such techniques include radiosondes (RAOBs), microwave radiometers (MWRs), remote sensing satellites, and the Global Positioning System (GPS) (Ha *et al.*, 2010).

- i) The radiosonde is composed of a meteorological sensor and a balloon, and the sensor measures pressure, temperature, and humidity as it soars up with the balloon as shown in

Figure 2.3. Based on radiosonde observation one can get vertical profiles of the atmosphere from the surface through to the upper atmosphere. In real-world situations, however, winds can cause the balloon to drift away from the zenith direction at the launch site. In those cases, the radiosonde measurements cannot provide a ‘true’ vertical. Currently, a radiosonde is the most widely used water-vapor measuring device. About 900 World Meteorological Organization radiosonde stations, under the World Weather Watch program, launch radiosondes several times a day (Ha *et al.*, 2010).

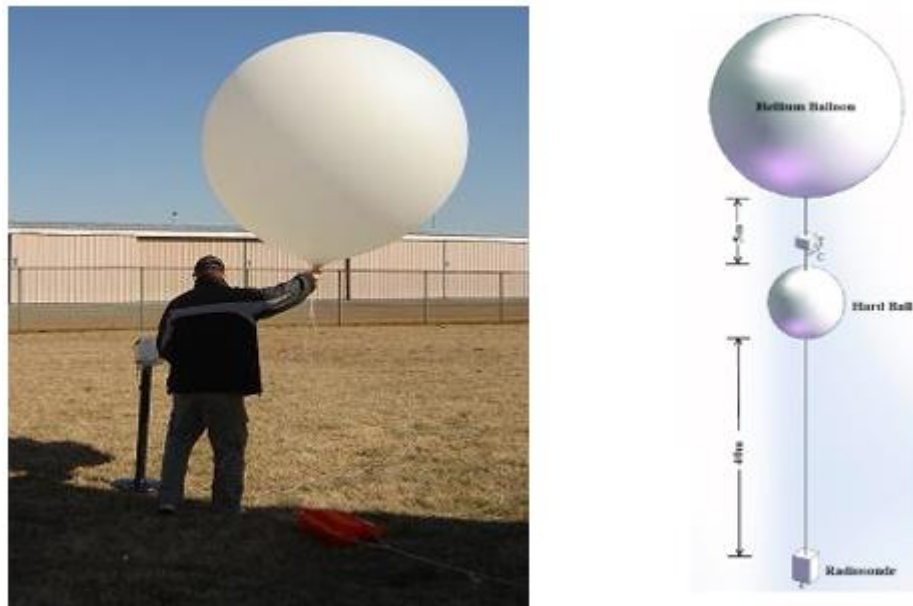


Figure 2.3 A radiosonde (National Weather Service, 2023)

- ii) Microwave radiometers (MWRs) detect water vapor and cloud liquid water in the atmosphere by measuring the brightness temperature of the atmosphere at frequencies of 18-32 GHz (Ha *et al.*, 2010). Some old MWR models, such as the WVR-1100 manufactured by radiometric, observe only the total amount of water vapor along its line of sight.
- iii) Remote sensing satellites can measure water vapor by observing the brightness temperature of the atmosphere using onboard infrared and microwave sensors. Compared to other devices, satellite sensors can monitor a much larger area, and thus they are adequate for observing atmospheric water vapor on a global scale. Microwave sensors can measure water vapor even under clouds, but they only work in oceanic parts of the Earth (Ha *et al.*, 2010). One of the disadvantages of satellite-based measurements is that one cannot use infrared sensors to retrieve data on water vapor content under clouds and even though microwave sensors can measure water vapor even under cloud, but they only work in

oceanic parts of the Earth because of their relatively simple surface condition (Zhou *et al.*, 2016)

- iv) GNSS meteorology, from GPS measurements, one can determine the amount of signal delay due to the atmosphere. Then, the time delay due to water vapor can be separated from the total delay with the use of on-site pressure and temperature measurements (Ha *et al.*, 2010). The GNSS meteorology (before GPS meteorology) was suggested by (Bevis *et al.*, 1992) and later in 1997; it was clarified more by (Solheim & Ware, 1999). The concept is based on propagation delays due to a neutral atmosphere as the magnitude of signal delay was treated to be proportional to the amount of water vapour in the atmosphere (Bevis *et al.*, 1992). The delayed GPS signals by atmosphere and ionosphere are considered as errors and not needed in geodetic applications but interestingly they become useful atmospheric parameters when well modeled (Schüler, 2001).

2.2.2 Relationship between water vapour and humidity

Water vapour is a gaseous substance and its concentration in the air is defined by its partial pressure, e . The sum of the partial pressures of all atmospheric gasses yields to the air pressure of the atmosphere.

$$P_{air} = e + p_d \dots \dots \dots Eq (2.1)$$

Where p_d : partial pressure of dry air. The equilibrium vapour pressure, e_s , is the partial pressure for which the water vapour is in thermodynamic equilibrium state with its condensed phase. It is given as a function of temperature, T , in Kelvin as:

$$e_s(T) = 0.6112 \cdot \exp\left(\frac{17.67 \cdot T}{T + 243.5}\right) \dots \dots \dots Eq (2.2)$$

The Relative Humidity (RH) is defined as a ratio (%) between the water vapour's partial pressure and the equilibrium vapour pressure:

$$RH = \frac{e}{e_s} \cdot 100\% \dots \dots \dots Eq (2.3)$$

RH describes how close the concentration of water vapour is to saturation or condensation. The humidity of the air can further be defined in terms of the mixing ratio, r in g/kg of an air parcel:

$$r = 1000 \cdot \frac{m_w}{m_d} \dots \dots \dots Eq (2.4)$$

where m_w , denotes the mass of water vapour and m_d is the mass of dry air. The mixing ratio can be expressed in terms of partial pressure as

$$r = 1000 \cdot \frac{mv_{ap}}{M_{air}} \cdot \frac{e}{P_{air} - e} \dots \dots \dots Eq (2.5)$$

with M_{vap} and M_{air} as the molar weight of water vapour and dry air respectively.

Another definition is the specific humidity, SH which describes the part (in mass) of water vapour in an air particle.

$$SH = 1000 \cdot \frac{m_w}{m_a} g/kg \dots\dots\dots Eq (2.6)$$

With m_w , the mass of water vapour and m_a , the mass of the whole humid air, m_w the mass of water vapour and m_a , the mass of the whole humid air in the air parcel.

Further, is the definition of Absolute Humidity, AH which is mass of water vapour in a given volume of air.

$$AH = \frac{m_w}{V_a} = e \cdot \frac{M_w}{RT} kg/m^3 \dots\dots\dots Eq (2.7)$$

2.2.2.1 Integrated Water Vapour (IWV) and Precipitable Water (PW)

Among parameters used to quantify atmospheric water vapour, IWV and PW are used when GNSS meteorology is the method to determine water vapour. Integrated water vapour, IWV denotes the amount of water vapour in a column between two levels of height or pressure (Acheampong, 2015). The units of IWV are kg/m^2 and the expression between the altitudes h_1 and h_2 is

$$IWV(h_1, h_2) = \int_{h_2}^{h_1} AH(h)dh \dots\dots\dots Eq (2.8)$$

In terms of two pressure levels, P_1 and P_2

$$IWV(p_1, p_2) = \int_{p_2}^{p_1} \frac{AH(P)}{p_{air}(P) \cdot g} dP = \frac{1}{100g} \int_{p_2}^{p_1} SH(P)dP \dots\dots\dots Eq (2.9)$$

where, g is the Earth's gravity and p_{air} is air density. It can also be expressed in terms of water vapour's partial pressure and temperature.

$$\Delta IWV(h_1, h_2) = \int_{h_2}^{h_1} \frac{e(h) \cdot M_w}{RT(h)} dh \dots\dots\dots Eq (2.10)$$

With $R = 8.314472 \text{ JK}^{-1}\text{mol}^{-1}$ is the ideal gas constant and T is air temperature.

Precipitable Water (PW) is used to express the height of an equivalent column of liquid water in units of length. PW relates to IWV by dividing with the density of liquid water, ρ_w .

$$PW = IWV / \rho_w \dots\dots\dots Eq (2.11)$$

Since PW is expressed in units of meters, its relationship to Zenith wet delay (ZWD) from GNSS signal as it passes atmosphere is just a dimensionless constant Π .

2.3 GNSS Meteorology

Global Navigation Satellite Systems (GNSS) meteorology is an emerging field that has revolutionized weather monitoring and forecasting (Larson & Axelrad, 2015). GNSS is a system of satellites that provide positioning, navigation, and timing services to users worldwide. In recent years, GNSS has been used to obtain atmospheric data, such as temperature, pressure, and water vapor content, which are critical for weather forecasting (Guldner *et al.*, 2020). One of the main advantages of using GNSS for meteorology is its ability to provide continuous, real-time measurements of atmospheric conditions over a wide area (Larson & Axelrad, 2015). Unlike traditional weather balloons and radiosondes, which provide only sporadic measurements at specific locations, GNSS provides a more comprehensive picture of atmospheric conditions across a large region. This is particularly useful for predicting the onset and severity of weather events, such as storms and floods. In order to obtain atmospheric data using GNSS, a GNSS receiver is needed, which can be either a standalone receiver or part of a network of receivers.

The receiver tracks the GPS or other GNSS signals and records the time of arrival of each signal. The receiver also measures the phase delay caused by the atmosphere, which is caused by the presence of water vapor, as well as other atmospheric effects (Larson & Axelrad, 2015). Once the data has been collected by the receiver, it is processed using a technique called "atmospheric tomography," which involves analyzing the signal delays at multiple elevation angles and using a mathematical model to reconstruct the atmospheric properties (Akhlaq *et al.*, 2018). This technique is used to obtain a three-dimensional map of atmospheric conditions, including temperature, pressure, and water vapor content. The data obtained through GNSS meteorology can be used to improve the accuracy of weather forecasting models (Guldner *et al.*, 2020). By providing real-time and high-resolution data on atmospheric conditions, GNSS meteorology can help forecasters predict the onset and severity of weather events, as well as provide early warning of extreme weather conditions. GNSS meteorology is a rapidly evolving field that has the potential to transform weather monitoring and forecasting. By providing continuous, real-time data on atmospheric conditions, GNSS can improve the accuracy and timeliness of weather predictions, and ultimately help save lives and protect property during extreme weather events.

2.4 Tropospheric delay.

Tropospheric layer also refracts GNSS signals, unlike the ionosphere, it is non-dispersive for radio waves (i.e., the refractive index is independent of the signals' frequency) (Acheampong,

2015). Measurements of code and carrier phases at the various frequencies experience a common delay (Misra & Enge, 2011). In Figure 2.4 The tropospheric medium slows the speed of propagation of the signal making range measurements to satellites longer. The earth's atmosphere affects microwave or radio signals passing through it in three ways:

- i) it causes propagation delays;
- ii) it causes ray bending; and
- iii) signal absorption (Kleijer, 2004)

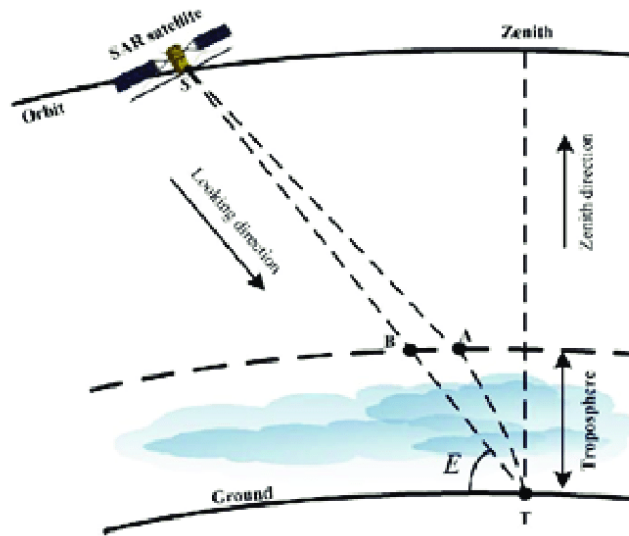


Figure 2.4 Tropospheric delay (Azeriansyah & Harintaka, 2019).

Propagation delays and ray bending effects on the neutral atmosphere were considered for this study and from literature the total delays depend on the refractivity along the traveled path (Solheim & Ware, 1999). This refractivity is a function of pressure and temperature at the receiving station. From Fermat's principle and following (Kleijer, 2004). The geometric distance of ray is given by:

$$L = \int_l dL \dots \dots \dots Eq (2.14)$$

where L is the geometrical distance and l is the geometrical path. The excess path length becomes.

$$\Delta L_a^i(\epsilon) = S - L = \int_s (n(s) - 1)ds + \{\int_s ds - \int_s dl\} \dots \dots \dots Eq (2.15)$$

Where is excess path length (Delay) in the slant direction for a signal from satellite, i to receiver's antenna, a , at elevation angle, ϵ . on the right-hand side is the excess path length caused by the propagation delay and is the excess path length caused by ray bending. The aspects caused by ray bending are negligible at higher satellite elevations based. The tropospheric effects can introduce errors from 2.5 m to as high as 25 m depending on the elevation of the satellite (Seeber, 2003). Δ_{trop} , cannot be estimated from GNSS observables and as such its effects are mitigated

by using models. Δd_{trop} on range measurements to satellites are made up of two components: the dry component and the wet component. Hence, Δd_{trop} can further be defined as:

$$\Delta d_{trop} = \Delta d_{tropd} + \Delta d_{tropw} \dots \dots \dots Eq (2.16)$$

where, Δd_{tropd} is the dry or hydrostatic component and Δd_{tropw} is the wet component. Δd_{tropw} , which comprises only 10% of total tropospheric refraction, depends on the distribution of water vapour in the atmosphere and the harder of the two components to model (Seeber, 2003). Whereby, Δd_{tropd} can be precisely described within an accuracy of $\pm 1\%$ by tropospheric models. Wet delays on the other hand, can be modeled using precise surface meteorological parameters with an accuracy not better than 2cm. Models for tropospheric refraction are based on functions of meteorological parameters and refractive index of air mass along signal path (Acheampong, 2015). An empirical formula for computing the reduced index of tropospheric refraction, N , and $N(s)$ is given below:

$$N = k_1 \frac{p_d}{T} Z_d^{-1} + k_2 \frac{e}{T} Z_w^{-1} + k_3 \frac{e}{T^2} Z_w^{-1} \Rightarrow N(s) = [n(s) - 1]10^6 \dots \dots \dots Eq (2.17)$$

where p_d and e are partial pressures of the dry gasses and water vapour in hPa, T is absolute temperature in Kelvin; and are inverse are compressibility factors for dry and moist air respectively and are used to describe the deviation of the atmospheric constituents from an ideal gas; k_1 , k_2 and k_3 are constants based on laboratories estimates and their values were found to be $k_1 = 77.60 \pm 0.05$ K/hPa, $k_2 = 77.40 \pm 2.2$ K/hPa, $k_3 = 373900 \pm 1200$ K²/hPa and $k_2' = 22.10 \pm 2.2$ K/hPa (Bevis *et al.*, 1994).

Eq (2.17), can further be expressed in terms of integrals of the two components and ignoring all other terms which are zero in the zenith direction, becomes:

$$\Delta d_{trop} = 10^{-6} \int_{atm} N(s).ds = \int_{atm} [\Delta d_{tropd}(s) + \Delta d_{tropw}(s)].ds \dots \dots \dots Eq (2.18)$$

Most tropospheric delays estimations are based on average meteorological conditions at the antenna location from models of the standard atmosphere using the day of the year, latitude and altitude (Misra & Enge, 2011). Two approaches that are used to estimate Δd_{trop} are:

Estimation of the Zenith tropospheric delay (ZTD) in terms of the corresponding dry (ZHD) and wet delays (ZWD);

$$ZHD = ZHD + ZWD \dots \dots \dots Eq (2.19)$$

i. Define a mapping function to scale the ZTD as a function of the elevation angle (ϵ)

$$\Delta d_{trop}(\epsilon) = \Delta d_{tropz,d}.m_d(\epsilon) + \Delta d_{tropz,w}.m_w(\epsilon) \dots \dots \dots Eq (2.20)$$

where m_d and m_w are mapping functions for the dry and wet components. Simple models normally use a common mapping function for both the dry and wet components ignoring the atmospheric profile differences (Misra & Enge, 2011) .

There are various tropospheric models that have been developed based on the assumptions of changes in temperature and water vapour with altitude. gLAB®, one of software used for this dissertation uses a model that does not require any surface meteorological data (Ramos-Bosch, 2019). The model shown below also uses the Niell mapping functions that considers different obliquity factors for the wet and dry components.

$$T_{z,dry} = ae^{-bH} \dots\dots\dots Eq (2.21)$$

$$T_{z,wet} = T_{z_0,wet} + \Delta T_{z,wet} \dots\dots\dots Eq (2.22)$$

Where $a = 2.3m$, $b = 0.116 \cdot 10^{-3}$, and H is station height above sea level, in meters. $T_{z_0, wet} = 0.1$ m and $\Delta T_{z,wet}$ is estimated as a random-walk process using Kalman filtering together with the station coordinates, and other parameters (Subriana *et al.*, 2014). There is a caution that this model has a huge simplification for the vertical delays.

2.4.1 Mapping function.

Mapping functions are defined as the ratio of electric path through the atmosphere at geometric elevation ϵ to path in zenith direction. Mapping functions (also referred to as obliquity factors) are models used to convert the slant tropospheric delays to zenith delays. These functions make computations of total tropospheric delays easier as signals arrive at the antenna location from various angles (Acheampong, 2015). The simplest model for both dry (hydrostatic) and wet delays according is $1/\sin \epsilon$ works well when the earth is considered to be flat and satellites are above 15o elevation angles (ϵ) (Misra & Enge, 2011). Several models have been developed to counter the effects of the earth's curvature and low-elevation satellites. Below is the model used by gLAB®, which is based on a modified Niell (1996) model using the Marini (1972) model normalized to unity at the zenith (Niell, 1996; Ramos-Bosch, 2019). The models are presented below, where E is the elevation angle and H is receiver's height above sea level in km.

Hydrostatic mapping function:

$$M_{dry}(E, H) = m(E, a_d, b_d, c_d) + \Delta m(E, H) \dots\dots\dots Eq (2.23)$$

With,

$$\Delta m(E, H) = [\frac{1}{\sin E} - m(E, a_{ht}, b_{ht}, c_{ht})]. H$$

Wet mapping function

$$M_{wet}(E, H) = m(E, a_w, b_w, c_w) \dots\dots\dots Eq (2.24)$$

With

$$m(E, a, b, c) = \left[\frac{1 + \frac{a}{b}}{\sin E + \frac{a}{\sin E + c}} \right]$$

Following (Subriana *et al.*, 2014) and (Niell, 1996) the hydrostatic parameters ad, bd, cd are time (t) and latitude (θ) dependent and can be evaluated using the expression

$$\xi(\theta, t) = \xi_{avg}(\theta) - \xi_{avg}(\theta) \cos\left(2\pi \frac{t-T_0}{365.25}\right) \dots\dots\dots Eq (2.25)$$

where t is the time from January 0.0, in days, and T0 is taken as Day of Year (DoY).

2.4.2 ZWD from total zenith delay.

From the equation of state for ideal gasses, $p_d/T = R_d p_d$, where, R_d is the specific gas constant of the dry constituent, ($R_d = R/M_d$, R is the universal gas constant and M_d is the molar mass of the dry gasses). Using simple approximations and the assumption of hydrostatic equation being valid for total pressure and not for partial pressures, Davis *et al.* (1985) reformatted Eq (2.17) to be:

$$N = k_1 R_d \rho + k_2 \frac{e}{T} + k_3 \frac{e}{T^2} \dots\dots\dots Eq (2.26)$$

which has been given earlier is derived by the expression $N = k_2 - (M_w/M_d)k_1$, where M_w is the molar mass of water vapour; ρ is the total density of dry air and water vapour.

When all the slant delays are mapped onto the zenith direction, zenith hydrostatic delays, ZHD can be obtained by considering the assumption that hydrostatic equilibrium have been satisfied (Davis *et al.*, 1985);

$$\frac{dp}{dh} = -p(h)g(h) \dots\dots\dots Eq (2.27)$$

where g is the acceleration due to gravity in the vertical direction; p is the total pressure.

The resultant integration of the first term in Eq (2.26) gives:

$$ZHD = (10^{-6} k_1 R_d g_m^{-1}) * P_s \dots\dots\dots Eq (2.28)$$

where P_s is the total ground pressure in hPa, g_m is gravitational acceleration at the mass center of a vertical column of the atmosphere and $g_m = (9.784 \pm 0.001 \text{ m/s}^2) \cdot f(\theta, H)$, and

$$f(\theta, H) = (1 - 2.66 * 10^{-3} * \cos(2\theta) - 2.8 * 10^{-7} H) \dots\dots\dots Eq (2.29)$$

(Bevis *et al.*, 1992).

The parameters θ and H are the latitude of the site in degrees and surface height above the geoid in meters respectively.

Substituting all the constants in Eq (2.28), the expression for solving ZHD in units of length become

$$ZHD = 0.002277(1 + 0.0026 \cos 2\theta + 0.00028H) \cdot P_s \dots\dots\dots Eq (2.30)$$

With ZTD already computed and knowledge of the precise coordinates of the antenna position (θ, H) and surface pressure values from meteorological file or nearby weather station, ZWD can be computed using Eq (2.19) and Eq (2.30).

2.4.3 PW/IWV from ZWD.

Two parameters are used to refer to the atmospheric water vapour content. These are Integrated Water Vapour (IWV) in units of kg/m^2 which refers to the quantity of the atmospheric water vapour over a specific location and Precipitable Water (PW) used to express the height of an equivalent column of liquid water in units of length.

$$IWV = \int_0^\infty p_v(h) dh = \frac{1}{R_w} \int_0^\infty \frac{e(h)}{T(h)} dh \dots\dots\dots Eq (2.31)$$

where p_v is the partial density of water vapour in kg/m^3 ; the height h in meters and R_w is the specific gas constant for water vapour in $\text{J}/(\text{kgK})$. PW relates to IWV by dividing with the density of liquid water, ρ_w . Again IWV is related to the ZWD using a dimensionless quantity as conversion factor, Π :

$$IWV = \frac{ZWD}{\Pi} \text{ and } PW = \frac{ZWD}{\rho_w \Pi} \dots\dots\dots Eq (2.32)$$

From Eq (2.18) and considering second and third terms of Eq (2.26), zenith wet delays become,

$$ZWD = 10^{-6} \int_z (k'_2 \frac{e(z)}{T(z)} + k_3 \frac{e(z)}{T(z)^2}) dz \dots\dots\dots Eq (2.33)$$

substituting the constants and introducing a concept of mean temperature, T_m , which is defined as

$$T_m = 0.72T_s + 70.2 \dots\dots\dots Eq (2.34)$$

where T_s is the surface temperature, the conversion factor finally becomes:

$$\Pi = 10^{-6} p_w R_w (k'_2 + \frac{k_3}{T_m}) \dots\dots\dots Eq (2.35)$$

The conversion factor was computed by Bevis *et al*, (1994) and gave a result of ≈ 0.15 with variation of over 20% (Bevis *et al.*, 1994).

2.5 Time series analysis.

Time series analysis is a statistical technique used to identify and analyze patterns in time-based data. Time series analysis requires breaking down the data into its pattern, seasonal, and irregular components, according to (Athanasopoulos 2018). This makes it possible to spot patterns throughout time and anticipate future values. The ARIMA (autoregressive integrated moving

average) model is one of the most often used approaches to time series analysis. In order to predict future values, this model examines the correlation and lag effects of previous observations (Box *et al.*, 2015). Numerous disciplines, including meteorology, finance, and economics, have used time series analysis. This model involves analyzing the correlation and lagged effects of past observations to forecast future values (Box *et al.*, 2015). Time series analysis has been applied in various fields, including economics, finance, and meteorology.

2.6 Correlation analysis.

Correlation analysis is a statistical technique used to measure the strength of the relationship between two or more variables. According to Hair *et al.* (2019), correlation analysis involves calculating the correlation coefficient between two variables, with values ranging from -1 to 1. A value of -1 indicates a perfect negative correlation, while a value of 1 indicates a perfect positive correlation. A value of 0 indicates no correlation. Correlation analysis is commonly used in meteorology to study the relationship between meteorological variables, such as temperature and precipitation (Barrett *et al.*, 2016). The strength and direction of the correlation can provide insights into the underlying mechanisms and interactions between these variables.

There are three types of correlation coefficient;

i) **Pearson correlation coefficient.**

This is the correlation which is more used in statistics to measure the degree of relationship between the linear related variables. The Pearson correlation coefficient (r) can be computed through the Eq (2.36) below;

$$r = \frac{\sum_{i=1}^n (x_i - \bar{x})(y_i - \bar{y})}{\sqrt{\sum_{i=1}^n (x_i - \bar{x})^2 \sum_{i=1}^n (y_i - \bar{y})^2}} \dots\dots\dots \text{Eq (2.36)}$$

Whereby r is the Pearson correlation coefficient, \bar{x} is the mean of variable x and \bar{y} is the mean of variable y .

ii) **Kendall's Tau rank correlation coefficient.**

This is the correlation which is a non-parametric test that can be used to determine the strength of dependence between the two variables. And this coefficient is obtained from the equation below.

$$\tau = \frac{nc - nd}{0.5n(n-1)} \dots\dots\dots \text{Eq (2.37)}$$

Whereby τ is the Kendall's rank correlation coefficient, nc is number of concordant (ordered in the same way) and nd is number of discordant (ordered in differently).

iii) Spearman rank correlation coefficient.

This is also a non-parametric test that can be used to measure the degree of association between the two variables. The test in this correlation does not have any assumption about the distribution of the data and is the appropriate correlation analysis when the two variables are measured on a scale that is at least ordinal (Shi & Conrad, 2009). The formula below shows how to obtain Spearman rank correlation coefficient, whereby ρ is the Spearman rank correlation coefficient, di is the difference between ranks corresponding in two variables and n is the number of values in each data set.

2.7 Related studies

Different researches have been conducted to assess the accuracy of estimated precipitate water vapour (PWV) from both GPS receiver and Global Atmospheric reanalysis datasets. In 2020, research was conducted on Atmospheric water vapor determination using GNSS signals in Tanzania that was able to obtain PW from GPS station by Precise Point Positioning (PPP) and those from Global reanalysis data, the result showed a positive correlation about with the lowest value of 0.9588. This is one of few researches on Atmospheric water vapor which was conducted in Tanzania based on DoDM GPS station. (Mlawa, 2020).

(Ssenyunzi *et al.*, 2020) This research was aimed for assessing performance of ERA-5 in retrieving Precipitate water vapour over the East African Region. This research is interested in evaluate a challenge on estimating waters vapour from Reanalysis datasets due to complexity of topographical nature in the East Africa region. Due to the essence of rift valley that creates mountainous features along the valley, because the differences in elevation generates variation of in situ data and predicted data. In the study for assessment obtained by comparing between the PWV determined from ERA-5 and GPS PWV from 13 GPS stations, the results shows that RMSE values at most the sites for the two datasets are in the range of 1.35mm-2.25mm with an average of RSME of 1.66mm.

(Jiang *et al.*, 2016) Moreover, Research paper for Retrieving Precipitable Water Vapor Data Using GPS Zenith Delays and Global Reanalysis Data in China, in research they use The NCEP FNL dataset provided by the NCEP (National Centers for Environmental Prediction) and over 600 observed stations from different sources were selected to assess the quality of the results. A one-year experiment was performed in this study. The types of stations selected include meteorological sites, GPS stations, radio sounding stations, and a sun photometer station. The results of this experiment were at more than 96% of selected stations, PWV differences caused by the differences between the interpolation results and real measurements were less than 1.0 mm and

study indicates that GPS PWV products that use interpolated surface meteorological elements were very close to those based on real meteorological observations, with differences within ± 0.4 mm and a RMSE mainly below 0.6 mm.

2.7.1 On this research

This research study focuses on the evaluation of atmospheric reanalysis datasets using GPS measurements as in-situ observations for analysis. Despite the primary usage of GPS in positional measurement, navigation, tracking, monitoring, mapping, and surveying, it can also be utilized for measuring atmospheric water vapor. In this study, three GPS stations from the northern, middle, and southern parts of Tanzania were equipped with dual-frequency receivers and meteorological devices were used. These stations were employed to assess the performance of various global atmospheric reanalysis products. The assessment primarily involved comparing the precipitable water vapor (PWV) derived from the GPS stations (ARSH, DODM, and MTWE) with the PWV values obtained from global reanalysis products (ERA-5, ERA-Interim, MERRA2, JRA55, NCEP1, and NCEP2). The motivation for conducting this research in Tanzania lies in the region's complex topography, diverse climate, and since the products may still be subject to large uncertainty on the one hand, this is due to the fact that the reanalysis comes from different providers and different versions are inconsistent in the input data, assimilation schemes, besides using different physical schemes and representations come with different updates and advancement. By comparing the atmospheric water vapor derived from reanalysis products with measurements obtained from GPS receivers, our aim is to gain insights into the strengths and limitations of these products, enabling us to identify the most suitable reanalysis product for Tanzania

CHAPTER THREE

METHODOLOGY

The methodology used in this study focused assessment the accuracy and performance of global atmospheric reanalysis products in representing local atmospheric water vapour in Tanzania which ERA5, ERA-interim, JRA-55, CFSR, NASA MERRA, NASA's MERRA 2, NCEP (R2) and NCEP datasets was obtained on one year and statistically analyzed against water vapour retrieved from different located GPS station in Tanzania using GAMIT processing software specifically in Arusha (ARSH), Dodoma (DODM), Mtwara (MTVE) .Data identification was the first step of the approach, which also included data acquisition, preparation, and processing, followed by analysis and result interpretation.

3.1 Data identification

3.1.1 Reanalysis datasets

The primary data were recognized based on a number of Global reanalysis datasets that were ERA5, ERA-interim, JRA-55, CFSR, NASA MERRA, NASA's MERRA 2, NCEP (R2) and NCEP. The total precipitate water vapour was required to be downloaded on all reanalysis data sets. Table 3.1 shows a detailed summary of the identified reanalysis datasets.

Table 3.1 Reanalysis datasets identified

Reanalysis Dataset	Temporal Coverage	Spatial Resolution	Data Source
ERA 5	1979 – present	31 km	ECMWF
ERA-Interim	1979 – 2019	0.75° × 0.75°	ECMWF
JRA-55	1958 – 2019	1.25° × 1.25°	JMA
NASA MERRA-2	1980 – present	0.5° × 0.625°	NASA/GMAO
NCEP/NCAR Reanalysis I	1948 – 2018	2.5° × 2.5°	NOAA/NCEP
NCEP/DOE Reanalysis II	1979 – 2010	2.5° × 2.5°	NOAA/NCEP

3.1.2 GNSS datasets

The accurate and reliable identification of data is critical in any scientific research. In this study, the GNSS data were identified based on objectives on obtaining water vapour from GPS stations. The data from ARSH, DODM and MTVE including the IGS stations were used in GNSS positioning processing. The observation navigation files, meteorological files, precise ephemeris

were major components for GPS processing using GAMIT software. Table 3.2 gives a detailed summary on identified data with their sources, data format and where they were used.

Table 3.2 GPS data identification

DATA	FORMAT	SOURCE	USE
GNSS observation and navigation files for experiment and IGS sites station for 1 year (Jan 2015-Dec 2015)	Compressed RINEX (HATANAKA) xxxxsddd.yy.d.z	UNAVCO https://www.unavco.org/data/gps-gnss/data-access-methods/dai1/campaign.php	PPP processing
GNSS Meteorological files for GPS station for 1 year (Jan 2015-Dec 2015)	RINEX xxxxsddd.yy.m.z	UNAVCO https://www.unavco.org/data/gps-gnss/data-access	ZWD, PW and IWW computation
GNSS precise ephemeris and precise clock files	cccwwwd.sp3.z cccwwwd.clk.z	CDDIS ftp://cddis.gsfc.nasa.gov/pub/gps/products/	For PPP processing

3.2 Data sources and acquisition.

3.2.1 Reanalysis datasets acquisition.

All Reanalysis data was acquired based on the specific location of the GPS station in which was ARSH, DODM, and MTVE. Based to Total integrated precipitate water vapour (PWV) with unit of with Kg/m^2 or mm was obtained with the temporal resolution of 6 hours interval 00:00, 06:00, 12:00 up to 18:00. All reanalysis data was obtained at period of one year that starts from 1st January, 2015 to 31st December, 2015 and also all data were acquired at a spatial coverage 0°S , -15°S , 27°E , 43°E . Table 3.3 provides the formats and source links to download Reanalysis dataset.

Table 3.3 Reanalysis data access

Reanalysis Dataset	Format	Download Links
ERA 5	NetCDF	https://cds.climate.copernicus.eu/cdsapp#!/dataset/reanalysis-era5-single-levels?tab=form
ERA-Interim	NetCDF	https://cds.climate.copernicus.eu/cdsapp#!/dataset/reanalysis-era-interim-pressure-levels?tab=form

JRA-55	GRIB	https://rda.ucar.edu/datasets/ds628.0/
CFSR	GRIB	https://rda.ucar.edu/datasets/ds093.1/
NASA MERRA	NetCDF	https://disc.gsfc.nasa.gov/datasets/M2I6NPANA_V5.2.0/summary
NASA MERRA-2	NetCDF	https://disc.gsfc.nasa.gov/datasets/M2I6NPANA_V5.12.4/summary
NCEP/NCAR Reanalysis I	NetCDF	https://www.esrl.noaa.gov/psd/data/gridded/data.ncep.reanalysis.html
NCEP/DOE Reanalysis II	NetCDF	https://www.esrl.noaa.gov/psd/data/gridded/data.ncep.reanalysis2.html

3.2.2 RINEX observation files, Metrological, Navigation files from GPS stations.

RINEX observation, meteorological and navigation files for the experiment site ARSH, DODM and MTVE. all IGS sites were downloaded from UNAVCO archives with the help of DAIV1 (Data Archive Interface version 1) with link <https://www.unavco.org/data/gps-gnss/data-accessmethods/dai2/app/dai2.html> . Figure 3.1 gives a simplified graphical user interface large amount data downloading from UNAVCO. The IGS sites which were downloaded included ABDO, ADIS, ACRG, DARK, DEAR, HARB, MAL2, MSA1. All RINEX datafiles were downloaded within a one-year coverage that started at 01 Jan 2015 to 12 Dec 2015.

ABPO - Data Download Options

[<< Back to ABPO Search Result Page](#)

NOTICE - By downloading data from UNAVCO, you are agreeing to abide by the acknowledgments section of the [UNAVCO Data Policy](#).

Data Type Download Option	Estimated File Count	Estimated File Size	Start Time	End Time	Choose Option
RINEX Data					
<div>All RINEX Data</div> <div>Individual File Links (hatanaka_obs_nav_qc)</div>	4649	~4649MB	2007-11-16	2023-04-23	<div>Bundle Data</div>
<div>Time-Windowed RINEX Data</div>	361	~361MB	2015-01-01	2015-12-31	<div>Bundle Data</div>
<div>Latest RINEX Data File</div>	1	~1MB		2023 Apr 23 23:59:30	<div>Download</div>

Figure 3.1 UNAVCO Data Download center

RINEX observation files downloaded from UNAVCO were compressed in Hatanaka(.d) that tends to minimize storage capacity of observation files (.yyo) for the web transmission to local users. The data format RINEX observation, meteorological and navigation files were

xxxxdds.yy.d.z, xxxdds.yy.m.z and xxxdds.yy.n.z respectively in which xxxx is station marker name, ddd is day of year, s is session, yy are last two digits of year, d,n,m are file types.

3.2.3 Precise ephemeris and precise clock files.

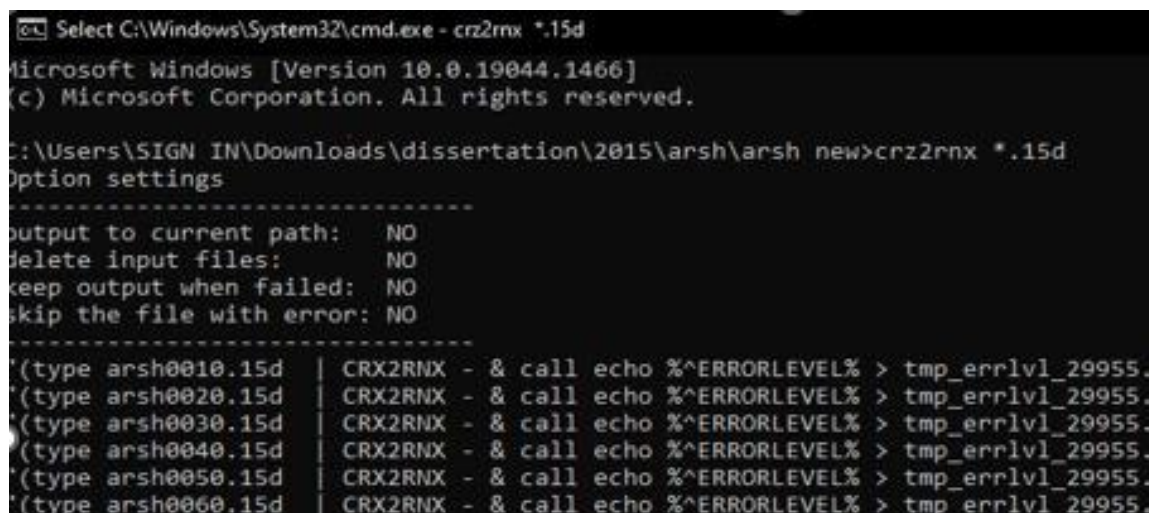
The final satellite position files (precise ephemeris) in sp3 format and precise clock files in clk format were downloaded from data archives covering the interval specified above by corresponding the GPS week and day and so these data were from GPS. The precise ephemeris files were downloaded using get_orb command with help of GAMIT/GLOBK software from data archives of cddis and corresponding clock files were downloaded through file transfer protocol (ftp) from cddis with the link <ftp://cddis.gsfc.nasa.gov/pub/gps/products/>. The downloaded precise ephemeris and clock files were in cccwwwd.sp3.z and cccwwwd.clk.z respectively in which ccc- three letter ID for the center which generated the file www- four digits GPS week d- single digit day of week 0=Sunday, 1=Monday...6 sp3/clk-file type.

3.3 Data preparation & Quality check.

The acquired data were prepared so as to meet requirements of specific tasks in need to accomplish this research objective. Data were manipulated in terms of changing their file type (extension), arranging them and extracting them from different formats so as they can be read by software under research.

3.3.1 RINEX observation files.

Observation files of all stations were acquired in compressed and crinexed format (xxxxdds.yy.d.z). The data were first uncompressed using windows winRAR app to remove .z and then the hatanaked file (xxxxdds.yy.d) was uncrinexed to get xxxdds.yyo observation files by using CRX2RNX_4.08 app in windows command line in Figure 3.2



```

C:\Windows\System32\cmd.exe - crx2rnrx *.15d
Microsoft Windows [Version 10.0.19044.1466]
(c) Microsoft Corporation. All rights reserved.

C:\Users\SIGN IN\Downloads\dissertation\2015\arsh\arsh new>crx2rnrx *.15d
Option settings
-----
output to current path: NO
delete input files: NO
keep output when failed: NO
skip the file with error: NO
-----
(type arsh0010.15d | CRX2RNX - & call echo %^ERRORLEVEL% > tmp_errlvl_29955.
(type arsh0020.15d | CRX2RNX - & call echo %^ERRORLEVEL% > tmp_errlvl_29955.
(type arsh0030.15d | CRX2RNX - & call echo %^ERRORLEVEL% > tmp_errlvl_29955.
(type arsh0040.15d | CRX2RNX - & call echo %^ERRORLEVEL% > tmp_errlvl_29955.
(type arsh0050.15d | CRX2RNX - & call echo %^ERRORLEVEL% > tmp_errlvl_29955.
(type arsh0060.15d | CRX2RNX - & call echo %^ERRORLEVEL% > tmp_errlvl_29955.

```

Figure 3.2 Extraction of Observation files from Crinex to Rinex

3.3.2 RINEX meteorological file

The RINEX meteorological files were first uncompressed using windows WinRAR app to get its uncompressed file (xxxxddd.yym) so as it can be read by GAMIT/GLOBK software.

3.3.3 Preparation of atmospheric reanalysis datasets.

The reanalysis datasets (ERA-5, ERA-Interim, NASA-MERRA2, JRA-55, NCEP, and NCEP2) were obtained in the Network Common Data Format (NetCDF) due to its convenient storage capabilities for information such as latitude, longitude, time, and scientific measurements. While all reanalysis datasets were downloaded with a one-year coverage as a single file, the NASA MERRA2 data was downloaded daily throughout the entire year as separate slices. As a result, it was necessary to consolidate all the data from the separate slices into a single year to properly extract the required information. To accomplish this, a Python script was used to merge all the relevant datasets into a single file. Presented on Appendix 4.

3.4 Data processing

After preparing all necessary data for processing and arranging them in respective folders for each year (rinex, brdc, gsoln, igs and meteofiles) the data were subjected to GAMIT/GLOBK processing. GAMIT/GLOBK is a comprehensive GPS analysis package developed at MIT, the Harvard Smithsonian Centre for Astrophysics (CfA), Scripps Institution of Oceanography (SIO), and Australian National University for estimating station coordinates and velocities, stochastic or functional representations of post-seismic deformation, atmospheric delays, satellite orbits, and Earth orientation parameters (Herring *et al.*, 2015). The reanalysis data processing was based on extracting information depending on geographical location of GPS stations (ARSH, DODM, MTVE).

3.4.1 Extraction PW/IWV from Reanalysis datasets

The ArcGIS software was used to read and extract information based on the geographic position of the experiment GPS stations ARSH, DODM and MTVE. Data selection was considered based on a weighted distance from GPS station site to corner points of gridded reanalysis data. The following are the procedures used to extract measurement from reanalysis datasets.

- i. Identification of specific geographical locations of points of interest for which data should be extracted. Table 3.4 shows the coordinates for all three GPS stations.

Table 3.4 Geographical position of GPS stations

Station ID	Longitude °	Latitude °	Location
ARSH	36.698	-3.387	Arusha
DODM	35.748	-6.187	Dodoma
MTVE	40.166	-10.26	Mtwara

- ii. From ArcGIS tool (make NetCDF table view tool) used to extract reanalysis data by selecting a desired variable, time and location in which filters the information based on user input criteria.
- iii. The extracted data were obtained in the form of a table that was composed with time and values of required information and also data can be visualized in a graph of time series. Figure 3.3 shows the plot of the time series.

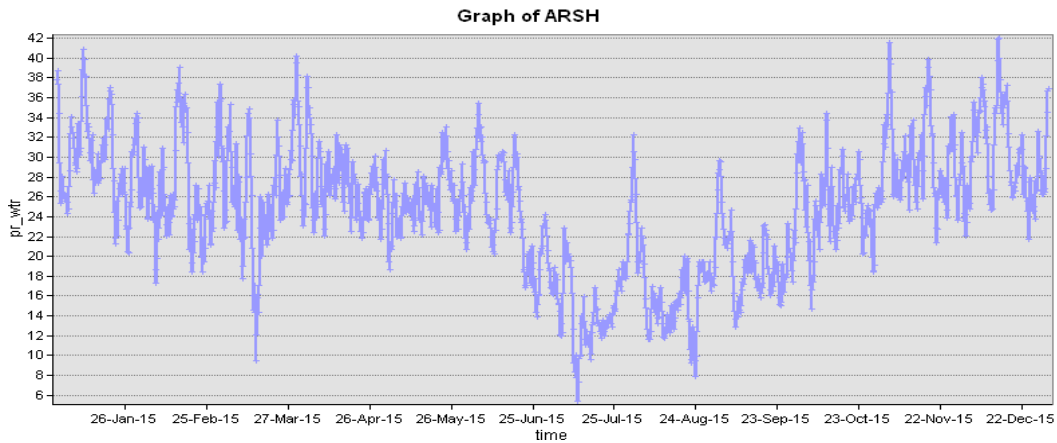


Figure 3.3 Time series of ARSH-pw from reanalysis

- iv. Also, all data from a table were able to be exported in CSV format for further analysis and integration with other tools and software.

3.4.1 Determining PW/IWV from GAMIT/GLOBK

The data from GPS stations (ARSH, DODM and MTVE) is required to process and provide integrated precipitate water vapour (PWV) for each station. For that GAMIT software was used for processing, in order to obtain the results of data the following procedures required to be accomplished.

3.4.1.1 Creating working directory

Since the data processed include one year then one top directory was set up for year 2015. In figure 3.4 shows the year directory, three directories were set up where the data for processing were inputted which were rinex, meteofiles, and brdc.

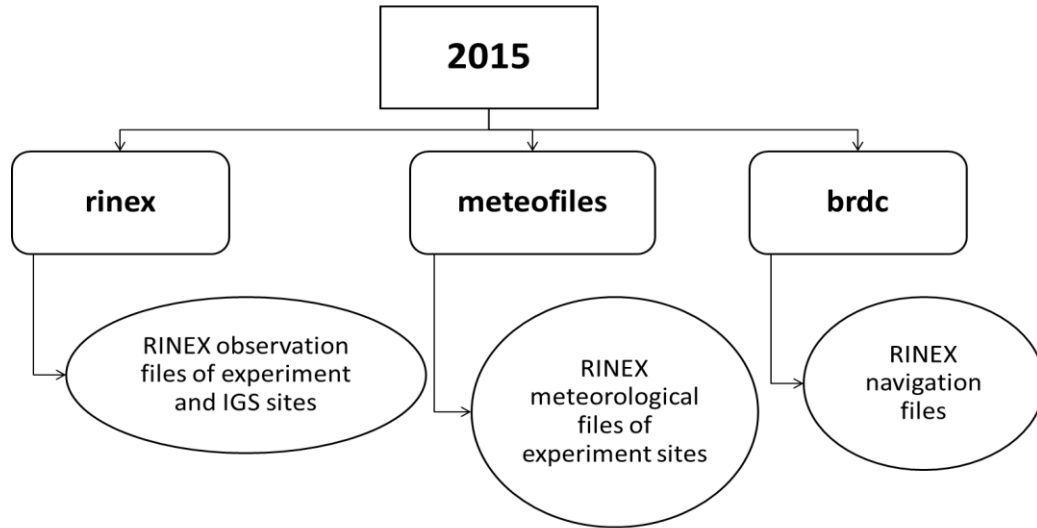


Figure 3.4 Workflow for processing GNSS Data by using GAMIT/GLOBK Software

3.5.2.1 Creation of tables

The GAMIT tables directory was set up on the year directory runned by `2015> sh_setup -yr. 2015`. This copies the default tables/ folder from `~/gg/` for gamit to get started. All the setup and metadata information for the year 2015 goes here. The created tables directory contained several files with different station information including `lfile.`, `lfile.old`, `igs14_comb.apr`, `station.info` and other files (Ayubu, 2020).

3.5.2.2 Updating site information on station.info file

The information on different sites was updated to `station.info` file. First the global sites from `lfile.` were updated using the command and then in the table's directory, `station.info` file was updated for sites from MIT using `sh_upd_stnfo -l sd` command and the output was `station.info.new` file. The output file was renamed from `station.info.new` to `station.info` and then the `station.info` file was updated using experiment and IGS sites from `rinex` directory using a command `sh_upd_stnfo -files ../rinex/*.yyo` which extracts information from the RINEX header for each site in each year.

3.5.2.3 Running sh_gamit to get O-files

With tables already created and updated, the tool `sh_gamit` which comprises of several GAMIT processes to create daily constrained and loosely estimates were run at year level directory. The syntax of the command was as follows

sh_gamit -expt test -d [yyyy] [ddd] -pres ELEV -orbit IGSF -copt x k p -dopt c ao in which the experiment name was set as *test* with an orbit file used as IGS final orbit. The command executed in each day following the below described steps.

- i) Assign parameters of program flow, giving precedence first to the command-line arguments, then to the parameters set in process. Defaults and sites. defaults, and then to default assignments within *sh_gamit* itself.
- ii) Create the day-directory and/or standard directories which do not yet exist
- iii) Link into the day directory the standard tables sing script links. Day and the RINEX files that contain data at 24hrs interval
- iv) Run *makexp* to create the input files for *makex* (*scal.makex.batch*) and *fixdrv*
- v) Run *sh_check_sess* to make sure that all of the satellites included in the RINEX obs files are present in the nav file and in the g-file (created previously at MIT from an IGS sp3 file)
- vi) Run *sh_makej* to create a j-file of satellite clock estimates from the sp3 file.
- vii) Run *makex* to create x-files (observations) and k-files (receiver clock estimates) using phase and pseudorange data from RINEX obs, nav and j-file.
- viii) Run *fixdrv* to create the batch file for GAMIT processing
- ix) Execute the batch run to generate a tabular orbital ephemeris (*arc*), model the phase observations (*model*), edit the data (*autcln*), and estimate parameters (*solve*) and save the cleaning summary.
- x) Create sky plots of phase residuals and plots of phase vs elevation angle using the DPH files written by *autcln*.
- xi) Invoke *sh_cleanup* to delete or compress files as specified by *-dopt* and *-copt*.

With this sequence of operation, a lot of outputs were produced and the output o-file was of interest for this research. The o-file is an output from *solve run* which is a summary of q-file (output of *solve*) which contains necessary information which are inputs to utility *sh_metutil*. It contains the parameters of the piecewise-linear model estimated from the data, which *metutil* will interpolate to obtain ZTD (Herring *et al.*, 2015). In this computation, the software used SAAS model to get nominal value of both wet and dry delay and the mapping function employed was Global Mapping Function (GMF) (Herring *et al.*, 2015).

3.5.2.4 Running the utility sh_metutil

After getting the outputs from sh_gamit, the o-files, o[expt]a.ddd were copied to the meteofiles directory which also had RINEX met files, xxxxxxxx.ymm. The utility sh_metutil was then run in which the inputs were the o-files o[expt]a.ddd and RINEX met files so as to produce the output files in format *met_[site].[yyddd]* and logs for each output in format *metutil.o[expt]a.ddd*. The output had results after every 7200 sec with scale of 1.0 and then other outputs from sh_gamit were removed so as to optimize disk space for more processing of other days. The sh_metutil function was required to be repeated for each day for the whole year and so 3 scripts were prepared covering all 365 days in which to create a repetition of such processes for all days. The output files contained ZTD, ZHD, ZWD and PW together with their uncertainties and so the macro 'pwgamit' was recorded to get weighted mean of daily PW values for each day after renaming all outputs from *met_[site].[yyddd]* to site *met_[site].[yyddd].csv* to get excel files.

CHAPTER FOUR

RESULTS, ANALYSIS AND DISCUSSION

In this chapter, the results from different processes such as time series, mean bias, root mean squared deviation (RMSD) and Pearson coefficient correlation analysis were discussed based on the needs of this research. The discussion was centered on comparison of integrated precipitate water vapour from Arusha (ARSH), Dodoma (DODM) and Mtwara (MTVE) as (GPS-pw) against Reanalysis products ERA-5, ERA-Interim, NASA MERRA2, JRA-55, NCEP and NCEP2 as (RA-pw) in which the expected is determine a best fits Reanalysis product.

4.1 Time series analysis of GPS-pw

From the continuous observing stations ARSH, DODM and MTVE, the precipitate water vapour was obtained and plotted into time series. The GPS-pw Figure 4.1 was plotted against time from 1st January/2015 to 31th/December/2015.

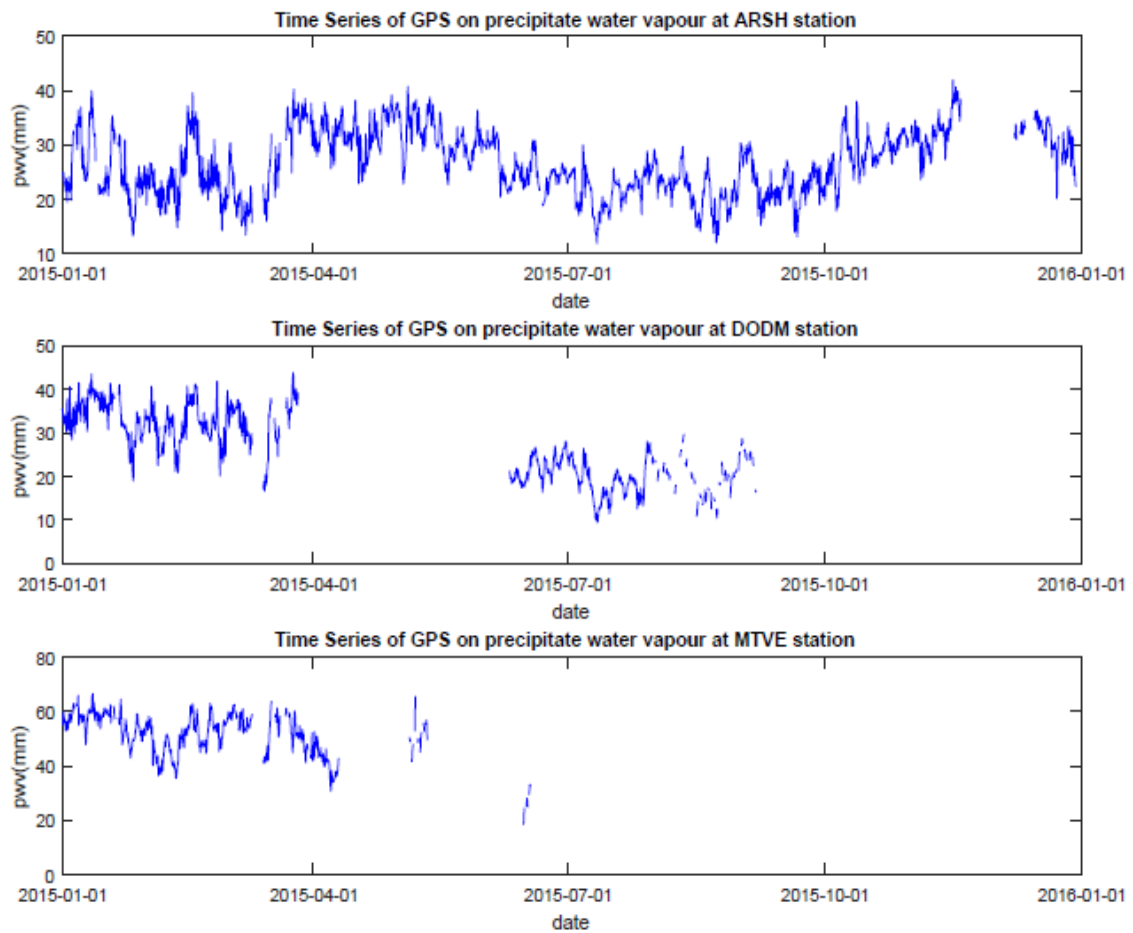


Figure 4.1 Time series plots of GPS-pw for ARSH, DODM, and MTVE stations.

The time series plot Figure 4.1 depicts the overall daily measurement of precipitable water (PW) across all stations: ARSH, DODM, and MTVE. However, several irregularities and breaks were observed in the plot. These anomalies can be attributed to missing navigation data and meteorological data caused by maintenance and hardware changes in GPS devices and meteorological instruments, resulting in gaps in the time series plots. Specifically, the ARSH-pw exhibits a small missing window of data from 19th November to 8th December 2015. On the other hand, DODM-pw shows larger missing windows from 26th March to 10th June 2015, as well as from 9th September to December 2015. Moreover, MTVE-pw displays significant missing windows from 10th April to 5th May, 11th May to 15th June, and 17th June to 31st December 2015. Due to these extensive data gaps, it becomes challenging to construct yearly time series plots and assess the overall accuracy of reanalysis products across all seasons throughout the year, particularly at DODM and MTVE stations.

4.2 Time series analysis of RA-pw

The time series plots of precipitable water vapor (PW) Figure 4.2 were generated for all six reanalysis-PW datasets extracted from the ARSH, DODM, and MTVE GPS stations. These plots encompassed the period from January 1, 2015, to December 31, 2015, allowing for an examination and visualization of the overall similarities and differences in trends, based on the geographical positions of the experimental stations.

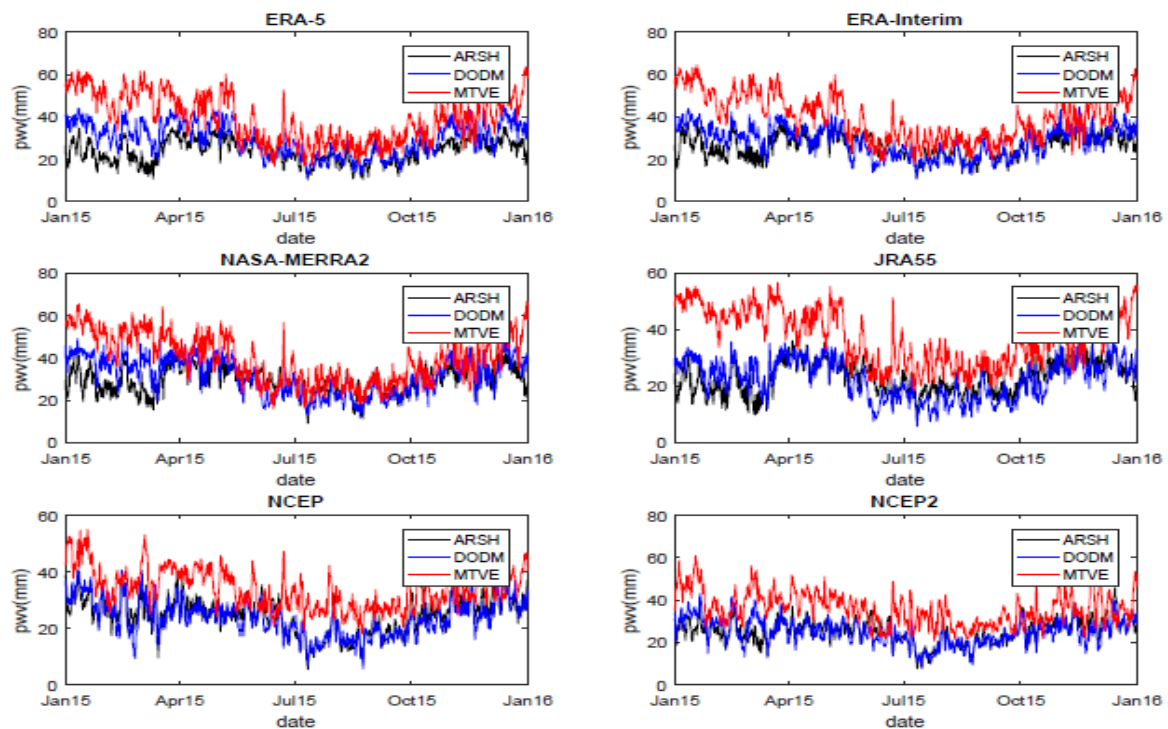


Figure 4.2 The time series of RA-pw from all GPS stations

Figure 4.2 provides, the overall trends of precipitation water (PW) exhibit smaller values between June and November, followed by relatively larger values from November to May across all stations. Despite some variations in the trends, Mtwara consistently displays higher values compared to the other stations, Arusha and Dodoma. These trends align with the weather pattern observed in Mtwara, a coastal region characterized by a relatively long wet season spanning from November to June.

4.3 Mean Bias, Root mean square (RMSD) and Correlation (r) Statistics analysis.

The mean bias, root mean square and correlation statistics analysis were conducted to quantitatively assess the agreement between the global atmospheric reanalysis products and GPS water vapour measurements. The following analysis was based on all GPS stations from Arusha, Dodoma and Mtwara examining the tendency of mean bias, root mean square deviation (RMSD) and Pearson correlation coefficient (r).

4.3.1 Arusha Statistics analysis

Based on ARSH station a comparison on descriptive statistics of GPS-pw and RA-pw was performed and the differences between them are shown in Table 4.2.

Table 4.1 Descriptives statistics based on ARSH station

	GPS	NCEP	NCEP2	JRA-55	Merra2	ERA-Interim	ERA5
Mean(mm)	26.588	24.758	25.172	23.129	29.490	26.605	23.895
Standard deviation(mm)	5.865	6.452	5.596	5.567	6.430	5.536	5.310
Max_value(mm)	41.930	42.000	45.700	36.197	45.955	44.328	36.742
Min_value(mm)	11.930	5.400	7.500	8.475	9.064	10.684	10.141
Median(mm)	26.025	25.300	25.450	23.103	29.292	26.500	23.968

Table 4.2 Difference in descriptive statistics between GPS-pw and RA-pw

	Δ NCEP	Δ NCEP2	Δ JRA-55	Δ Merra2	Δ ERA-Interim	Δ ERA5
Mean(mm)	1.830	1.416	3.459	-2.902	-0.017	-2.693
Standard deviation(mm)	-0.586	0.270	0.299	-0.565	0.330	0.555
Max_value(mm)	-0.070	-3.770	5.733	-4.025	-2.398	5.188
Min_value(mm)	6.530	4.430	3.455	2.866	1.246	1.789
Median(mm)	0.725	0.575	2.922	-3.267	-0.475	2.057

4.3.1.1 Mean Bias, Root mean square (RMSD) for ARSH station

The statistical analysis was performed to assess the agreement between the global atmospheric reanalysis products (ERA-5, ERA-interim, NASA-MERRA 2, JRA-55, NCEP1, and NCEP2) and the GPS water vapor measurements. Mean bias and root mean square error (RMSD) were used as the statistical metrics for the analysis. The mean bias measures the average systematic difference between the reanalysis products and GPS measurements. After removing missing values, the mean bias results showed that ERA-5, ERA-interim, JRA-55, NCEP1, and NCEP2 showed a negative bias of -2.9536mm, -0.30858mm, -3.7508mm, -2.3057mm and -1.7231mm, respectively, indicating an underestimation. NASA-MERRA 2 showed positive bias of. 2.6633mm indicating an overestimation. ERA-interim showed nearly mean biases close to zero of -0.30858mm. Regarding RMSD, ERA-interim had the lowest value of 2.9294mm, indicating a relatively tight agreement with GPS measurements. ERA-5 and NASSA-MERRA2 showed slightly higher RMSD values of 3.7216mm and 3.9918mm, respectively, suggesting a slightly larger dispersion of differences. JRA-55, NCEP1, and NCEP2 exhibited relatively higher RMSD values of 4.9668mm, 6.055mm, and 5.0721mm, respectively, indicating a larger scatter of differences. These statistical results provide insights into the agreement between the reanalysis products and GPS measurements, highlighting differences in bias and dispersion among the products. Table 4.3 and Figure 4.3 shows the Mean Biases and Root Mean Square (RMSD) of all reanalysis datasets from GPS

Table 4.3 Mean bias and Root mean squared deviation for ARSH station

Reanalysis products	Mean Bias (mm)	RMSD (mm)
ERA-5:	-2.954	3.722
ERA-interim:	-0.309	2.929
NASA-MERRA2	2.663	3.992
JRA-55:	-3.751	4.967
NCEP1:	-2.306	6.055
NCEP2:	-1.723	5.072

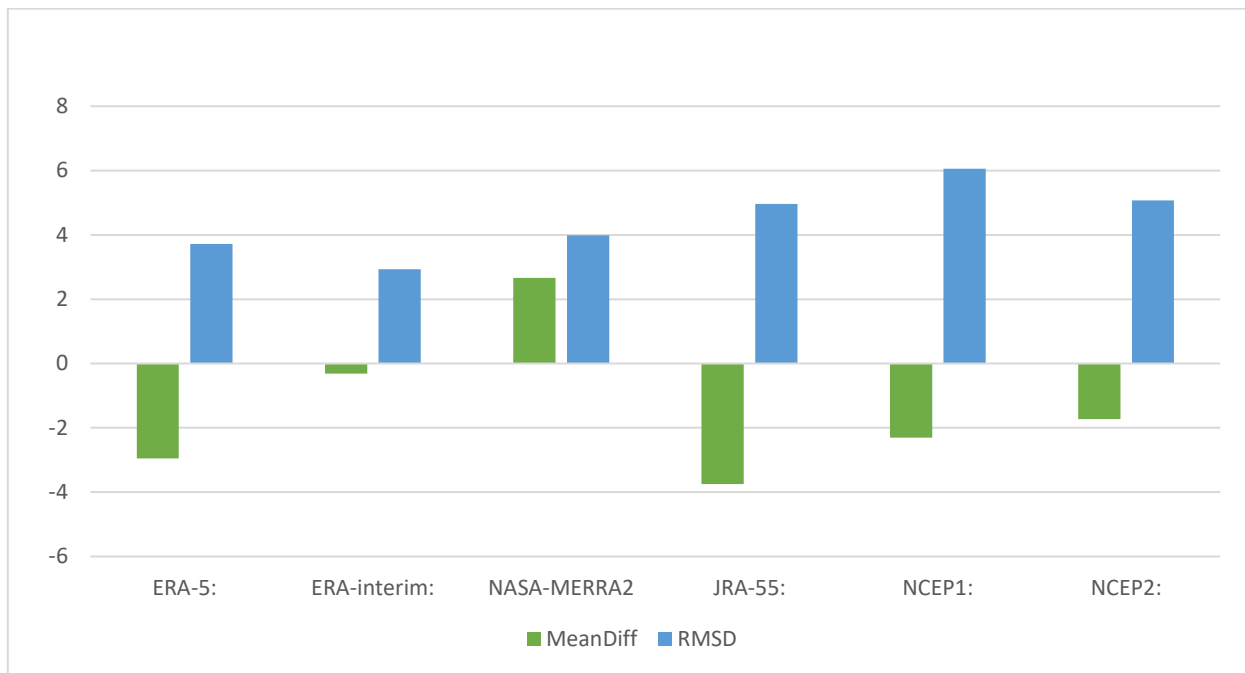


Figure 4.3 the graph shows the difference between GPS-pw and RA-pw in mean bias and RMSD of ARSH stations.

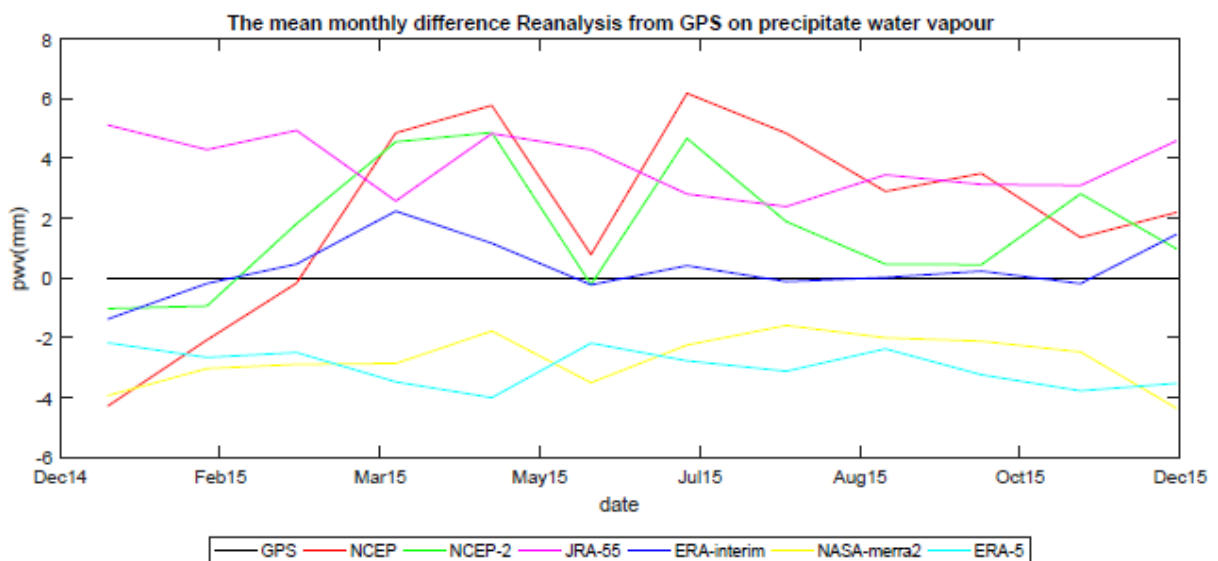


Figure 4.4 the difference between GPS-pw and RA-pw against time of ARSH station

Figure 4.4 illustrates the time series plot of ARSH station for all reanalysis products, highlighting the bias between RA-pw and GPS-pw for each monthly mean measurement of precipitable water vapor. Among these reanalysis products, ERA-5 demonstrates a relatively superior fit to the straight-line GPS-pw data, particularly during the summer season (June - November). Conversely, JRA-55, NCEP, and NCEP2 consistently deviate from the straight-line GPS-pw data across all seasons throughout the year

4.3.1.2 Correlation analysis between GPS-pw and RA-pw for ARSH station

Correlation analysis between GPS-pw and RA-pw was conducted for ARSH station to determine the relationship between the reanalysis products (ERA-5, ERA-interim, NASA-MERRA 2, JRA-55, NCEP1, and NCEP2) and GPS water vapor measurements. This assessment utilized the Pearson correlation coefficient (Eq. 2.36) to determine the strength of the correlation in each dataset pair, as depicted in table 4:4. The results of the RA-PW against GPS-PW analysis revealed a strong positive correlation for all datasets, with ERA-5 exhibiting the highest correlation coefficient of 0.923, while NCEP displayed a lower correlation coefficient of 0.585. Figure 4.5 presents a bar chart illustrating the correlation between all reanalysis products and GPS water vapor measurements.

Table 4.4 Pearson correlation coefficient in all datasets of ARSH station

	GPS	NCEP	NCEP2	JRA55	ERA-Interim	NASA-MERRA2	ERA_5
GPS	1	0.585	0.65	0.838	0.871	0.887	0.923
NCEP	0.585	1	0.814	0.563	0.634	0.632	0.62
NCEP2	0.65	0.814	1	0.65	0.671	0.677	0.69
JRA55	0.838	0.563	0.65	1	0.832	0.844	0.856
ERA-Interim	0.871	0.634	0.671	0.832	1	0.877	0.899
NASAMERRA2	0.887	0.632	0.677	0.844	0.877	1	0.908
ERA_5	0.923	0.62	0.69	0.856	0.899	0.908	1

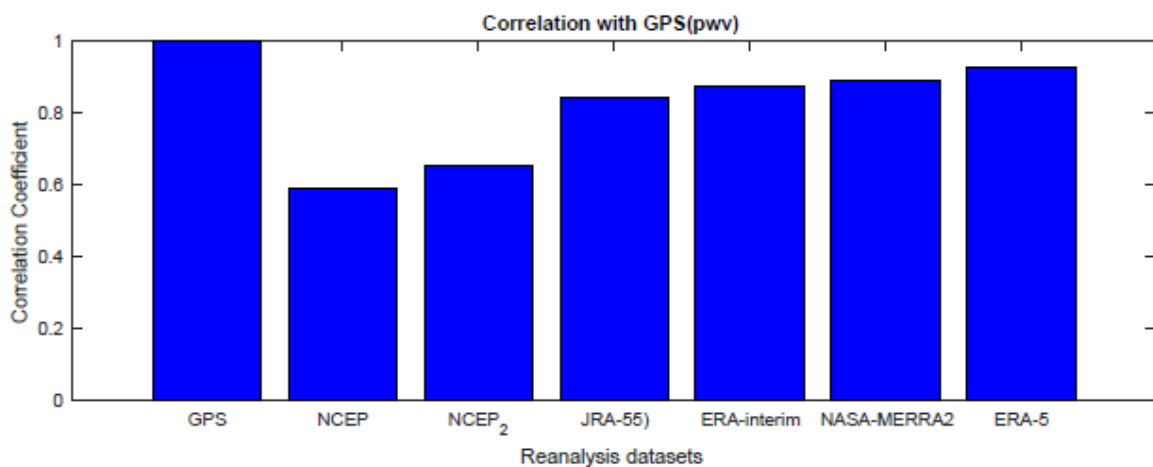


Figure 4.5 the graph shows a variation of Pearson correlation coefficient on all RA-pw against GPS-pw of ARSH station

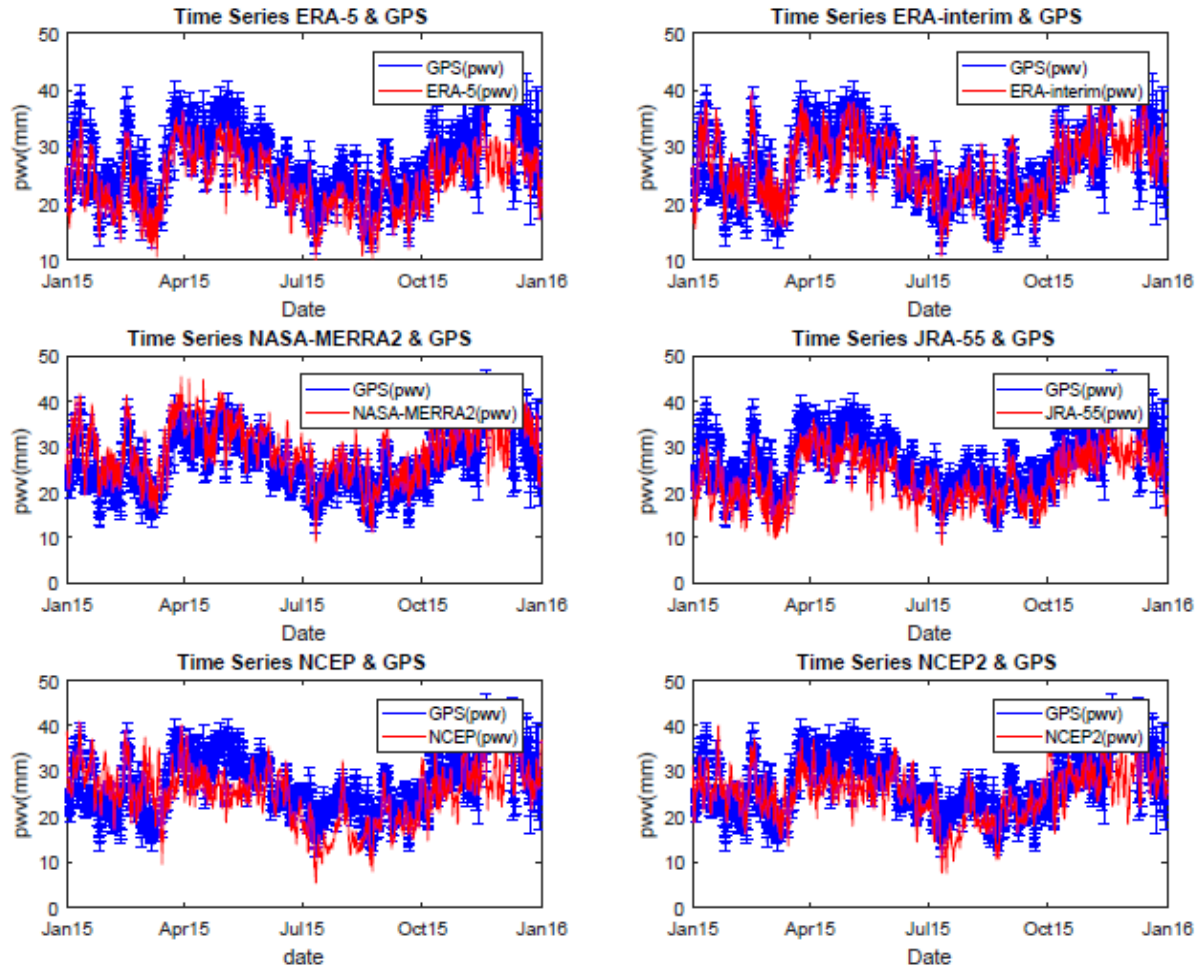


Figure 4.6 the time series plots of GPS-pw with error bars and RA-pw of ARSH station

The time series plots depicted in Figure 4.6 illustrate the variations in precipitation water vapor (PW) at Arusha station, encompassing both RA-PW and GPS-PW, along with their corresponding residuals for daily measurements. This visual representation effectively demonstrates the interplay of trends within tolerance intervals for each measurement, based on the data obtained from Arusha station.

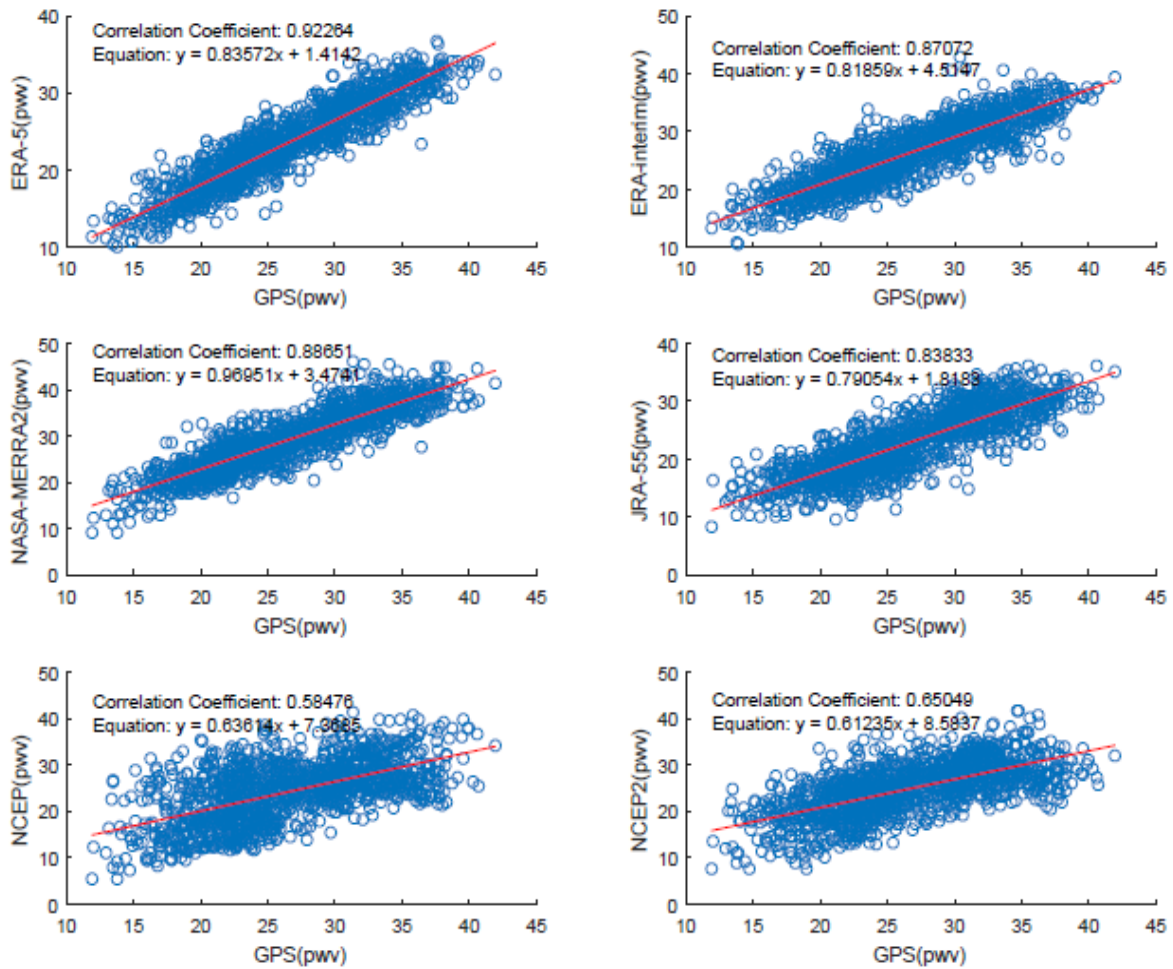


Figure 4.7 scatter plots of all RA-pw against GPS-pw of ARSH station

The scatter plots presented in Figure 4.7 depict the relationship between RA-pw and GPS-pw at Arusha station. By analyzing the overall pattern, direction, and strength of the relationship, it is evident that ERA-5, NASA-MERRA2, ERA-Interim, and JRA-55 exhibit a strong linear correlation, surpassing that of NCEP and NCEP2. The graph also includes a linear equation representing the best fit line.

4.3.2 Dodoma Statistics analysis

Based on DODM station a comparison on descriptive statistics of GPS-pw and RA-pw was performed and the differences between them are shown in Table 4.6.

Table 4.5 Descriptives statistics based of DODM station

	GPS	NCEP	NCEP2	JRA-55	Merra2	ERA-Interim	ERA5
Mean(mm)	26.450	23.679	24.810	22.384	31.477	28.279	29.546
Standard deviation(mm)	7.911	6.466	6.063	6.898	8.699	7.121	7.796

Max_value(mm)	43.810	40.600	43.100	37.404	50.569	44.695	45.885
Min_value(mm)	9.500	5.500	8.300	5.756	11.535	11.429	11.207
Median(mm)	25.650	23.700	24.700	22.908	32.328	28.982	29.526

Table 4.6 Difference in descriptive statistics between GPS-pw and RA-pw of DODM station

	Δ NCEP	Δ NCEP2	Δ JRA-55	Δ Merra2	Δ ERA-Interim	Δ ERA5
Mean(mm)	2.770	1.640	4.066	-5.027	-1.829	-3.096
Standard deviation(mm)	1.445	1.848	1.013	-0.788	0.790	0.115
Max_value(mm)	3.210	0.710	6.406	-6.759	-0.885	-2.075
Min_value(mm)	4.000	1.200	3.744	-2.035	-1.929	-1.707
Median(mm)	1.950	0.950	2.742	-6.678	-3.332	-3.876

4.3.2.1 Mean Bias, Root mean square (RMSD)

At DODM station the statistical analysis was performed after removing missing values, the mean bias results showed that JRA-55, NCEP1, and NCEP2 showed a negative bias indicating an underestimation. ERA-5, ERA-Interim, NASA-MERRA 2 showed positive bias indicating an overestimation. ERA-interim showed nearly mean biases close to zero of 0.80583mm. Regarding RMSD, ERA-5, ERA-interim had the lowest value indicating a relatively tight agreement with GPS measurements. NAS-MERRA 2, JRA-55, NCEP1, and NCEP2 exhibited relatively higher RMSD values indicating a larger scatter of differences. Table 4.7 and Figure 4.8 shows the Mean Biases, and Root Mean Square (RMSD) of all reanalysis datasets from GPS (PW).

Table 4.7 Mean bias and Root mean squared deviation of DODM station

Reanalysis products	Mean Bias (mm)	RSME (mm)
ERA-5	1.458	2.755
ERA-interim	0.806	2.852
NASA-MERRA2	3.835	5.104
JRA-55	-5.922	6.741
NCEP1	-3.605	6.279
NCEP2	-2.435	5.519

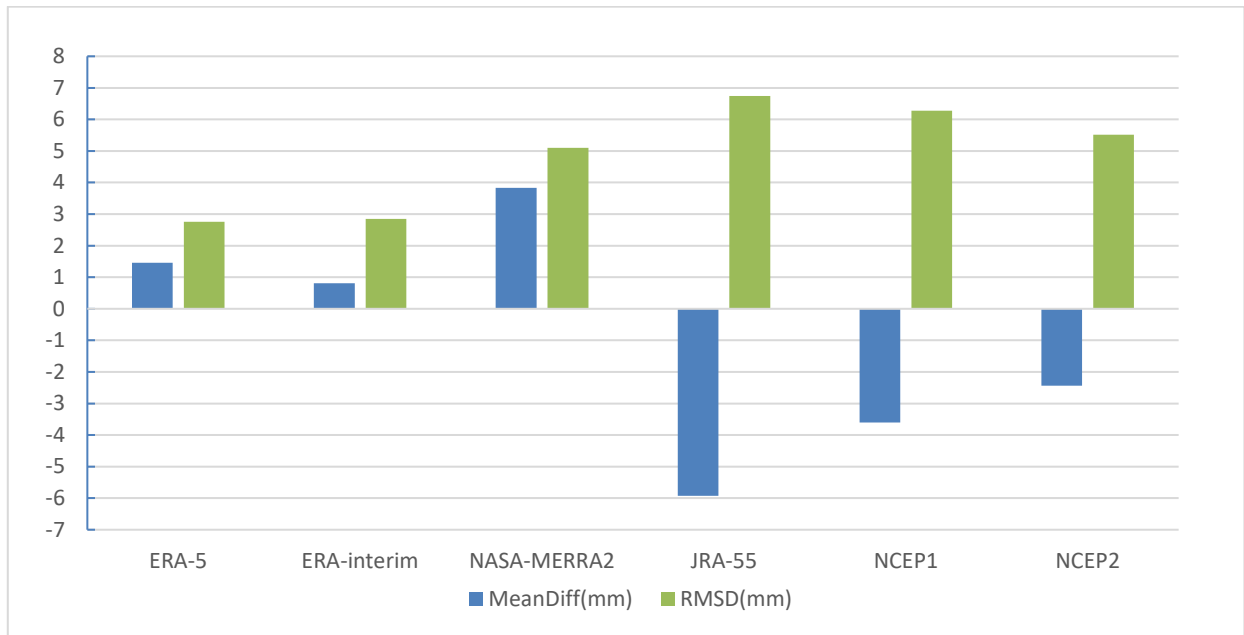


Figure 4.8 The graph shows the difference between GPS-pw and RA-pw in mean bias and RMSD of DODM stations.

4.3.2.2 Correlation analysis between GPS-pw and RA-pw for DODM station

Correlation analysis between GPS-pw and RA-pw was conducted for DODM station to determine the relationship between the reanalysis products (ERA-5, ERA-interim, NASA-MERRA 2, JRA-55, NCEP1, and NCEP2) and GPS water vapor measurements. This assessment utilized the Pearson correlation coefficient (Eq. 2.36) to determine the strength of the correlation in each dataset pair, as depicted in the table 4:8. The results of the RA-pw against GPS-pw analysis revealed a strong positive correlation for all datasets, with ERA-5 exhibiting the highest correlation coefficient of 0.957, while NCEP displayed a slightly lower correlation coefficient of 0.783. Figure 4.9 presents a bar chart illustrating the correlation between all reanalysis products and GPS water vapor measurements.

Table 4.8 Pearson correlation coefficient in all datasets of DODM station

	GPS	NCEP	NCEP2	JRA55	ERA-Interim	NASA-MERRA2	ERA_5
GPS	1	0.783	0.794	0.915	0.939	0.94	0.957
NCEP	0.783	1	0.899	0.79	0.82	0.789	0.802
NCEP2	0.794	0.899	1	0.806	0.806	0.796	0.813
JRA55	0.915	0.79	0.806	1	0.932	0.913	0.935
ERA-Interim	0.939	0.82	0.806	0.932	1	0.947	0.956

NASAMERRA2	0.94	0.789	0.796	0.913	0.947	1	0.952
ERA_5	0.957	0.802	0.813	0.935	0.956	0.952	1

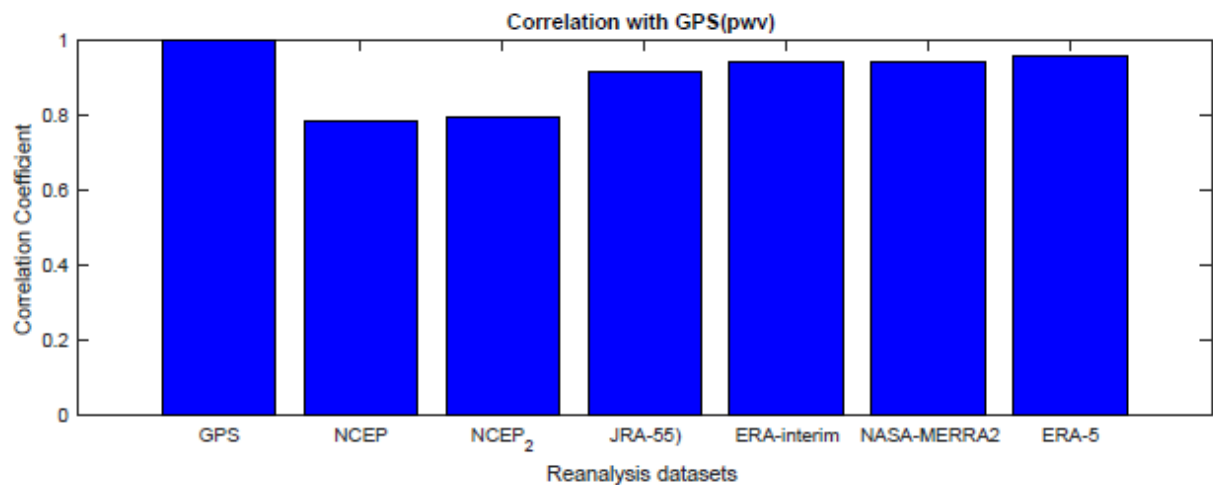


Figure 4.9 The graph shows a variation of pearson correlation coefficient on all RA-pw against GPS-pw of DODM station

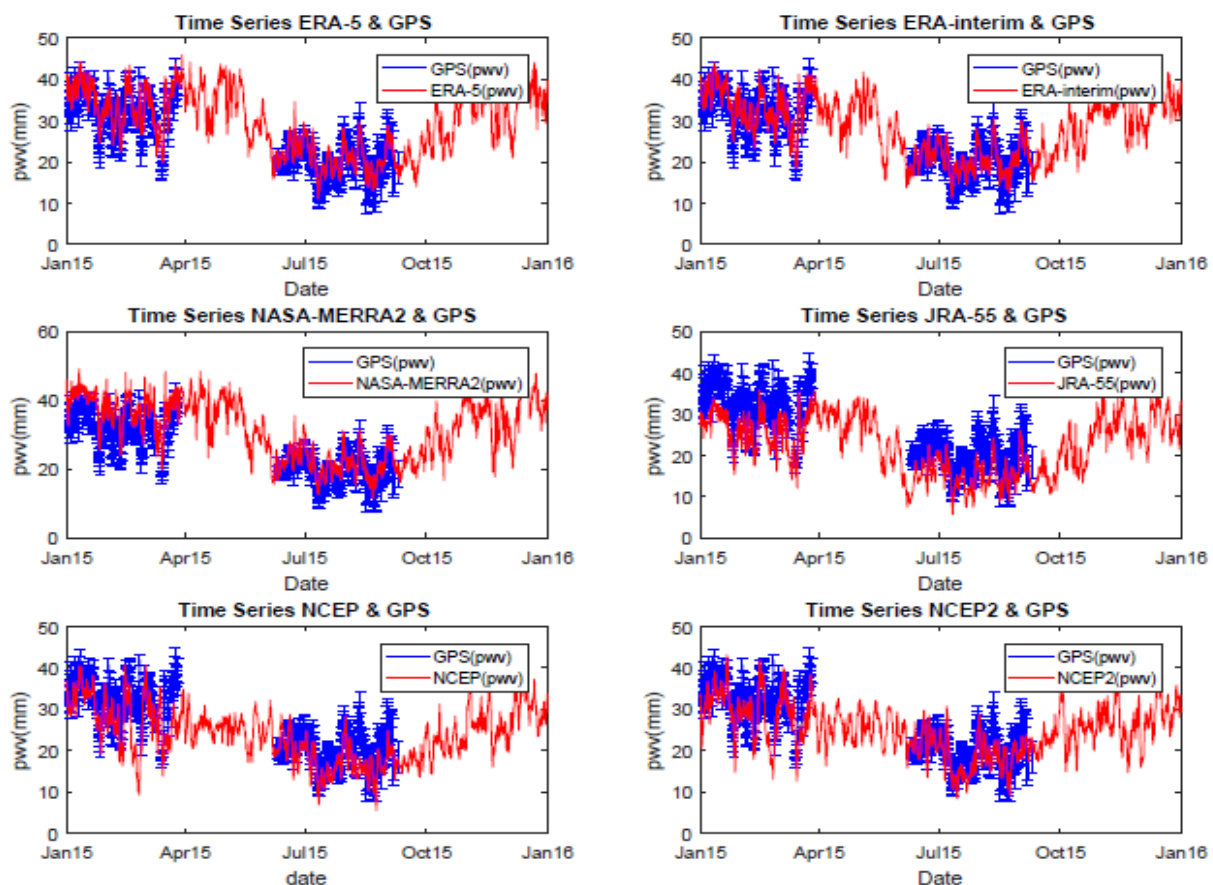


Figure 4.10 The time series plots of GPS-pw with error bars and RA-pw of DODM station

The time series plots depicted in Figure 4. 10 illustrate the variations in precipitation water vapor (PW) at Dodoma station, encompassing both RA-pw and GPS-pw, along with their

corresponding residuals for daily measurements. This visual representation effectively demonstrates the interplay of trends within tolerance intervals for each measurement, based on the data obtained from Dodoma station was only possible to analyze wet season from January to April and dry season June to September.

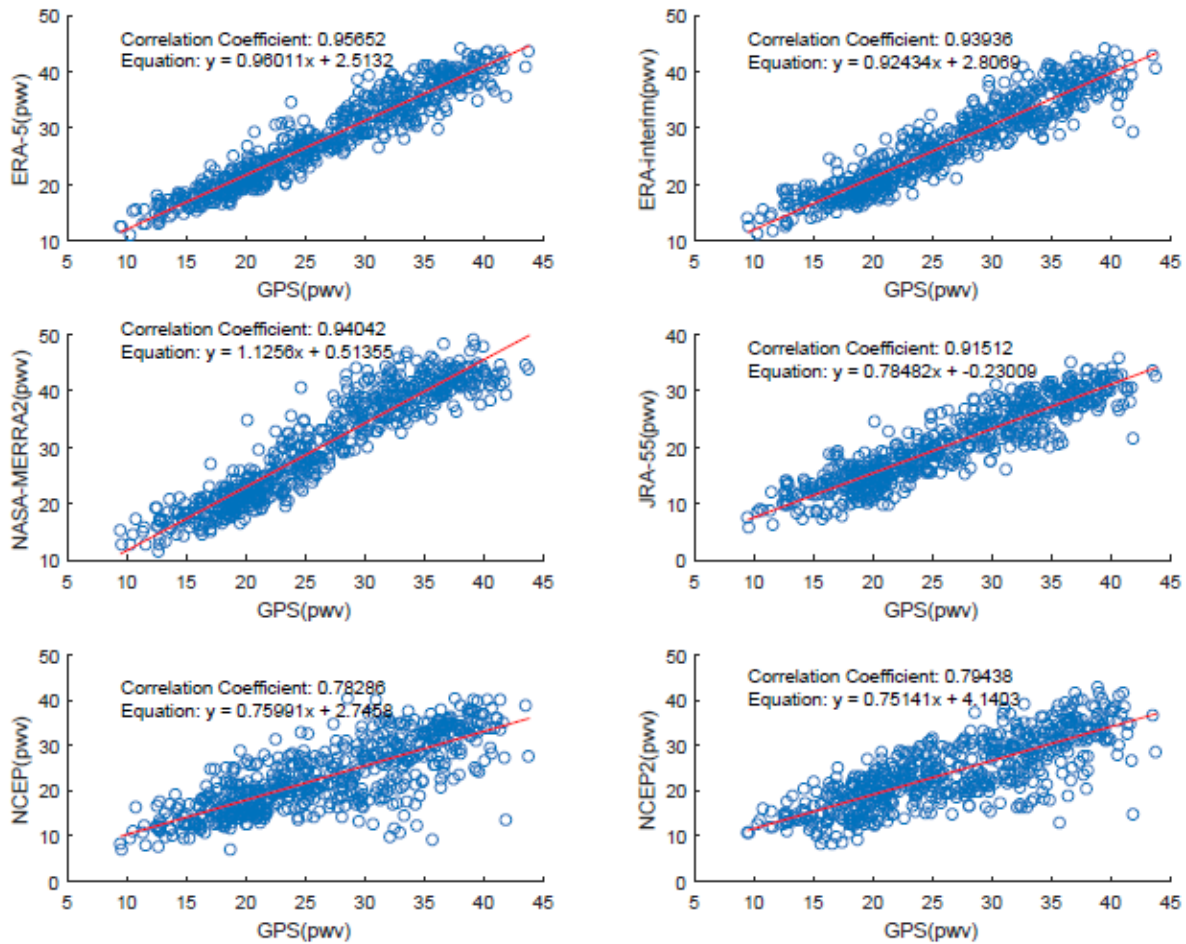


Figure 4.11 scatter plots of all RA-pw against GPS-pw of DODM station

The scatter plots presented in Figure 4.11 depict the relationship between RA-pw and GPS-pw at Dodoma station. By analyzing the overall pattern, direction, and strength of the relationship, it is evident that ERA-5, NASA-MERRA2, ERA-Interim, and JRA-55 exhibit a strong linear correlation, surpassing that of NCEP and NCEP2. The graph also includes a linear equation representing the best fit line.

4.3.3 Mtwara Statistics analysis

Based on MTVE station a comparison on descriptive statistics of GPS-pw and RA-pw was performed and the differences between them are shown in Table 4.10.

Table 4.9 Descriptives statistics based of MTVE station

	GPS	NCEP	NCEP2	JRA-55	Merra2	ERA-Interim	ERA5
Mean(mm)	51.399	34.024	35.769	37.756	39.849	39.903	39.650
Standard deviation(mm)	7.947	6.990	7.723	9.669	11.474	10.719	11.212
Max_value(mm)	66.400	55.000	60.900	56.711	66.672	64.482	63.686
Min_value(mm)	18.460	18.000	20.300	18.516	15.846	17.966	16.646
Median(mm)	52.785	33.500	35.100	38.006	38.848	39.543	39.285

Table 4.10 Difference in descriptive statistics between GPS-pw and RA-pw of MTVE station

	Δ NCEP	Δ NCEP2	Δ JRA-55	Δ Merra2	Δ ERA-Interim	Δ ERA5
Mean(mm)	17.375	15.630	13.643	11.550	11.496	11.750
Standard deviation(mm)	0.957	0.224	-1.722	-3.527	-2.772	-3.265
Max_value(mm)	11.400	5.500	9.689	-0.272	1.918	2.714
Min_value(mm)	0.460	-1.840	-0.056	2.614	0.494	1.814
Median(mm)	19.285	17.685	14.779	13.937	13.242	13.500

4.3.3.1 Mean Bias, Root mean square (RMSD)

At MTVE station the statistical analysis was performed after removing missing values, the mean bias results showed all Reanalysis products a negative bias indicating an underestimation. NASA MERRA 2 showed nearly small biases compare to others of -1.053mm. Considering RMSD, ERA-5, ERA-interim and NASA- MERRA 2 had similar lowest value indicating a relatively agreement with GPS measurements. JRA-55, shows intermediate value of 6.7424mm. NCEP1, and NCEP2 exhibited relatively higher RMSD values indicating a larger scatter of differences. Table 4.11 and Figure 4.12 shows the Mean Biases and Root Mean Square (RMSD) of all reanalysis datasets from GPS-pw.

Table 4.11 Mean bias and Root mean squared deviation of MTVE station

Reanalysis products	Mean Bias (mm)	RSMD (mm)
ERA-5	-1.776	3.330

ERA-interim	-1.629	3.568
NASA-MERRA 2	-1.053	3.791
JRA-55	-5.160	6.742
NCEP1	-12.153	13.855
NCEP2	-11.039	13.176

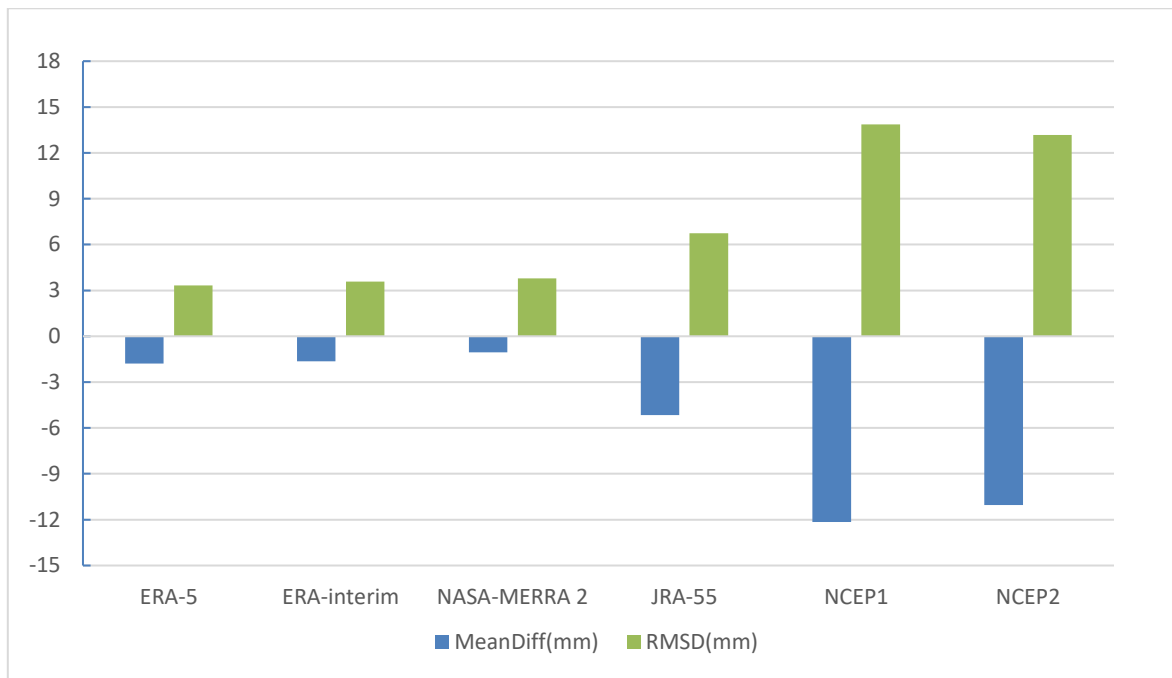


Figure 4.12 The graph shows the difference between GPS-pw and RA-pw in mean bias and RMSD of MTVE stations

4.3.3.2 Correlation analysis between GPS-pw and RA-pw for MTVE station

Correlation analysis between GPS-pw and RA-pw was conducted for MTVE station to determine the relationship between the reanalysis products (ERA-5, ERA-interim, NASA-MERRA 2, JRA-55, NCEP1, and NCEP2) and GPS water vapor measurements. This assessment utilized the Pearson correlation coefficient (Eq. 2.36) to determine the strength of the correlation in each dataset pair, as depicted in the table 4:12. The results of the RA-pw against GPS-pw analysis revealed a strong positive correlation for all datasets, with ERA-5 exhibiting the highest correlation coefficient of 0.935, while NCEP2 displayed a lower correlation coefficient of 0.573. Figure 4.13 presents a bar chart illustrating the correlation between all reanalysis products and GPS water vapor measurements.

Table 4.12 Pearson correlation coefficient in all datasets of DODM station

	GPS	NCEP	NCEP2	JRA55	ERA-Interim	NASA-MERRA2	ERA_5
GPS	1	0.591	0.573	0.847	0.918	0.893	0.935
NCEP	0.591	1	0.771	0.672	0.65	0.534	0.617
NCEP2	0.573	0.771	1	0.585	0.614	0.548	0.61
JRA55	0.847	0.672	0.585	1	0.872	0.842	0.867
ERA-Interim	0.918	0.65	0.614	0.872	1	0.905	0.937
NASAMERRA2	0.893	0.534	0.548	0.842	0.905	1	0.901
ERA_5	0.935	0.617	0.61	0.867	0.937	0.901	1

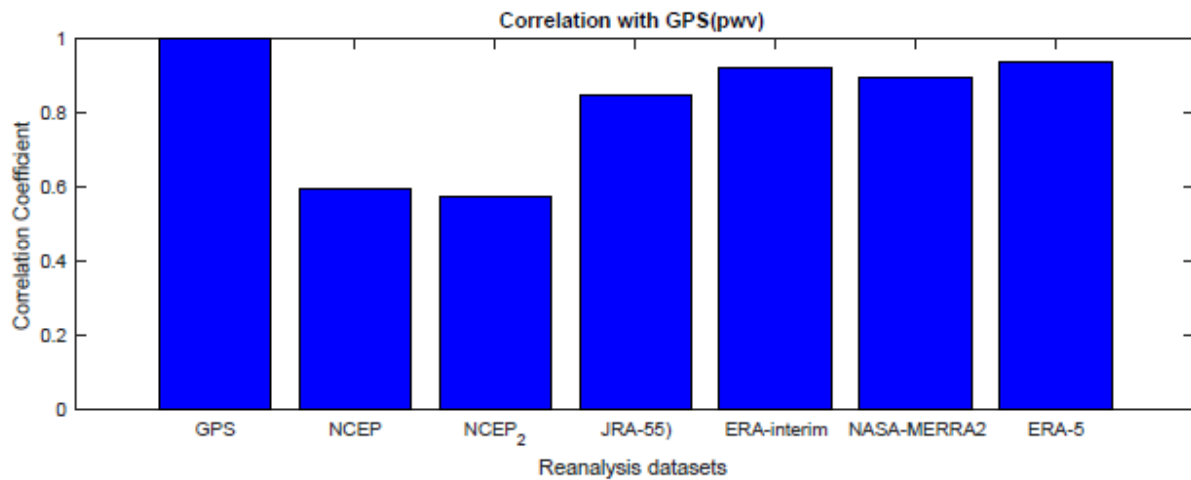


Figure 4.13 The graph shows a variation of pearson correlation coefficient on all RA-pw against GPS-pw of MTVE station

The time series plots in Figure 4.14 illustrate the variations in precipitation water vapor (PW) at Mtwara station, encompassing both RA-pw and GPS-pw, along with their corresponding residuals for daily measurements. This visual representation effectively demonstrates the interplay of trends within tolerance intervals for each measurement, based on the data obtained from Mtwara station was only possible to analyze only wet season from January to April.

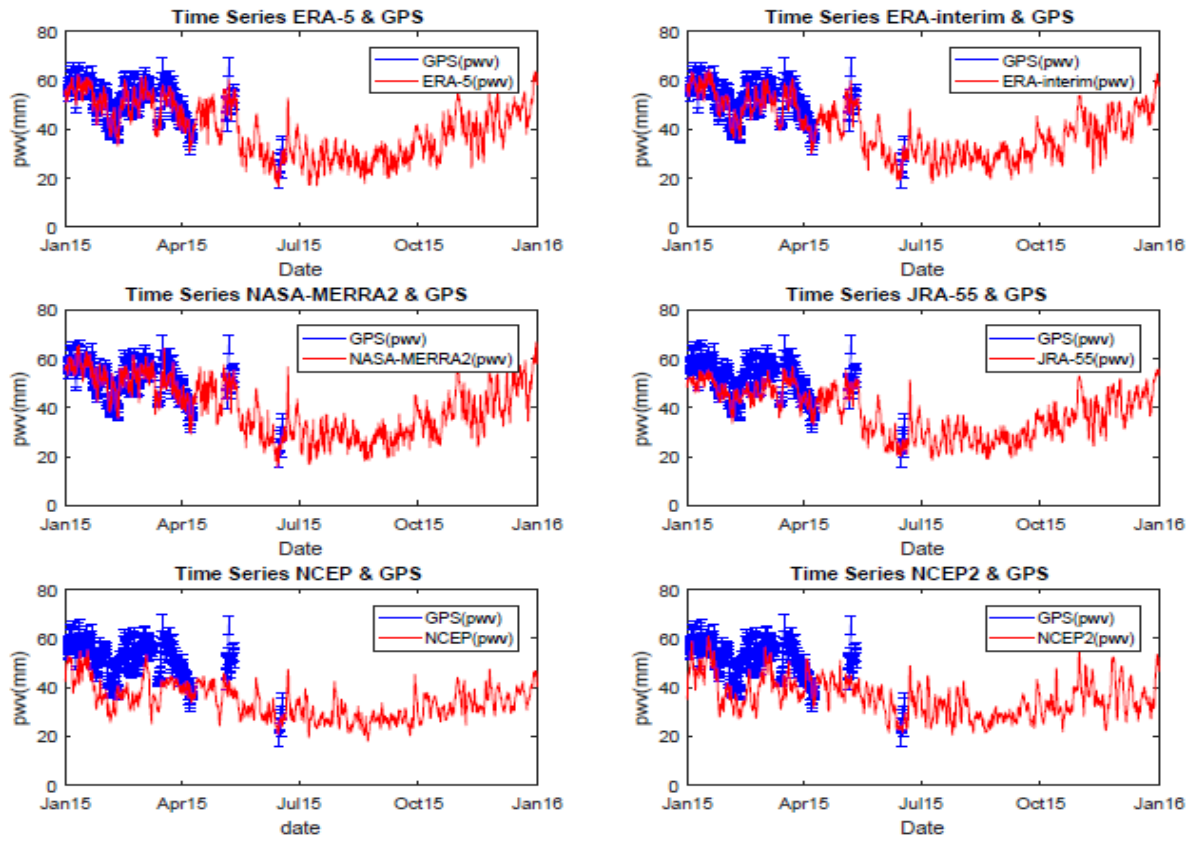


Figure 4.14 The time series plots of GPS-pw with error bars and RA-pw of MTVE station

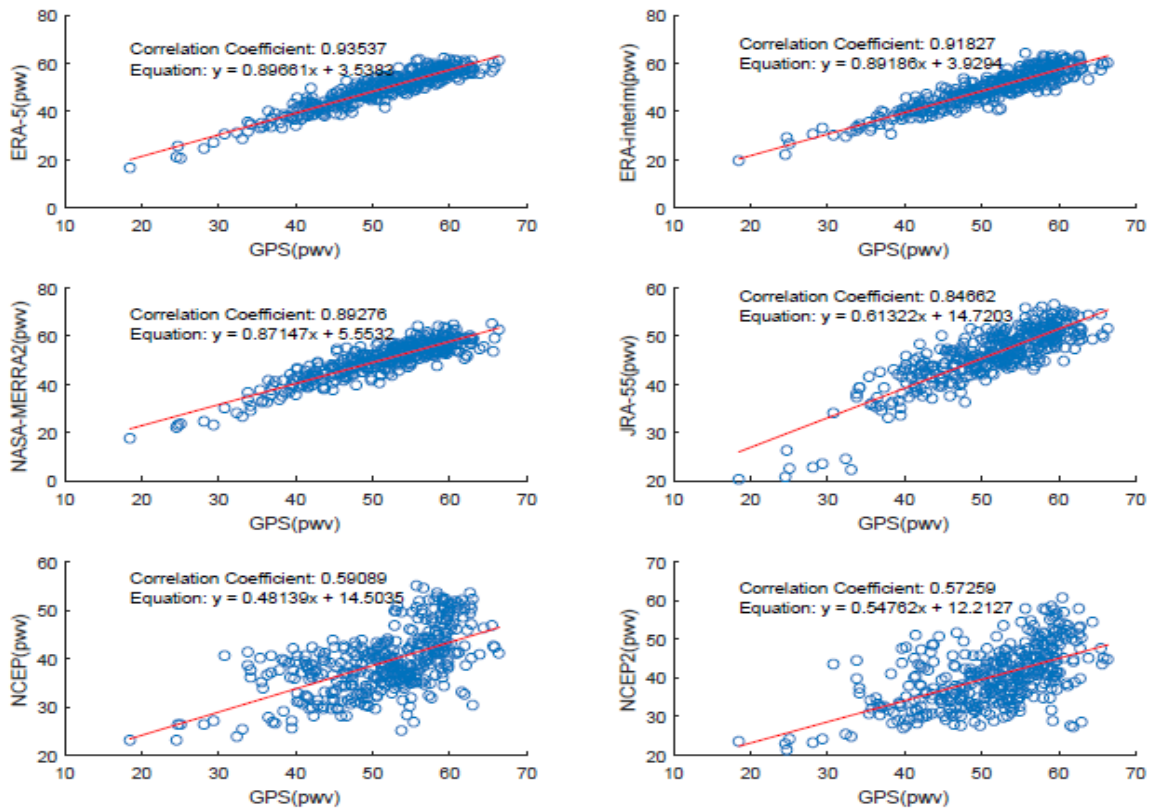


Figure 4.15 scatter plots of all RA-pw against GPS-pw of DODM station

The scatter plots presented in Figure 4.15 depict the relationship between RA-pw and GPS-pw at Mtwara station. By analyzing the overall pattern, direction, and strength of the relationship, it is evident that ERA-5, NASA-MERRA2, ERA-Interim, and JRA-55 exhibit a strong linear correlation, surpassing that of NCEP and NCEP2. The graph also includes a linear equation representing the best fit line.

4.4 Summary discussion of the results

In order to have an accurate and fair discussion of an overall result, all results from three GPS-stations were contributed in different percentages because of availability and successful outputs from PW computation. Figure 4.16 shows the distribution of total weights on results from the analysis in which it was based on numbers of observations from GPS stations. ARSH, DODM, and MTVE were 57%, 26% and 17% respectively.

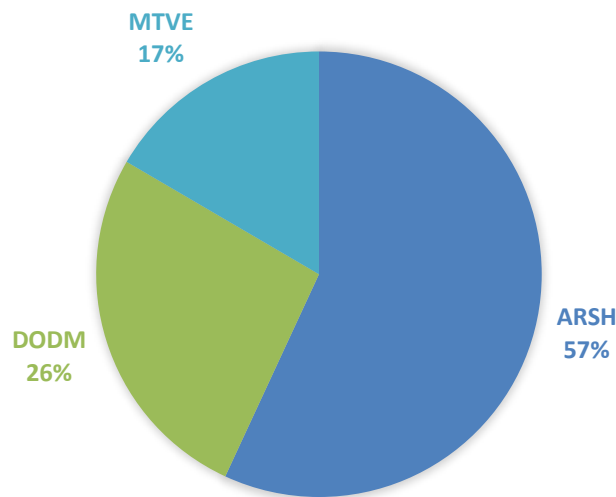


Figure 4.16 The pie chart shows the distribution of contribution of GPS station in data analysis and comparison.

Then all results from each GPS station were weighted to find the average of mean bias, root mean squared deviation (RMSD) and correlation coefficient(r) from ARSH, DODM and MTVE. Consider the Eq 4.1 below

$$\bar{x} = \frac{\sum_{i=1}^n x_i \cdot \omega_i}{\sum_{i=1}^n \omega_i} \dots \dots \dots \text{Eq 4.1}$$

Where \bar{x} is the weighted mean, x_i is results from each station and ω_i is the weight from each station.

Table 4.13 weighted average of mean bias, RSMD, and correlation from all GPS stations

REANALYSIS DATASET	Mean Bias (mm)	RSMD (mm)	Correlation coefficient (r)
ERA-5	-1.607	3.404	0.934
ERA-interim	-0.244	3.018	0.897
NASA-MERRA 2	2.336	4.247	0.902
JRA-55	-4.555	5.730	0.860
NCEP1	-4.318	7.439	0.674
NCEP2	-3.492	6.566	0.638
Overall average	-1.980	5.067	0.817

Generally, the overall results from all GPS-stations (ARSH, DODM and MTVE) showed that ERA-5 and ERA- interim from ECMWF have good results compared to other reanalysis. The ERA-5 had best correlation coefficient of 0.934 while NCEP2 had a worse correlation coefficient of 0.638. the results for mean bias and root mean squared deviation showed that ERA-interim had best results of -0.244mm and 3.018mm respectively while JRA-55 had worse mean bias of -4.555mm and NCEP1 had worse root mean squared deviation of 7.439mm. The overall average from all reanalysis datasets products (ERA-5, ERA-interim, NASA-MERRA 2, JRA-55, NCEP1, and NCEP2) showed a good statistical result in which mean bias, root mean squared deviation and correlation coefficient were -1.980mm, 5.067mm and 0.817 respectively.

CHAPTER FIVE

CONCLUSION AND RECOMMENDATION.

5.1 Conclusion.

The assessment of reanalysis datasets using atmospheric water vapour retrieved from GNSS signals in Tanzania was achieved. The evaluation of accuracy and performance of global reanalysis product was based in three different GPS stations ARSH, DODM and MTVE. With help from GNSS processing software (GAMIT/GLOBK) we were able to determine the GPS-pw which was used to examine the reanalysis datasets. The overall averaged results from all Global reanalysis datasets for weighted mean bias, weighted root mean squared deviation and weighted coefficient correlation computation obtained were -1.980mm, 5.067mm, and 0.817 respectively. The results have showed a good agreement with GPS-pw, for that reason global reanalysis datasets can be used by TMA for weather prediction and climate monitoring. Despite all of this reanalysis shows a good result but ERA-5 and ERA-interim from ECMWF showed a best result compared to others. Since ERA-interim is the predecessor of ERA-5 hence there was improvement that showed in correlation results 0.897 to 0.934. NASA-MERRA2 also had good results of 2.336mm, 4.247mm, and 0.902 while NCEP1 and NCEP2 showed a poor result compared to others. Overall, it can be concluded that the reanalysis successfully reproduces the spatiotemporal PW variability over Tanzania, as assessed with the GPS-pw dataset, with ERA5 slightly outperforming the other reanalysis over a period of one year.

5.2 Recommendations.

From the findings of this study, the following recommendations are given:

- i) Extending a similar approach from this research by dealing with more GNSS stations across Tanzania to get a more refined analysis on all zones of the country.
- ii) Designing a network of ground-based GPS stations across Tanzania basing on available stations and by considering the optimum separation between stations so as to fully suffice needs of meteorological applications such as weather tomography.
- iii) Determining and analyzing PW from non-meteorological GNSS sites by interpolating ground weather data from nearby weather stations and assessing them if they can be depended on.
- iv) Determining of PW from meteorological GNSS site from interpolated data from Reanalysis products and in-situ meteorological data and assess if they can be dependent.

REFERENCE

- Abraha, K. E., Lewi, E., Masson, F., & Boy, J. (2017). Spatial-temporal variations of water vapour content over Ethiopia: a study using GPS observations and the ECMWF model. *GPS solutions*.
- Alshawaf, F., Hinz, S., Mayer, M., & Meyer, F. J. (2015). Constructing accurate maps of atmospheric water vapour by combining interferometric synthetic aperture radar and GNSS observations. *Journal of Geophysical Research: Atmosphere* 120(4), 1391-1403.
- Alshawaf, K., Balidakis, G., Dick, S., & Heise, S. (2017). Estimating trends in atmospheric water vapour and temperature time series over Germany. *Atmospheric Measurement Techniques* 10(9), 3117-3132.
- Balasubramanian, A. (2016, February). Weather forecastin. Retrieved from <http://doi.org/10.4314/sajg.v6i3.13>
- Bennitt, G. V., & Jupp, A. (2012). Operational assimilation of GPS zenith total delay observations into the met office numerical weather prediction models. *Monthly Weather Review*, pp.2706-2719.
- Bevis, M., Businger, S., Herring, T. A., Rocken, C., Anthes, R. A., & Ware, R. H. (1992). GPS meteorology: Remote sensing of atmospheric water vapour using the Global Positioning System. *Journal of Geophysical Research: Atmosphere* 97(D14), pp. 379-386.
- Brenner, L. (2020). *sciencing.com*. Retrieved from Four Types of Forecasting. Sciencing: <http://sciencing.com/fourtypes-forecasting-8155139.html>
- Durre, I., Vose, S., & Wuertz, D. (2006). Overview of integrated global radiosonde archive. *Journal of Climate* , 53-68.
- Gleisner, H., & Thelji, P. (2016). *Reanalysis data*.
- Hangemann, S., Bengtsson, L., & Gendt, G. (2003). On the determination of atmospheric water vapor from GPS measurement. *Journal of Geophysical Research: Atmosphere* 108(D21), p.108.
- Huffman, G. (2020). Weather Forecasting. Retrieved from <http://www.scholastic.com/teachers/article/weather-forecasting>.
- Jiang, P., Shirong, Y., Dezhong, C., Yanyan, L., & Pengfei, X. (2016, May 6). Retrieving Precipitable Water Vapor Data Using GPS Zenith Delays and Global Reanalysis Data in China. *Remote Sensing*, 389. Retrieved from <https://doi.org/10.3390/rs8050389>
- Kalnay, E., Kanamitsu, M., Kistler, R., Collins, W., Deaven, D., Gandin, D., . . . Chelliah, M. (1996). The NCEP/NCAR 40-Year Reanalysis Project. *Bulletin of the American Meteorological Society*, 437-471.
- Li, X., Dick, G., Wickert, J., & Bender, M. (2014). Real time GPS sensing of atmospheric water vapour: Precise point positioning with orbity, clock, and phase delay corrections. *Geophysical research*, pp.3615-3621.
- Mlawa, A. (2020). *Atmospheric Water Vapour Determination Using GNSS Signals for Numeric Weather Prediction in Tanzania*. Dar es salaam: Ardhi University.

- Moustafa, T. (1992). The hydrological cycle and its influence on climate. *Nature*, 359.
- Namaoui, H., Kahlouche, S., Belbachir, A., Van Malderen, R., Brenot, H., & Pottiaux, E. (2017). GPS water vapour and its comparison with radiosonde and ERA-Interim data in Algeria. *Advances in Atmospheric Science* 34, 623-634.
- Potter, T. D., & Colman, B. R. (2003). *HANDBOOK OF WEATHER, CLIMATE, AND WATER. Dynamics, Climate, Physical Meteorology, Weather Systems, and Measurements*.
- Ssenyunzi, R. C., Oruru, B., D'ujanga, F. M., Realini, E., & Barindelli, S. (2020, april 15). Performance of ERA% data in retrieving Precipitate Water Vapour over East African Tropical Region. *Advances in Space Research*, 65(8), 1877-1893.
- Tylor, J. W., & Buizza, R. (n.d.). Density forecasting for Weather Derivative Pricing. *International Journal of forecasting*, 22(0),29-42.
- Wang, X., Zhang, & Dai, A. (2016). Water vapour weighted mean temperature and its impact on the determination of precipitable water vapour and its trend. *Journal of geophysics*, pp.833-352.
- Weber, M. (2004). *General Meteorology*.
- WMO. (2004). Implementation plan for the Global systems for climate in support of the UNFCCC.
- WMO. (2018). Guide to instruments and methods of observation volume I-measurement of Meteorological Variables.
- Yunk, T. P., Liu, C. H., & Ware, R. (2000). A history of GPS soundings. *Terrestrial, Atmospheric and Oceanic Sciences*, 1-20.

APPENDICES

Appendix 1: Sample of processed data and results from ARSH station

GPS_RESULTS			REANALYSIS_RESULTS					
DATE	GPS (mm)	sig (mm)	NCEP (mm)	NCEP 2 (mm)	JRA-55 (mm)	ERA-Interim (mm)	Merra2 (mm)	ERA-5 (mm)
1/1/15 12:00 AM	24.740	1.330	37.800	31.100	24.499	26.759	29.515	26.640
1/1/15 6:00 AM	24.800	0.820	38.700	30.600	20.772	24.322	25.007	22.306
1/1/15 12:00 PM	24.950	0.800	37.400	28.000	20.614	23.536	25.936	23.261
1/1/15 6:00 PM	23.170	0.730	34.400	24.000	22.341	23.470	26.905	22.981
1/2/15 12:00 AM	22.740	1.240	29.400	21.400	20.050	20.001	24.995	20.088
1/2/15 6:00 AM	21.500	0.800	26.600	18.700	18.335	16.554	22.043	17.943
1/2/15 12:00 PM	23.830	0.780	25.300	18.700	18.605	19.313	20.844	19.275
1/2/15 6:00 PM	19.550	0.720	25.600	21.000	17.194	20.002	22.660	19.728
1/3/15 12:00 AM	23.230	1.360	28.100	23.300	14.987	18.516	23.245	17.504
1/3/15 6:00 AM	21.560	0.870	27.000	24.900	14.498	15.567	21.980	15.714
1/3/15 12:00 PM	24.190	0.870	26.000	26.900	13.991	17.217	23.146	17.368
1/3/15 6:00 PM	21.400	0.790	26.200	28.000	14.476	18.822	31.417	19.015
1/4/15 12:00 AM	22.960	1.370	25.900	26.000	15.650	20.714	31.703	19.390
1/4/15 6:00 AM	19.880	0.970	26.100	25.500	16.689	20.820	26.453	18.181
1/4/15 12:00 PM	27.870	0.950	25.600	26.500	18.214	21.086	29.158	22.761
1/4/15 6:00 PM	29.430	0.880	24.300	28.200	20.809	22.904	36.712	26.064
1/5/15 12:00 AM	32.610	1.710	25.400	27.500	21.542	23.928	36.290	26.590
1/5/15 6:00 AM			24.800	26.000	20.399	26.832	32.712	25.157
1/5/15 12:00 PM			27.000	26.200	18.479	28.641	31.516	28.640
1/5/15 6:00 PM			28.600	30.300	18.786	31.595	34.233	29.312
1/6/15 12:00 AM	33.880	1.230	32.400	31.800	19.786	33.670	35.763	27.987
1/6/15 6:00 AM	30.860	0.790	34.100	32.200	19.938	32.757	35.189	29.261
1/6/15 12:00 PM	29.170	0.800	33.000	33.200	20.735	31.230	32.772	27.399
1/6/15 6:00 PM	36.370	0.750	32.500	32.000	22.681	34.491	33.486	30.274
1/7/15 12:00 AM	33.650	1.520	32.500	30.000	26.674	35.665	36.824	30.734
1/7/15 6:00 AM	33.580	0.800	31.900	28.400	26.747	35.405	37.720	31.111
1/7/15 12:00 PM	33.280	0.790	30.900	26.900	25.012	33.249	35.639	27.634
1/7/15 6:00 PM	36.950	0.730	29.400	25.300	29.259	33.161	38.801	29.955
1/8/15 12:00 AM	28.760	1.440	29.200	25.800	30.009	31.375	40.546	29.803
1/8/15 6:00 AM	25.590	0.950	28.500	27.600	28.852	28.457	34.501	27.801
1/8/15 12:00 PM	29.520	0.930	28.800	28.100	26.765	27.416	33.401	27.101
1/8/15 6:00 PM	26.410	0.870	30.300	28.500	28.781	31.785	33.488	24.973
1/9/15 12:00 AM	23.510	1.630	33.400	26.600	25.840	33.783	33.078	25.414
1/9/15 6:00 AM	25.820	0.950	30.500	23.500	22.433	29.323	28.886	24.071
1/9/15 12:00 PM	23.350	0.930	30.200	20.900	21.554	27.615	27.682	21.607
1/9/15 6:00 PM	23.550	0.900	30.900	22.900	22.785	31.993	30.095	22.310
1/10/15 12:00 AM	24.200	1.710	33.600	24.800	24.446	32.079	33.982	24.314
1/10/15 6:00 AM	25.470	1.280	36.100	24.500	24.070	31.000	34.166	25.509
1/10/15 12:00 PM	29.410	1.250	38.800	24.500	22.906	34.104	36.693	28.284
1/10/15 6:00 PM	35.800	1.190	40.900	27.300	25.142	36.072	40.141	28.607

1/11/15 12:00 AM	36.220	1.980	39.900	32.000	28.997	37.873	41.669	31.003
1/11/15 6:00 AM	34.830	0.900	39.800	31.100	29.803	37.660	39.897	30.689
1/11/15 12:00 PM	39.940	0.850	38.000	31.100	28.882	36.501	38.981	32.505
1/11/15 6:00 PM	38.730	0.800	38.100	31.100	31.595	37.493	41.169	34.045
1/12/15 12:00 AM	36.000	1.460	35.200	32.700	31.235	36.275	36.013	34.653
1/12/15 6:00 AM	32.820	0.940	33.400	31.600	27.937	33.150	34.514	34.266
1/12/15 12:00 PM	31.660	0.910	32.600	30.800	25.418	29.983	33.384	30.640
1/12/15 6:00 PM	32.000	0.920	33.000	31.800	27.841	31.489	34.096	25.654
1/13/15 12:00 AM	27.000	1.570	31.900	32.100	25.267	30.454	35.254	22.212
1/13/15 6:00 AM			30.400	30.000	21.913	28.352	28.077	21.924
1/13/15 12:00 PM			29.700	26.900	18.762	25.971	25.997	21.229
1/13/15 6:00 PM			30.400	26.600	21.298	27.196	27.560	21.223
1/14/15 12:00 AM	22.890	1.260	31.700	27.500	24.494	29.711	25.871	19.720
1/14/15 6:00 AM	20.900	0.820	32.300	24.500	19.196	25.451	23.772	19.444
1/14/15 12:00 PM	22.570	0.780	27.700	21.700	17.191	25.601	24.232	20.253
1/14/15 6:00 PM	21.040	0.750	26.400	20.600	13.729	27.115	22.629	19.187
1/15/15 12:00 AM	21.030	1.360	28.700	21.100	13.632	26.003	19.346	19.273
1/15/15 6:00 AM	21.640	0.750	27.400	20.600	13.632	23.796	21.073	18.578
1/15/15 12:00 PM	22.120	0.680	27.600	23.200	13.693	22.839	22.669	18.696
1/15/15 6:00 PM	22.080	0.650	28.700	23.500	14.364	24.869	26.468	21.655
1/16/15 12:00 AM	20.920	1.200	28.400	25.400	17.463	26.464	29.701	23.293
1/16/15 6:00 AM	23.980	0.790	30.300	26.100	16.231	24.634	27.409	20.642
1/16/15 12:00 PM	21.490	0.750	27.400	25.400	17.902	25.913	27.270	22.156
1/16/15 6:00 PM	26.090	0.750	27.800	25.800	19.759	29.678	30.997	22.417
1/17/15 12:00 AM	22.990	1.260	27.800	25.800	18.213	30.440	32.675	19.994
1/17/15 6:00 AM	24.220	0.770	29.500	25.400	16.935	29.162	25.587	21.141
1/17/15 12:00 PM	20.680	0.720	29.600	25.500	17.296	27.701	30.353	20.607
1/17/15 6:00 PM	23.000	0.720	31.200	27.400	18.788	29.573	34.178	24.050
1/18/15 12:00 AM	24.850	1.280	31.000	25.300	18.631	29.374	34.082	28.278
1/18/15 6:00 AM	25.660	1.020	31.900	24.800	18.842	29.163	29.583	23.929
1/18/15 12:00 PM	29.090	0.930	31.200	23.700	19.266	29.320	30.010	24.721
1/18/15 6:00 PM	33.830	0.960	29.800	23.500	21.408	33.077	32.373	28.169
1/19/15 12:00 AM	35.340	1.590	32.000	27.200	22.590	36.575	34.970	30.444
1/19/15 6:00 AM	32.670	0.890	33.800	28.200	21.064	35.963	31.233	26.708
1/19/15 12:00 PM	33.250	0.730	33.800	28.700	21.636	31.159	32.757	27.774
1/19/15 6:00 PM	30.290	0.770	33.800	31.300	23.778	30.929	33.792	29.639
1/20/15 12:00 AM	32.260	1.310	32.800	30.600	27.265	33.567	37.419	29.827
1/20/15 6:00 AM			35.900	33.400	27.490	35.088	39.459	28.796
1/20/15 12:00 PM			37.000	38.800	27.892	33.861	38.711	27.616
1/20/15 6:00 PM			36.700	39.800	29.037	33.781	37.162	30.134
1/21/15 12:00 AM	30.500	1.26	36.300	40.000	26.701	33.899	38.195	29.980
1/21/15 6:00 AM	29.760	0.86	35.300	36.000	25.211	32.219	36.331	28.275
1/21/15 12:00 PM	31.930	0.77	32.200	31.500	22.802	32.007	34.522	26.741
1/21/15 6:00 PM	31.490	0.82	28.800	28.300	23.947	32.979	36.410	28.590
1/22/15 12:00 AM	26.950	1.28	27.600	28.400	21.223	28.668	31.863	24.907
1/22/15 6:00 AM	22.470	0.74	24.400	26.400	20.670	24.185	27.789	20.774

1/22/15 12:00 PM	24.550	0.64	21.300	24.800	20.400	23.570	27.597	21.597
1/22/15 6:00 PM	23.870	0.7	21.800	24.900	21.050	25.496	32.934	24.884
1/23/15 12:00 AM	22.360	1.13	25.600	26.700	20.090	25.872	33.102	23.901
1/23/15 6:00 AM	21.590	0.94	22.100	24.800	18.264	24.625	30.872	22.076
1/23/15 12:00 PM	30.920	0.83	23.600	24.400	18.133	27.595	30.678	24.616
1/23/15 6:00 PM	23.560	0.92	26.000	25.900	22.277	28.306	32.667	25.144
1/24/15 12:00 AM	22.360	1.4	27.400	28.400	25.540	27.903	32.158	23.149
1/24/15 6:00 AM	20.930	0.99	26.800	24.600	22.874	22.901	27.212	20.122
1/24/15 12:00 PM	22.850	0.89	27.900	24.000	17.577	22.132	27.993	20.013
1/24/15 6:00 PM	19.010	0.96	28.300	25.800	19.402	23.145	31.923	21.130
1/25/15 12:00 AM	21.980	1.45	28.800	26.800	20.749	23.678	28.074	19.641
1/25/15 6:00 AM	16.910	0.99	26.300	25.200	18.814	17.389	19.607	15.478
1/25/15 12:00 PM	20.160	0.85	27.400	25.000	14.430	16.617	19.426	14.992
1/25/15 6:00 PM	16.400	0.95	26.500	25.900	13.606	19.285	22.229	17.953
1/26/15 12:00 AM	16.670	1.38	28.900	27.700	16.598	19.629	23.834	14.623
1/26/15 6:00 AM	13.490	0.94	26.300	24.800	15.416	17.124	20.403	13.686
1/26/15 12:00 PM	13.360	0.82	22.700	22.100	13.652	17.299	19.245	15.239
1/26/15 6:00 PM	16.730	0.92	23.100	20.700	13.193	19.847	19.616	18.202
1/27/15 12:00 AM	16.060	1.38	22.700	21.200	14.901	20.499	23.370	18.302
1/27/15 6:00 AM	17.450	0.83	20.500	19.400	14.513	20.371	23.160	17.712
1/27/15 12:00 PM	24.030	0.68	20.400	18.700	15.112	22.218	23.971	21.446
1/27/15 6:00 PM	22.310	0.76	22.800	19.800	15.284	23.146	25.079	24.033
1/28/15 12:00 AM	23.020	1.15	25.500	22.400	17.602	23.318	27.874	21.900
1/28/15 6:00 AM	22.160	0.81	25.000	21.700	16.976	22.552	27.681	19.713
1/28/15 12:00 PM	26.140	0.72	26.700	22.800	16.010	21.788	27.053	20.197
1/28/15 6:00 PM	20.360	0.81	30.600	26.100	15.876	22.763	26.369	21.439
1/29/15 12:00 AM	22.960	1.27	30.600	26.900	19.694	25.713	25.608	19.242
1/29/15 6:00 AM	23.140	0.83	30.200	27.900	19.664	24.633	21.680	19.275
1/29/15 12:00 PM	24.820	0.72	31.900	26.900	17.536	25.039	23.738	20.613
1/29/15 6:00 PM	20.860	0.82	31.200	31.900	17.541	26.304	24.389	20.790
1/30/15 12:00 AM	22.190	1.15	33.400	29.900	21.963	27.700	25.832	22.030
1/30/15 6:00 AM	22.340	0.88	34.000	28.300	19.581	22.043	21.735	21.158
1/30/15 12:00 PM	26.220	0.78	34.400	29.500	17.146	23.066	22.356	22.012
1/30/15 6:00 PM	22.690	0.9	33.500	31.200	16.792	27.919	24.422	23.078
1/31/15 12:00 AM	24.650	1.38	33.900	29.600	18.645	28.879	25.132	21.106
1/31/15 6:00 AM	19.000	0.95	28.000	27.100	16.845	23.767	21.020	17.766
1/31/15 12:00 PM	25.650	0.85	24.900	26.000	13.764	21.110	24.375	18.764
1/31/15 6:00 PM	22.690	0.99	26.500	26.700	13.530	23.349	28.141	19.926
2/1/15 12:00 AM	23.370	1.31	27.600	25.600	19.003	26.122	29.339	21.683
2/1/15 6:00 AM	21.880	0.9	25.000	24.500	17.622	22.974	26.711	20.985
2/1/15 12:00 PM	26.690	0.79	26.000	25.800	17.239	21.483	25.863	20.286
2/1/15 6:00 PM	24.730	0.94	27.000	26.600	19.668	22.143	29.963	20.210
2/2/15 12:00 AM	26.560	1.2	31.000	27.300	23.113	23.801	29.650	23.528
2/2/15 6:00 AM	22.300	0.83	29.800	27.100	19.889	23.507	26.369	21.136
2/2/15 12:00 PM	25.110	0.77	27.300	26.800	18.255	22.268	22.851	21.461

Appendix 2: Sample of processed data and results from DODM station

GPS_RESULTS			REANALYSIS_RESULTS					
DATE	GPS (mm)	sig (mm)	NCEP (mm)	NCEP 2 (mm)	JRA-55 (mm)	ERA-Interim (mm)	Merra2 (mm)	ERA-5 (mm)
1/1/15 12:00 AM	35.580	1.560	36.900	32.900	26.999	40.459	46.015	40.736
1/1/15 6:00 AM	34.990	0.780	35.000	33.500	29.678	40.545	39.866	41.019
1/1/15 12:00 PM	33.130	0.860	35.000	31.900	30.583	39.451	40.858	36.419
1/1/15 6:00 PM	32.080	0.720	34.100	29.500	27.403	39.134	41.718	37.169
1/2/15 12:00 AM	33.990	1.330	31.900	24.600	27.425	36.892	37.034	36.524
1/2/15 6:00 AM	32.350	0.940	31.500	20.700	27.772	36.488	34.191	34.803
1/2/15 12:00 PM	30.220	1.050	30.000	21.700	27.668	35.400	32.938	35.673
1/2/15 6:00 PM	37.740	0.920	28.800	23.600	27.257	33.832	36.308	40.958
1/3/15 12:00 AM	32.380	1.530	30.800	24.300	29.909	33.163	40.816	34.975
1/3/15 6:00 AM	30.560	1.180	30.200	26.400	24.764	33.533	38.035	35.133
1/3/15 12:00 PM	32.910	1.300	29.400	27.300	24.179	32.693	38.255	34.825
1/3/15 6:00 PM	40.580	1.070	29.400	28.100	27.413	34.050	38.253	37.973
1/4/15 12:00 AM	29.450	1.860	28.500	28.300	28.619	32.749	40.742	38.550
1/4/15 6:00 AM	33.000	0.750	28.300	28.900	27.501	33.222	39.640	37.448
1/4/15 12:00 PM	28.420	0.850	29.600	31.100	28.589	34.972	41.619	32.788
1/4/15 6:00 PM	34.360	0.690	30.600	31.500	26.966	39.687	45.353	34.076
1/5/15 12:00 AM	35.780	1.190	30.400	31.800	26.636	39.018	45.571	38.406
1/5/15 6:00 AM	31.860	0.890	29.000	29.800	26.618	33.444	39.353	32.937
1/5/15 12:00 PM	29.990	0.970	31.300	30.800	28.323	33.400	41.555	35.818
1/5/15 6:00 PM	35.660	0.850	32.300	34.000	27.505	35.057	43.827	38.107
1/6/15 12:00 AM	37.060	1.450	35.000	35.500	25.693	37.573	43.997	39.622
1/6/15 6:00 AM	31.970	0.700	35.900	35.200	28.469	36.976	40.955	38.261
1/6/15 12:00 PM	34.100	0.760	35.700	36.500	27.892	36.511	40.803	40.308
1/6/15 6:00 PM	37.240	0.670	36.400	36.100	27.462	40.283	42.424	39.432
1/7/15 12:00 AM	41.560	1.150	35.000	34.700	28.205	41.235	43.293	40.719
1/7/15 6:00 AM	34.930	0.700	33.000	30.700	29.872	41.137	43.627	40.581
1/7/15 12:00 PM	35.800	0.770	31.800	29.700	29.606	39.472	40.998	35.250
1/7/15 6:00 PM	32.580	0.670	30.400	26.800	29.540	40.893	41.958	36.464
1/8/15 12:00 AM	37.690	1.190	31.000	27.700	30.884	41.405	44.015	38.520
1/8/15 6:00 AM	37.330	0.900	28.300	26.300	30.821	37.143	43.782	39.619
1/8/15 12:00 PM	38.110	0.960	29.300	27.600	29.796	36.031	43.557	37.171
1/8/15 6:00 PM	36.650	0.860	31.500	31.800	29.969	36.466	44.379	41.223
1/9/15 12:00 AM	32.290	1.470	35.200	33.400	27.090	36.194	43.359	39.747
1/9/15 6:00 AM	32.990	0.900	34.800	31.400	24.308	32.488	42.917	37.548
1/9/15 12:00 PM	35.940	0.990	34.500	31.000	26.710	34.562	40.292	35.016
1/9/15 6:00 PM	38.000	0.950	35.600	31.600	32.191	36.930	40.697	35.837
1/10/15 12:00 AM	30.360	2.100	36.900	32.300	31.071	35.779	42.060	39.397
1/10/15 6:00 AM	40.010	0.820	36.900	31.300	30.227	37.099	47.963	39.343
1/10/15 12:00 PM	38.890	0.870	37.800	32.000	31.187	35.417	47.177	38.269
1/10/15 6:00 PM	39.100	0.780	40.300	33.700	32.048	39.819	49.141	42.586
1/11/15 12:00 AM	41.360	1.400	40.100	34.900	30.685	42.781	44.559	43.676
1/11/15 6:00 AM	38.070	0.760	39.000	34.200	33.771	41.817	41.865	44.213

1/11/15 12:00 PM	43.460	0.790	39.000	36.800	33.538	42.826	44.684	40.967
1/11/15 6:00 PM	39.540	0.750	39.700	39.100	32.564	44.016	44.872	42.756
1/12/15 12:00 AM	40.300	1.340	40.200	38.600	32.767	43.508	42.481	43.731
1/12/15 6:00 AM	38.680	0.720	38.100	38.600	32.953	41.407	42.545	43.223
1/12/15 12:00 PM	40.000	0.760	36.900	37.500	32.855	41.838	43.399	39.121
1/12/15 6:00 PM	37.130	0.730	36.000	35.200	32.060	42.571	44.752	40.973
1/13/15 12:00 AM	39.890	1.350	35.200	35.500	30.642	41.484	44.676	40.620
1/13/15 6:00 AM	38.300	0.800	34.300	33.600	31.006	38.790	44.202	39.952
1/13/15 12:00 PM	38.780	0.830	33.900	33.500	32.419	37.568	44.450	37.015
1/13/15 6:00 PM	39.290	0.830	33.400	34.500	31.767	38.817	43.052	40.936
1/14/15 12:00 AM	37.370	1.530	34.400	34.300	29.556	40.329	43.238	39.112
1/14/15 6:00 AM	37.980	0.970	33.600	31.000	28.134	39.530	41.702	37.522
1/14/15 12:00 PM	34.970	0.980	32.800	33.000	30.628	38.845	40.849	35.380
1/14/15 6:00 PM	39.340	1.000	31.100	33.100	32.511	41.414	44.239	37.816
1/15/15 12:00 AM	35.370	1.890	33.000	33.400	30.195	40.705	44.275	41.230
1/15/15 6:00 AM	38.630	0.850	34.800	32.400	30.226	39.041	44.143	41.767
1/15/15 12:00 PM	39.490	0.840	35.200	33.600	31.021	38.250	44.138	37.676
1/15/15 6:00 PM	34.760	0.880	33.000	34.600	31.505	37.674	43.866	38.751
1/16/15 12:00 AM	36.230	1.640	34.100	35.300	29.041	37.542	41.920	39.070
1/16/15 6:00 AM	38.730	0.740	37.100	36.200	28.450	35.794	42.448	38.067
1/16/15 12:00 PM	37.000	0.730	35.900	36.500	30.246	35.914	43.356	36.236
1/16/15 6:00 PM	35.100	0.800	32.800	36.800	31.728	38.091	42.551	34.782
1/17/15 12:00 AM	36.490	1.570	34.200	35.500	29.338	38.057	39.003	37.870
1/17/15 6:00 AM	33.280	0.720	34.400	34.900	28.185	33.400	39.485	33.379
1/17/15 12:00 PM	30.750	0.720	34.300	32.800	28.796	35.236	39.299	32.191
1/17/15 6:00 PM	36.730	0.790	34.000	34.300	31.663	38.834	40.475	33.888
1/18/15 12:00 AM	36.550	1.570	34.600	35.200	29.694	37.864	40.410	39.040
1/18/15 6:00 AM	41.380	0.830	33.500	32.800	30.186	37.516	41.005	41.581
1/18/15 12:00 PM	39.470	0.790	32.900	31.400	30.016	38.173	42.658	34.861
1/18/15 6:00 PM	35.080	0.910	32.700	30.700	30.814	39.514	42.608	36.775
1/19/15 12:00 AM	37.750	1.770	33.800	32.000	28.496	39.034	41.485	40.153
1/19/15 6:00 AM	39.070	0.670	34.000	32.300	27.907	36.433	40.327	40.077
1/19/15 12:00 PM	38.050	0.640	33.900	33.200	28.167	37.285	41.210	37.514
1/19/15 6:00 PM	37.990	0.770	34.600	34.200	30.700	39.941	41.292	38.530
1/20/15 12:00 AM	38.040	1.580	33.400	33.700	29.250	39.832	40.981	39.899
1/20/15 6:00 AM			33.700	34.200	30.911	39.608	39.865	40.264
1/20/15 12:00 PM			35.800	37.600	30.580	39.178	39.852	37.417
1/20/15 6:00 PM			36.700	41.300	31.209	41.457	41.162	39.595
1/21/15 12:00 AM	39.02	1.27	38.100	41.800	27.326	39.764	41.477	39.968
1/21/15 6:00 AM	38.92	0.81	38.000	43.100	26.695	37.997	42.674	38.382
1/21/15 12:00 PM	41.07	0.78	36.000	41.700	27.505	37.917	42.725	40.286
1/21/15 6:00 PM	37.24	0.93	34.700	40.100	30.650	38.641	40.066	39.644
1/22/15 12:00 AM	35.54	1.56	33.600	39.000	28.488	37.904	40.434	38.166
1/22/15 6:00 AM	31.47	0.74	32.700	37.100	24.701	33.993	39.852	33.968
1/22/15 12:00 PM	32.76	0.63	29.900	35.000	21.415	32.744	42.230	31.471
1/22/15 6:00 PM	32.11	0.82	27.200	33.600	21.941	35.136	43.777	33.794

1/23/15 12:00 AM	31.29	1.31	27.300	32.100	22.168	35.006	42.290	35.030
1/23/15 6:00 AM	31.92	0.8	27.200	29.700	22.452	32.742	42.490	35.843
1/23/15 12:00 PM	30.85	0.75	27.700	29.300	23.227	32.922	41.991	35.898
1/23/15 6:00 PM	31.71	0.93	26.800	29.500	25.620	34.255	44.276	37.048
1/24/15 12:00 AM	30.4	1.44	26.000	30.400	26.290	35.099	42.299	35.706
1/24/15 6:00 AM	29.47	0.78	24.900	27.300	24.655	32.068	38.994	34.082
1/24/15 12:00 PM	28.36	0.7	26.600	26.900	23.452	31.894	36.517	33.126
1/24/15 6:00 PM	30	0.89	27.700	27.700	24.496	33.984	38.876	32.137
1/25/15 12:00 AM	24.93	1.31	28.800	31.100	25.280	32.350	34.723	31.317
1/25/15 6:00 AM	23.02	0.88	25.900	28.700	22.532	29.533	30.068	30.923
1/25/15 12:00 PM	23.96	0.79	26.200	29.100	19.367	26.852	29.035	28.866
1/25/15 6:00 PM	30.18	1.02	27.800	27.900	19.309	28.437	30.213	29.125
1/26/15 12:00 AM	23.77	1.4	28.100	28.300	19.223	26.861	26.287	25.674
1/26/15 6:00 AM	20.36	0.75	25.700	24.700	17.494	24.911	26.208	24.703
1/26/15 12:00 PM	18.99	0.65	24.300	23.400	16.746	26.225	25.847	25.061
1/26/15 6:00 PM	28.26	0.85	23.900	19.800	16.365	28.755	29.225	26.764
1/27/15 12:00 AM	27.77	1.14	22.200	18.900	15.385	30.079	32.628	27.272
1/27/15 6:00 AM	26.72	0.89	19.200	14.700	16.982	29.487	33.246	27.528
1/27/15 12:00 PM	29.9	0.77	19.300	15.500	17.690	31.625	34.525	29.300
1/27/15 6:00 PM	34.85	1	22.000	18.000	20.175	36.029	36.868	31.515
1/28/15 12:00 AM	33.42	1.29	23.100	22.000	21.071	36.727	38.304	33.003
1/28/15 6:00 AM	32.17	0.84	22.500	21.900	21.226	34.917	39.416	32.159
1/28/15 12:00 PM	32.33	0.75	23.600	22.300	22.339	34.595	39.896	29.568
1/28/15 6:00 PM	33.76	0.99	28.100	25.900	25.376	37.296	40.588	30.723
1/29/15 12:00 AM	28.46	1.3	31.100	29.400	26.726	34.869	42.874	32.073
1/29/15 6:00 AM	28.21	0.98	30.000	30.400	24.039	30.855	34.867	31.388
1/29/15 12:00 PM	27.66	0.87	31.100	29.500	22.661	31.709	33.699	30.829
1/29/15 6:00 PM	29.8	1.12	32.500	32.800	25.822	37.313	35.912	31.902
1/30/15 12:00 AM	29.72	1.35	34.300	31.700	29.182	38.413	35.175	31.623
1/30/15 6:00 AM	31.59	1.03	36.100	29.100	26.706	35.737	35.985	33.707
1/30/15 12:00 PM	31.75	0.92	35.500	30.500	23.864	35.325	37.653	32.328
1/30/15 6:00 PM	35.38	1.12	35.000	29.700	26.917	37.946	41.594	35.123
1/31/15 12:00 AM	33.85	1.54	34.500	31.700	28.395	36.929	41.687	35.999
1/31/15 6:00 AM	32.9	1.07	31.600	27.900	26.064	31.727	44.348	32.543
1/31/15 12:00 PM	33.47	0.99	29.100	28.300	24.139	31.628	46.235	30.829
1/31/15 6:00 PM	33.86	1.2	27.100	27.900	26.717	32.456	40.212	32.283
2/1/15 12:00 AM	33.34	1.42	25.900	27.000	27.222	32.129	40.668	34.011
2/1/15 6:00 AM	30.04	1.15	24.300	27.100	24.247	29.006	35.297	32.536
2/1/15 12:00 PM	33.5	1.07	26.600	27.400	21.692	29.215	34.394	31.704
2/1/15 6:00 PM	35.01	1.29	27.800	28.600	23.293	30.821	36.072	35.091
2/2/15 12:00 AM	40.7	1.48	28.200	30.000	26.660	31.241	40.642	37.270
2/2/15 6:00 AM	34.05	1.13	27.300	29.000	25.311	29.523	39.322	32.831
2/2/15 12:00 PM	32.65	1.05	26.600	30.600	27.193	30.786	37.258	33.900

Appendix 3: Sample of processed data and results from MTVE station

GPS_RESULTS			REANALYSIS_RESULTS					
DATE	GPS (mm)	sig (mm)	NCEP (mm)	NCEP 2 (mm)	JRA-55 (mm)	ERA-Interim (mm)	Merra2 (mm)	ERA-5 (mm)
1/1/15 12:00 AM			42.500	36.400	48.186	55.460	56.046	55.726
1/1/15 6:00 AM	55.030	1.210	42.500	35.200	49.459	57.435	55.538	54.199
1/1/15 12:00 PM	59.630	1.130	45.300	40.500	51.458	58.456	56.530	56.138
1/1/15 6:00 PM	57.680	1.900	47.800	44.600	50.216	58.695	57.187	54.592
1/2/15 12:00 AM	55.800	1.570	48.400	44.100	50.612	55.994	55.878	52.204
1/2/15 6:00 AM	52.790	1.100	49.800	44.600	51.116	53.603	55.645	51.213
1/2/15 12:00 PM	55.090	1.500	49.700	46.300	52.074	53.796	56.673	52.236
1/2/15 6:00 PM	56.460	1.100	49.500	45.200	51.538	54.972	57.292	54.971
1/3/15 12:00 AM	53.130	1.520	50.900	47.200	51.737	55.496	56.550	54.242
1/3/15 6:00 AM	55.650	0.720	50.700	49.300	51.811	57.663	53.551	52.679
1/3/15 12:00 PM	59.210	0.650	51.800	47.500	52.273	58.835	57.349	57.554
1/3/15 6:00 PM	58.990	0.610	52.600	49.700	52.507	60.885	60.191	55.412
1/4/15 12:00 AM	55.960	1.260	51.800	52.700	50.244	59.377	58.836	54.538
1/4/15 6:00 AM	56.370	0.630	50.100	54.700	52.001	59.314	58.406	54.083
1/4/15 12:00 PM	59.320	0.580	52.300	57.500	51.839	59.459	59.807	57.202
1/4/15 6:00 PM	59.120	0.530	52.200	58.600	50.309	63.286	60.743	57.416
1/5/15 12:00 AM	62.590	1.150	51.200	53.100	49.167	62.857	60.337	58.170
1/5/15 6:00 AM	62.860	2.700	50.400	53.400	50.368	61.464	59.290	58.515
1/5/15 12:00 PM	60.930	2.630	49.900	51.100	52.667	62.250	59.789	58.855
1/5/15 6:00 PM			51.500	49.800	50.755	62.393	55.202	56.613
1/6/15 12:00 AM			51.700	48.500	50.693	60.598	55.091	60.889
1/6/15 6:00 AM	61.940	1.310	50.400	44.700	52.750	60.994	58.658	61.011
1/6/15 12:00 PM	62.790	1.200	47.100	47.700	51.548	59.577	59.459	61.086
1/6/15 6:00 PM	65.880	1.160	42.300	45.100	49.837	59.513	59.424	58.293
1/7/15 12:00 AM	54.920	1.600	38.300	43.800	46.017	58.728	58.277	57.750
1/7/15 6:00 AM	55.990	0.920	37.600	40.000	47.716	57.939	54.955	56.203
1/7/15 12:00 PM	58.790	0.830	38.100	38.800	49.950	57.516	55.873	57.347
1/7/15 6:00 PM	57.880	0.810	42.400	43.000	49.415	56.837	56.020	54.779
1/8/15 12:00 AM	58.990	2.130	42.700	47.800	49.978	58.502	53.062	55.292
1/8/15 6:00 AM	55.990	1.540	42.800	47.800	50.259	55.416	54.204	55.759
1/8/15 12:00 PM	56.780	1.420	40.300	45.900	50.858	56.224	56.791	55.254
1/8/15 6:00 PM	58.490	1.390	41.100	45.900	49.688	56.200	56.082	54.359
1/9/15 12:00 AM	58.550	1.600	41.600	45.100	47.434	55.972	55.281	51.785
1/9/15 6:00 AM	53.020	0.850	43.600	45.700	47.339	52.755	54.839	50.553
1/9/15 12:00 PM	47.760	0.720	42.600	46.200	46.460	52.464	53.995	50.143
1/9/15 6:00 PM	52.610	0.700	41.700	44.200	46.378	54.885	57.040	50.030
1/10/15 12:00 AM	55.940	1.310	43.500	43.600	49.728	56.658	59.810	52.895
1/10/15 6:00 AM	58.530	0.810	45.200	48.600	54.383	58.374	64.322	55.823
1/10/15 12:00 PM	60.520	0.730	47.300	51.500	54.593	61.736	64.849	59.771
1/10/15 6:00 PM	60.750	0.700	50.600	50.100	54.986	61.706	62.532	61.379
1/11/15 12:00 AM	59.280	1.160	50.500	48.100	52.216	58.055	63.903	62.251
1/11/15 6:00 AM	60.130	0.870	51.400	48.500	50.771	55.160	61.819	59.299

1/11/15 12:00 PM	59.560	0.730	48.900	50.700	50.913	55.798	63.075	57.046
1/11/15 6:00 PM	65.380	0.730	46.800	47.700	54.532	57.142	65.497	56.851
1/12/15 12:00 AM	66.400	1.170	41.100	44.900	51.579	60.299	62.716	61.139
1/12/15 6:00 AM	59.190	0.810	43.000	45.600	54.625	58.199	59.561	58.059
1/12/15 12:00 PM	62.920	0.710	52.400	50.400	51.465	58.421	58.649	57.571
1/12/15 6:00 PM	56.550	0.710	54.700	51.900	50.966	59.666	57.690	55.553
1/13/15 12:00 AM	59.830	1.140	51.400	46.600	53.049	58.399	56.769	58.174
1/13/15 6:00 AM	59.850	0.800	49.600	44.600	53.600	56.797	55.796	56.612
1/13/15 12:00 PM	58.790	0.680	48.100	44.800	52.075	58.694	58.200	55.905
1/13/15 6:00 PM	54.790	0.710	46.200	42.400	49.579	52.442	56.521	51.760
1/14/15 12:00 AM	59.650	1.140	45.400	45.100	48.244	51.423	54.019	53.612
1/14/15 6:00 AM	58.510	0.910	42.600	40.900	50.321	58.073	56.342	58.950
1/14/15 12:00 PM	58.580	0.800	44.900	42.800	50.222	58.311	53.115	56.972
1/14/15 6:00 PM	53.660	0.780	49.600	48.800	48.792	53.740	50.598	51.564
1/15/15 12:00 AM	56.920	1.190	48.100	47.300	53.289	59.821	52.119	58.154
1/15/15 6:00 AM	57.970	0.760	50.500	48.700	52.820	63.222	53.971	58.189
1/15/15 12:00 PM	59.060	0.620	50.900	49.500	53.521	62.463	54.872	59.070
1/15/15 6:00 PM	57.950	0.630	52.000	51.600	52.176	57.949	55.929	59.578
1/16/15 12:00 AM	61.000	0.940	51.600	52.300	52.432	57.182	57.685	57.205
1/16/15 6:00 AM	61.130	0.680	51.100	53.600	54.294	60.033	58.682	57.318
1/16/15 12:00 PM	59.710	0.570	49.000	56.600	51.996	60.497	60.247	58.503
1/16/15 6:00 PM	58.790	0.630	49.500	55.200	51.634	58.467	58.801	54.215
1/17/15 12:00 AM	59.270	0.910	50.400	55.800	52.557	58.911	56.816	58.900
1/17/15 6:00 AM	60.720	0.960	51.900	57.100	55.341	61.509	60.204	61.116
1/17/15 12:00 PM	60.400	0.880	49.000	60.900	54.265	63.036	62.830	57.256
1/17/15 6:00 PM	57.970	0.930	47.300	58.000	51.038	61.314	56.866	57.732
1/18/15 12:00 AM			50.200	59.100	51.444	62.197	58.082	54.765
1/18/15 6:00 AM	62.670	2.250	53.600	57.900	54.186	63.338	58.599	58.091
1/18/15 12:00 PM	55.720	2.160	55.000	58.100	53.984	64.482	60.924	61.051
1/18/15 6:00 PM	58.270	4.120	53.700	57.600	52.627	60.329	58.795	57.999
1/19/15 12:00 AM			51.800	54.600	51.996	58.255	56.938	58.756
1/19/15 6:00 AM	61.480	1.310	52.200	51.600	53.220	59.838	56.889	58.793
1/19/15 12:00 PM	61.810	1.180	48.600	50.200	54.386	60.292	59.304	59.934
1/19/15 6:00 PM	58.100	1.240	45.600	48.600	53.950	62.681	60.245	57.329
1/20/15 12:00 AM	57.120	4.920	44.400	49.000	52.203	60.160	61.669	60.080
1/20/15 6:00 AM			45.800	47.800	51.427	61.458	60.818	58.773
1/20/15 12:00 PM			44.500	49.200	52.361	59.832	56.711	56.695
1/20/15 6:00 PM			42.700	48.200	50.287	57.599	55.881	56.968
1/21/15 12:00 AM			42.600	51.400	50.544	55.729	52.305	57.279
1/21/15 6:00 AM	57.540	1.320	43.900	50.800	51.632	55.705	52.252	59.446
1/21/15 12:00 PM	55.140	1.150	45.900	54.400	51.333	56.707	57.366	58.409
1/21/15 6:00 PM	60.150	1.230	46.900	54.200	51.056	58.589	58.613	57.471
1/22/15 12:00 AM	64.430	1.480	46.400	54.500	49.332	57.527	55.778	57.949
1/22/15 6:00 AM	57.200	1.400	45.600	50.900	48.607	54.673	52.914	54.086
1/22/15 12:00 PM	47.730	0.850	43.500	49.600	48.744	53.671	53.949	47.576
1/22/15 6:00 PM	48.890	1.100	40.500	45.800	48.738	52.453	52.871	52.729

1/23/15 12:00 AM	51.640	1.390	38.500	44.200	49.027	52.264	49.477	54.912
1/23/15 6:00 AM	52.880	0.850	38.600	42.800	50.421	53.919	51.271	53.870
1/23/15 12:00 PM	53.010	0.700	40.100	45.100	48.368	54.649	51.772	54.256
1/23/15 6:00 PM	57.140	0.860	40.700	45.400	49.183	54.338	52.526	52.964
1/24/15 12:00 AM	54.890	1.180	40.700	47.100	48.149	55.299	48.111	50.123
1/24/15 6:00 AM	50.710	0.780	39.800	47.600	45.874	51.317	52.416	49.402
1/24/15 12:00 PM	51.900	0.650	36.900	43.700	45.624	50.560	56.173	51.489
1/24/15 6:00 PM	48.600	0.810	32.900	39.300	44.621	47.105	52.188	51.235
1/25/15 12:00 AM	47.720	1.140	31.000	35.500	44.827	46.053	49.082	48.863
1/25/15 6:00 AM	45.960	0.760	31.200	33.900	46.236	46.354	49.240	49.139
1/25/15 12:00 PM	42.840	0.600	31.500	30.900	46.289	47.259	48.676	41.892
1/25/15 6:00 PM	45.090	0.760	33.400	30.300	44.372	45.800	46.533	41.867
1/26/15 12:00 AM	46.340	1.200	34.400	28.100	43.645	46.035	43.279	42.231
1/26/15 6:00 AM	49.710	0.750	34.700	27.800	42.291	46.666	42.513	46.071
1/26/15 12:00 PM	49.140	0.600	34.400	28.500	43.809	45.081	47.285	51.699
1/26/15 6:00 PM	49.410	0.760	36.900	32.200	43.615	48.396	48.936	50.610
1/27/15 12:00 AM	50.170	1.100	36.100	33.000	42.213	49.445	50.300	51.402
1/27/15 6:00 AM	52.950	0.880	35.900	32.100	44.420	50.849	51.996	52.118
1/27/15 12:00 PM	53.910	0.700	35.300	31.000	47.002	51.355	54.510	52.249
1/27/15 6:00 PM	59.070	0.890	37.200	31.700	49.659	53.310	57.774	52.744
1/28/15 12:00 AM	58.950	1.140	41.100	34.800	49.430	50.672	54.710	54.587
1/28/15 6:00 AM	55.190	0.780	43.300	36.000	49.101	52.265	52.962	53.991
1/28/15 12:00 PM	54.600	0.630	41.900	34.500	47.042	51.717	52.209	50.563
1/28/15 6:00 PM	53.980	0.800	37.800	32.100	45.360	51.007	51.791	47.727
1/29/15 12:00 AM	51.070	1.600	35.000	30.500	46.476	49.037	50.968	51.313
1/29/15 6:00 AM	52.890	0.750	33.900	30.000	45.211	49.807	50.977	50.931
1/29/15 12:00 PM	49.010	0.600	32.900	31.700	43.364	47.466	51.464	47.424
1/29/15 6:00 PM	49.070	0.760	33.900	33.200	43.213	49.360	52.271	45.581
1/30/15 12:00 AM	52.990	0.980	35.100	35.800	43.760	51.551	51.191	50.994
1/30/15 6:00 AM	53.670	0.750	34.800	36.800	47.643	53.517	49.282	52.725
1/30/15 12:00 PM	51.370	0.600	34.900	36.600	49.739	52.696	52.840	54.811
1/30/15 6:00 PM	51.210	0.750	37.100	36.100	47.855	52.653	54.578	54.421
1/31/15 12:00 AM	55.050	1.100	35.300	39.400	46.520	52.706	55.968	57.397
1/31/15 6:00 AM	56.390	0.710	35.200	38.000	46.626	53.757	56.411	55.798
1/31/15 12:00 PM	54.860	0.550	35.700	39.400	46.514	53.969	57.047	52.298
1/31/15 6:00 PM	53.060	0.730	37.000	40.200	44.702	52.854	55.665	48.910
2/1/15 12:00 AM	58.190	0.930	36.500	41.500	44.941	53.228	51.714	51.496
2/1/15 6:00 AM	54.080	0.830	36.400	41.500	46.778	51.568	50.797	49.327
2/1/15 12:00 PM	54.590	0.670	36.500	39.500	46.489	50.216	52.706	54.138
2/1/15 6:00 PM	57.440	0.860	38.800	41.000	44.636	53.253	54.791	54.417
2/2/15 12:00 AM	51.560	1.600	37.000	39.200	45.301	52.553	54.564	52.812
2/2/15 6:00 AM	54.510	0.800	36.600	37.800	45.093	49.845	51.401	47.345
2/2/15 12:00 PM	40.100	0.630	32.900	35.100	45.755	45.933	46.805	45.807
2/2/15 6:00 PM	49.440	0.830	30.000	34.800	45.248	45.150	52.048	45.506

Appendix 4: Python script employed to merge daily reanalysis datasets

```
combiner.py > ...
1  import os
2  import glob
3  import xarray as xr
4
5  # Path to the directory containing the NetCDF files
6  dir_path = 'C:/Users/SIGN IN/Downloads/merra'
7
8  # Find all NetCDF files in the directory
9  file_pattern = os.path.join(dir_path, '*.nc4')
10 files = glob.glob(file_pattern)
11
12 # Open each file as an xarray dataset
13 datasets = [xr.open_dataset(file) for file in files]
14
15 # Merge the datasets along the time dimension (assuming 'time' is the common dimension)
16 merged = xr.concat(datasets, dim='time')
17
18 # Write the merged dataset to a new file
19 merged.to_netcdf('merged.nc4')
20
```